AMMRC CTR 75-29

PARAMETRIC STUDY OF DIFFUSION BONDED BUTT JOINTS

NOVEMBER 1975

M.E. GULDEN, A.G. METCALFE AND E.C. THORSRUD

SOLAR DIVISION OF INTERNATIONAL HARVESTER
P.O. BOX 80966
SAN DIEGO, CALIFORNIA 92138

FINAL REPORT - CONTRACT NUMBER DAAG46-75-C-0040

Approved for public release; distribution unlimited.

Prepared for
ARMY MATERIALS AND MECHANICS RESEARCH CENTER
Watertown, Massachusetts 02172

U.S. ARMY AVIATION SYSTEMS COMMAND
St. Louis, Missouri 63166

This project was accomplished as part of the U.S. Army Manufacturing Technology program. The primary objective is to develop, on a timely basis, manufacturing processes, techniques, and equipment for use in production of Army materials.

The findings in this report are not to be construed as an official Department of the Army position, unless so designated by other authorized documents.

Mention of any trade names or manufacturers in this report shall not be construed as advertising nor as an official indorsement or approval of such products or companies by the United States Government.

DISPOSITION INSTRUCTIONS

Destroy this report when it is no longer needed.
Do not return it to the originator.

UNCLASSIFIED

SECURITY CLASSIFICATION OF THIS PAGE (When Data Entered)

REPORT DOCUMENTATION PAGE		READ INSTRUCTIONS BEFORE COMPLETING FORM
1. REPORT NUMBER AMMRC CTR 75-29	2. GOVT ACCESSION NO.	3. RECIPIENT'S CATALOG NUMBER
4. TITLE (and Subtitle) PARAMETRIC STUDY OF DIFFUSION BONDED BUTT JOINTS		5. TYPE OF REPORT & PERIOD COVERED Final Report 6. PERFORMING ORG. REPORT NUMBER RDR 1801
7. AUTHOR(s) M.E. Gulden, A.G. Metcalfe and E.C. Thorsrud		8. CONTRACT OR GRANT NUMBER(s) DAAG46-75-C-0040
9. PERFORMING ORGANIZATION NAME AND ADDRESS Solar Division of International Harvester Company 2200 Pacific Highway, P.O. Box 80966 San Diego, California 92138		10. PROGRAM ELEMENT, PROJECT, TASK AREA & WORK UNIT NUMBERS D/A Project: XO12191 CC6300 AMCMS Code: 1497.94.2.P8041
11. CONTROLLING OFFICE NAME AND ADDRESS U.S. Army Aviation Systems Command St. Louis, Missouri 63166		12. REPORT DATE November 1975 13. NUMBER OF PAGES 148
14. MONITORING AGENCY NAME & ADDRESS(if different from Controlling Office) Army Materials and Mechanics Research Center Watertown, Massachusetts 02172		15. SECURITY CLASS. (of this report) Unclassified 15a. DECLASSIFICATION/DOWNGRADING SCHEDULE –

16. DISTRIBUTION STATEMENT (of this Report)

Approved for public release; distribution unlimited.

17. DISTRIBUTION STATEMENT (of the abstract entered in Block 20, if different from Report)

18. SUPPLEMENTARY NOTES

19. KEY WORDS (Continue on reverse side if necessary and identify by block number)

Titanium alloys
Diffusion bonding
Tensile strength
Bend strength
Fatigue

20. ABSTRACT (Continue on reverse side if necessary and identify by block number)

The objective of this program was to establish adequate technology background to apply continuous seam diffusion bonding to fabricate helicopter rotor spars from Ti-6Al-4V sheet material. The following areas were investigated: identification of the cause of joint failure along original sheet edge; a parametric study to determine the degree of control required to achieve high quality diffusion bonded joints; determination of the tolerance of the process for fit-up, material preparation and

DD FORM 1 JAN 73 1473 EDITION OF 1 NOV 65 IS OBSOLETE

UNCLASSIFIED

SECURITY CLASSIFICATION OF THIS PAGE (When Data Entered)

contaminants; identification of methods to repair defective joints; and applicability of various nondestructive inspection techniques.

Joint quality was determined by various mechanical tests, including bend, tensile and fatigue, metallography and scanning electron microscopy.

FOREWORD

This report was prepared by Solar Division of International Harvester Corporation under U.S. Army Contract Number DAAG-46-75-C-0040. The contract was administered by the Army Materials and Mechanics Research Center, Watertown, Massachusetts with Mr. Paul J. Doyle, AMXMR-K serving as Technical Supervisor. This is the final report and covers work conducted from October 15, 1974 to August 31, 1975.

The authors wish to acknowledge the contr ibutions of R. Bradley Domes and Richard L. Swoboda for assistance in fabrication and evaluation of the diffusion bonded panels.

SUMMARY

The objectives of this program were the establishment of adequate technology background to apply continuous seam diffusion bonding to fabricate helicopter main rotor blade spars from sheet material. The study was performed with 30 x 4 inch panels and was directed to: (1) identification of the cause of and solutions to the occurrence of flat fracture; (2) a parametric study to determine the degree of control required to achieve high quality diffusion bonded joints; (3) determination of the tolerance of the process for fit-up, material preparation and contaminants; and (4) identification of methods to repair defective joints. In addition, applicability of various nondestructive inspection techniques was evaluated.

The results showed a wide range of bonding parameters over which parent metal properties were obtained as indicated by: 5T bend tests in each direction; tensile tests; and resonant fatigue tests. Current could be varied six percent, speed by 30 percent and force by 18 percent without loss of properties. Failure in bend tests at the joint under a 5T bend occurred beyond these limits but was not accompanied initially by loss of tensile or fatigue strength.

The most damaging nonstandard conditions in bonding were: presence of nylon or cotton in butted material; heavy grease and fingerprints; and steel foil. Contaminated etching acids, preoxidation of sheets at 800° F, tap water rinse, molybdenum foil entrapment, grinding wheel dust and many other conditions did not affect tensile strength. Only the first two resulted in joint failures in 5T bend tests. Differences of sheet metal thickness and other geometrical variables within a reasonable range of conditions did not affect joint properties. Deliberate offset of the 0.125 inch thick sheets by 0.040 inch shims did not affect joint strength or bend ductility.

Substandard bonding conditions leading to joint failure resulted in increasing percentages of "flat" fracture following the original sheet edges. Joints showing no loss of mechanical properties fractured with the dimpled structure characteristic of ductile fractures. The scale of the dimpling became finer as joint quality decreased, and only in one or two severely contaminated cases did the dimpling disappear over small areas providing evidence of nonductile fracture. The scale of dimpling was as small as 400Å for badly contaminated conditions. The origin of the dimples could not be identified as a pore or inclusion in any case.

Preliminary work showed that certain repair procedures were feasible and that acoustic emission appeared promising as a nondestructive evaluation technique.

Recommendations are made on application of these results to manufacture of spars.

TABLE OF CONTENTS

TABLE OF CONTENTS (Continued)

LIST OF ILLUSTRATIONS

LIST OF ILLUSTRATIONS (Continued)

LIST OF ILLUSTRATIONS (Continued)

LIST OF TABLES

1

INTRODUCTION AND BACKGROUND

The Army Materials and Mechanics Research Center Report (TR74-37), "Continuous Seam Diffusion Bond Titanium Spar Evaluation" of April 1974, describes previous work on this subject. This report by M.J. Bonassar and John J. Lucas of Sikorsky Aircraft points out that "the titanium spar rotor blade provides a significant increase in helicopter performance, but a low cost fabrication method such as continuous seam diffusion bonding is needed for production." This conclusion was based on fabrication of test panels and three nine-foot spar sections at Solar, followed by mechanical testing. The fatigue testing of the spars showed "fatigue strength characteristics as good as, or better than, present fusion welded main rotor blade spar specimens." Further evaluation was recommended.

The continuous seam diffusion bonding, or CSDB, process was developed at Solar as a production method in 1971/1972. The first application was to Hastelloy X T-sections supporting the low pressure turbine seals in the General Electric CF6 engines used on the DC-10 airliner. However, a change in policy at the Solar Division of International Harvester in 1972 led to the decision to cease manufacture of aerospace subcomponents and concentrate on turbomachinery products. Some of the drive to achieve wider production application of the process was lost at this point, although production manufacture of this component is continuing successfully at the Heintz Division of Kelsey Hayes Company under license. The Research Department at Solar has maintained a capability for performing this process for evaluation, and, at the same time, is extending the technology to new applications in isothermal shape rolling, ring rolling, roll forging, and other processes. The test panels and spars discussed in Report TR74-37 were made in the Solar Research Laboratories.

Figure 1 shows manufacture of the first set of these spars. The success achieved on these spars led to a decision by the U.S. Army to initiate a program through Sikorsky Aircraft to establish a manufacturing capability to make spars by CSDB. Prior to the start of this manufacturing development program, it was recognized that several other technical problems remained that would require solutions before the CSDB process would be accepted as a manufacturing process for the critical joints in a helicopter rotor spar. The most important problems identified in this regard were:

- Understanding of and solutions to the flat fractures that occurred in some tensile and fatigue tests.

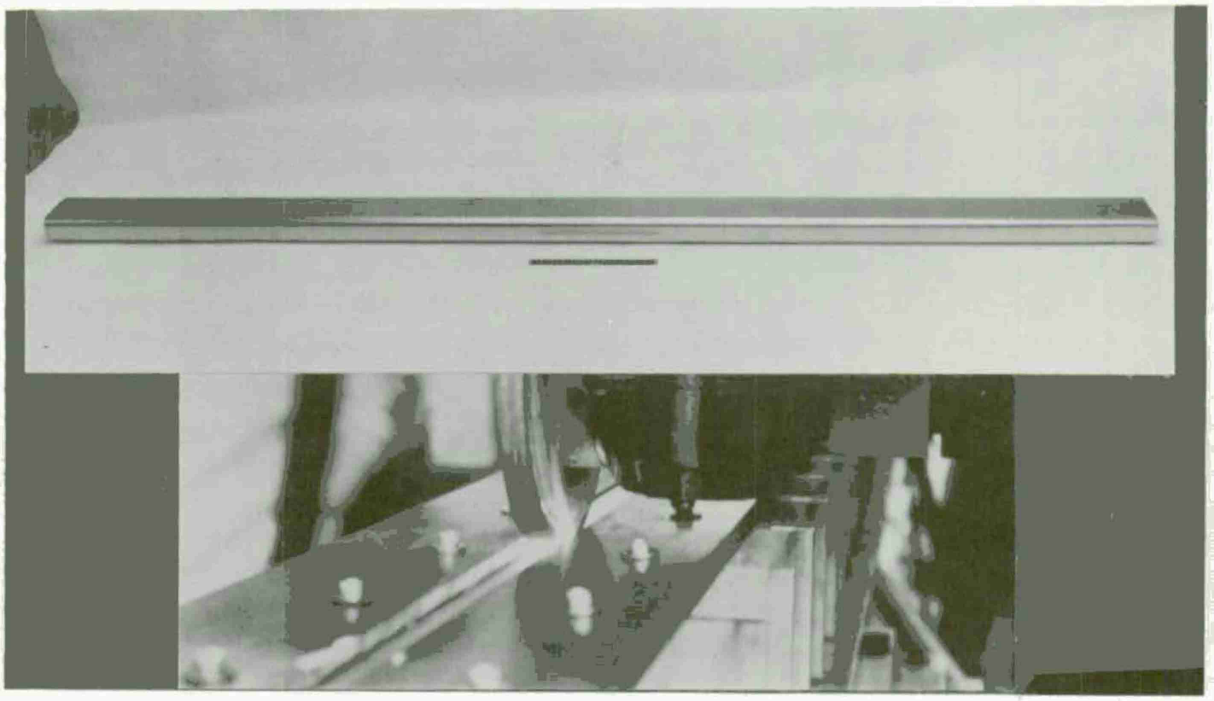

Figure 1. Fabrication of 9 foot spar by CSDB.

- Parametric study to establish optimum CSDB parameters and the controls required on each of the principal parameters. The method is based on electrical resistance heating by refractory metal roll electrodes that allow forging pressures to be exerted on the parts being joined.

- Determination of the tolerance of the process for joint variables including fit-up, material preparation and contaminants.

- Identification and establishment of methods to repair diffusion bonded joints.

- Establish NDI methods for diffusion bonded spars.

The present program was initiated to provide answers to the first three problems by work with flat panels. It was recognized that some additional work would be required to adapt the results to actual spars. Only identification of repair methods (Problem No. 4) could be included in the program because more extensive work on actual spars would be required to qualify a repair method for flight hardware. It was not planned to perform work on production NDI methods for the same reasons discussed above, although it was recognized that information from the program would aid in subsequent work on production NDI techniques. In this regard, the opportunity was taken to include a preliminary evaluation of acoustic emission to determine if this warranted subsequent work.

2

EXPERIMENTAL METHODS

2.1 DIFFUSION BONDING AND CSDB EQUIPMENT

Diffusion bonding by the continuous seam diffusion bonding (CSDB) process is an isothermal metal working process developed by Solar. The process is covered by U.S. Patent 3,644,698 and subsequent patents. The process features plastic deformation of metal parts under refractory metal rolls using electrical resistance heating. The plastic deformation is used to generate a forged weld.

Materials such as titanium and superalloys are worked at temperatures ranging from a low of approximately 1650° F for titanium alloys to as high as 2200° F for some superalloys. The CSDB process involves the application of forces at controlled rates to parts at controlled temperatures. Butt joints are made by clamping the parts in the bonding aid with lateral force and applying vertical pressure by a molybdenum alloy electrode wheel. The desired bonding temperature is attained by passing controlled electric current from the wheel through the part into the tooling and the time at temperature is controlled by the speed of the driven wheels.

Wheel forces range from a few hundred to six thousand pounds or more. Only that portion of the panel under the roll at any instant is heated to the bonding temperature and the time at peak temperature is typically one or two seconds.

Control of surface contours at the joint is achieved and results in joints with high fatigue strength.

2.1.1 Panel Size

Selection of the size for the bonded panel was based on prior work accomplished on flat panel butt bonding. The panels for this project were fabricated from two 2-inch widths of material, 1/8 inch thick by 32 inches long. When bonded together these make a 4 inch wide panel having a bonded area length of approximately 28 inches. The quality of butt bonds is greatly improved by having the best fit-up possible on the mating surfaces. This is most easily accomplished by machining the opposing edges of each half.

Machining accomplishes a second purpose. The halves must be machined enough to remove the rolled or radius edge left by the shearing operation.

2.1.2 Tooling

Tooling in the form of bonding aids is most important to the quality of the end product. Bonding aids for the CSDB process are subjected to high-temperature, quite high localized pressures and must maintain product alignment while in motion under a bonding wheel. The bonding aid for this project was designed to handle the above conditions. In addition, vacuum and inert gas bonding condition capabilities were required in the design.

Bonding aids are designed to perform three main functions. Positioning of the parts to be bonded in relation to the bonding wheel; positioning of the detail parts with relation to each other; generating and maintaining containment side pressure.

Further discussion of the bonding aid is facilitated by a cross section illustration, Figure 2.

Bonding Aid Materials

Several types of materials have been used for diffusion bonding tools and include high-temperature resistant materials such as A-11 and the stainless steels; high-strength materials such as 4130; and mild steel, both cold rolled and hot rolled. In the larger bonding aids, base plates and support structure out of the heat zones are made from aluminum tooling plate. The mandrel for the original spar fabrication project was built around a copper bar.

For the most part, the materials that have been most satisfactory are the aluminum-mild steel combination. When using aluminum, it must be protected from the bonding temperature, but equally important, the aluninum must not be allowed to conduct the heat away from the bond area. Thermal insulation of the tool is sometimes difficult because the fixture must remain electrically conductive. Ceramics, ceramic coatings or plastic-glass cloth laminates usually cannot be used.

There are occasions when it is necessary to create thermal barriers, at which time the high nickel-high chromium stainless steels can be used, or machined clearance may be required to create an air thermal barrier.

Butt Joint Bonding Aid Design

The design of the butt joint bonding aid differs from the bonding aid that will be used for a spar. There are, however, many basic similarities required for both tools and the design discussion will evolve around these physical characteristics.

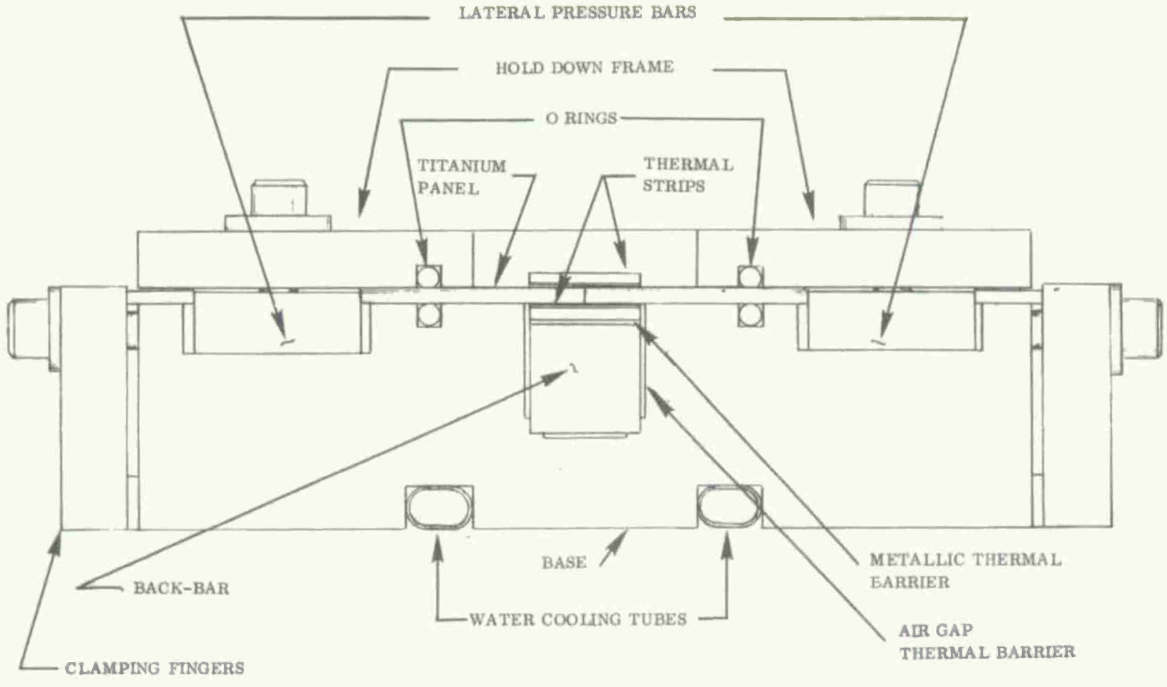

Figure 2. Bonding aid cross section.

Bonding Aid Base - The base of the butt joint tool is obviously unrelated to a spar bonding aid because of end product configuration. The base is of mild steel and quite heavy for maintaining position of the panel halves and strong enough to maintain lateral side pressure without distortion during the bonding operation.

In the center section of the base a slot is machined to accommodate the 1 inch square backup bar. The slot is machined to allow only contact of a 1/8 inch land on the sides and bottom, full length of the backup bar. The 1/8 inch land allows clearance between the backup bar and the fixture base; this is an example of an air thermal barrier. In this project fixture, the air thermal barrier was required because total physical contact between the fixture base and backup bar (three sides) allowed a heat loss so great that a satisfactory diffusion bond was difficult to achieve. A metallic thermal barrier was also required on top of the 1 inch square backup bar; this will be discussed in the backup bar section.

In the fixture bottom, two grooves were machined full length to accommodate copper tubes for water cooling. In actual use, it was determined that these two tubes removed too much heat; consequently, they were no longer used. Further discussion of water cooling is covered in the section on tool temperature control.

The top of the base is also grooved for an O-ring. The O-ring was used when making panels in vacuum or inert gas conditions. Grooves on the outside top of the base accommodate lateral pressure bars.

Back-up Bar and Thermal Barriers - Back-up bar usage was created to serve two purposes. The localized heating of the diffusion bonding process has, in the past, warped the bonding aid base and resulted in the loss of the bonding aid after approximately six parts were bonded. A cold-rolled steel back-up bar was then installed as a "throw-away" or consumable item for each bonding run. In this design concept, the back-up bar alone absorbs the warpage and extends the fixture life indefinitely.

The second and equally important purpose of the back-up bar is to create a condition to decrease thermal conductivity away from the bond area. The thermal barrier is created because of the gap between the back-up bar and fixture base. In the case of this project fixture, a gap of 0.032 inch, except at the 1/8 inch corner contact areas, was required to provide an air thermal barrier. A second type of thermal barrier, in the form of a low thermal conductive nickel-chromium alloy also performs this function. Thin gages are used, 0.030 to 0.060 inch thick, of the same width and length as the back-up bar and are reuseable. This type thermal barrier is located between the inside thermal strip and back-up bar (see Figure 2). A 1 inch square cross section back-up bar of mild steel was used for this project. This size was chosen because the width was necessary to control heat zone in the panel and the thickness could easily absorb the warpage.

Back-up bar length is important in that it should be at least 3 inches longer than the bond area for bonds up to 3 feet in length. Lengths for spars should extend 6 to 9 inches beyond the bonded length. Extra length is required to control heat buildup at the finish end of the bonding run. At the start of the bond, the backup bar should not extend more than 1 inch outside the bond. Longer lengths absorb heat and keep the joint area from attaining bonding temperatures as quickly as possible.

Thermal Strips - Thermal strips perform several functions. A better outer surface results on the part, distributing the wheel load over a wider area. The heat affected zone in the part is better controlled, heat is conducted through the whole width of the thermal strip and tends to eliminate the surface hot zones. Thermal strips also function as positioners of the titanium and molybdenum foils. Various thicknesses and widths of thermal strips have been tested but the best results have come from strips of cold-rolled steel, 1/8 inch thick by 1 inch wide. This size makes the consumable strips easily obtainable and quite inexpensive.

Foils - Two kinds of foils are used on each side of the diffusion bonded joint. Ti-6Al-4V foil, 1 inch wide and 0.004 to 0.006 inch thick, is used on each side of the joint, and when bonded to the butt joint, gives considerable reinforcement. The second foil, molybdenum, 0.003 inch thick by 1 inch wide, serves a twofold purpose. One, as a parting agent and two, as a protector to prevent an iron-titanium interaction. The interaction would result in a brittle iron-titanium eutectic alloy.

Positioning of the foils must be maintained throughout the bonding run. This is quite difficult because the part, the two foils and the thermal strip have different thermal expansion rates. When the part length is relatively short, in the 2-foot range, the foils can be resistance welded (spot tacked) to the thermal strips at the ends only.

A different method is recommended for attaching foils to each of the top and bottom thermal strips for parts longer than 2 feet. When using a 1-inch width thermal strip, our experience on this program suggests that the foil width should be increased from 1 inch to 1-1/4 inches. The foils would then be roll formed into a channel configuration with 1/8 inch legs prior to assembly. This will create automatic foil location, easily maintained in the bonding run. Attaching the foils to the bottom thermal strip can be accomplished by the resistance welding method. Welding should be done only on the 1/8 inch legs of the channels, and only enough welds to hold the foils in place during handling should be used.

The top thermal strip is not contained as is the bottom thermal strip. During the bonding process, elongation of the top strip occurs at a rate of 0.5-inch per foot (5 to 6 inches on a 10-foot spar length). Since the molybdenum and titanium foils have much lower expansion rates than mild steel, they cannot be resistance welded along the length of the thermal strip; however, it is permissible to resistance weld at the start end. On this project, 1 inch wide foils were used and positioning was maintained with spring tension.

Top Hold-Down Plate - Horizontal alignment is accomplished by applying enough force on each panel member to overcome distortion and hold it firmly against the foils and lower thermal strip. The hold-down plate for this project was a picture frame configuration of mild steel; with a bonding wheel opening 2 inches wide. An optimum distance from the bonding wheel must be maintained so that the hold-down plate does not remove heat from the joint area but must be close enough to maintain product alignment.

Bonding Aid Side Pressure Application - Applying and maintaining side pressure is another essential function of a bonding aid. The parts to be bonded must have uniform pressure applied over their lengths. Side pressure was created in the project fixture by six 5/16 inch diameter cap screws on each side, transmitted by 2 inch wide clamping fingers through continuous 1/8 x 3/4 inch wide strips to the full length of each 1/2 by 1-1/2 inch pressure bars.

2.1.3 Cleaning Procedure

An adequate cleaning procedure is required for materials to be diffusion bonded, however, special techniques are not required. The manufacturing process specification for cleaning parts for fusion welding is satisfactory for CSDB.

Materials used in procedure:

- Solvent, Metriclene MF, or equivalent
- Solvent, ND-150 solution, or equivalent
- Alkaline cleaner, Oakite 77, or equivalent
- Acid, Nitric 42° Baume (Fed. Spec. O-A-88)
- Acid, Hydrofluoric, 70% (Fed. Spec. A-H-795)
- Water, demineralized (commercial grade)

Cleaning Method

1. Solvent wash, using ND-150 solution of Metriclene M-4 as required to remove all mill marks, inks and dyes. (Chrloinated solvents will not be used on titanium parts.)

2. Immerse in the alkaline cleaner and allow to remain for a minimum of 5 minutes -

   a. Solution - 6 to 10 ounces of Oakite 77 per gallon of water maintained at 160-180° F.

   b. Immersion rinse and repeat alkaline cleaner cycle until a "water break free" surface condition is achieved.

3. Rinse - a thorough rinsing in water is required.

4. Immerse in nitric-hydrofluoric acid solution and hold as required to loosen scale, oxides and discoloration.

   a. Solution - 3 to 5 percent hydrofluoric acid by volume, plus 27 to 32 percent of nitric acid by volume in water maintained at a temperature of 130-140° F.

   b. Immersion time limits vary with solution conditions, long durations may be used as long as a detrimental etching is avoided.

5. Rinse - clear water

   a. Air-water blasting may be used to remove scale, oxides and discoloration.

6. Immerse in nitric acid solution, hold as required to loosen all smut and oxide residues.

   a. Solution - 40 to 50 percent solution of nitric acid by volume in water, maintained at 140-180° F.

7. Immersion rinse in clean water and follow with air-water blasting to remove all smut and other residues.

8. Rinse - demineralized water

9. Bake until dry - 250 ± 50° F.

10. Package

    a. Do not handle without clean white gloves.

    b. Wrap in paper until used.

NOTE: Clean only that quantity of parts that can be bonded in a single shift.

2.1.4 General Bonding Procedure

Prebonding preparation must be performed on the machine, bonding wheel, bonding aid and consumable details prior to loading the bonding aid.

The bonding wheel is checked for alignment with the machine table, establishing that the wheel face is parallel with the table and that the plane of the wheel is at a right angle to the table. The latter can be visually checked with a tool maker square when the wheel is loaded at the pre-established bonding pressure.

Locating of the bonding aid is established with reference to the bonding table and the bonding wheel. The centerline of the bonding aid and/or part joint shall be positioned to be on the centerline of the thickness of the wheel. This is visually accomplished with a "half wheel thickness pointer" while the fixture is traversed, start to finish, with the wheel in the up position.

The bonding aid is cleaned prior to the start of each run by removal of dirt particles, followed by wiping down with acetone and drying by a clean air blast. After each cleaning the fixture should be recoated with spray graphite. NOTE: Before a new bonding aid can be used for CSDB, it must be completely disassembled and vapor degreased. Only a dry lubricant, such as spray graphite, can be used when reassembling the fixture.

Consumable items are prepared using the following procedure:

- Metallic thermal barriers, if used, are cut to length, vapor degreased and graphite coated
- Back-up bars (one required) are cut to length, vapor degreased and graphite coated
- Thermal strips (two required) are cut to length and vapor degreased. The bottom (inside) strip, is coated both sides with graphite; the top strip is coated one side only with graphite
- Molybdenum foil is cut to length (two parts) and hand wiped with acetone; it may be alkaline cleaned and vapor degreased
- Titanium foil is cut to length (two parts). These are cleaned using the same process (and at the same time) as the parts to be bonded.

NOTE: Care should be taken with the cleaned and graphite coated parts to avoid subsequent contamination. Parts should not be handled with bare hands and should be protected (paper wrapped) until used.

Upon completion of the foregoing preparation, the titanium foil strips and the parts to be bonded are cleaned (see cleaning procedure, Section 2.1.3). The foils can then be attached to the thermal strips. NOTE: The top thermal strip will have foils attached to the graphite coated side only.

Loading of the bonding aid is accomplished in the following sequence, which is illustrated by photographs of selected operations:

1. Place back-up bar into slot, positioning the stainless steel thermal barrier (not shown in the photograph) between the thermal strip and back-up bar, shown in Figure 3.

2. Place two panel halves into fixture, positioning joint on the fixture centerline, using side pressure clamp blocks to fingertight condition. Figure 4 shows the parts in place preparatory to placement of the holddown top plate.

3. The holddown top plate is placed into position and clamped firmly, checking alignment of the two halves. Full side pressure can then be applied and the top thermal strip positioned, Figure 5.

4. Place fixture into bonding position and set wheel on thermal strip. Attach foil spring load device and place thermal strip guide into position at finish end (see Figure 6 and 7).

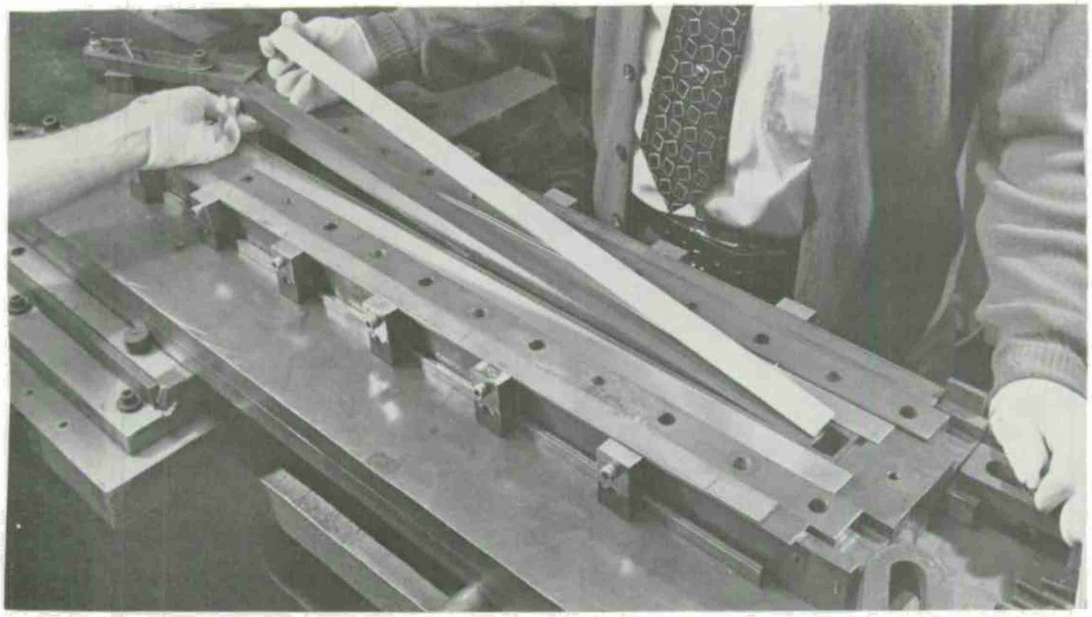

Figure 3. Placement of back-up bar and thermal strip.

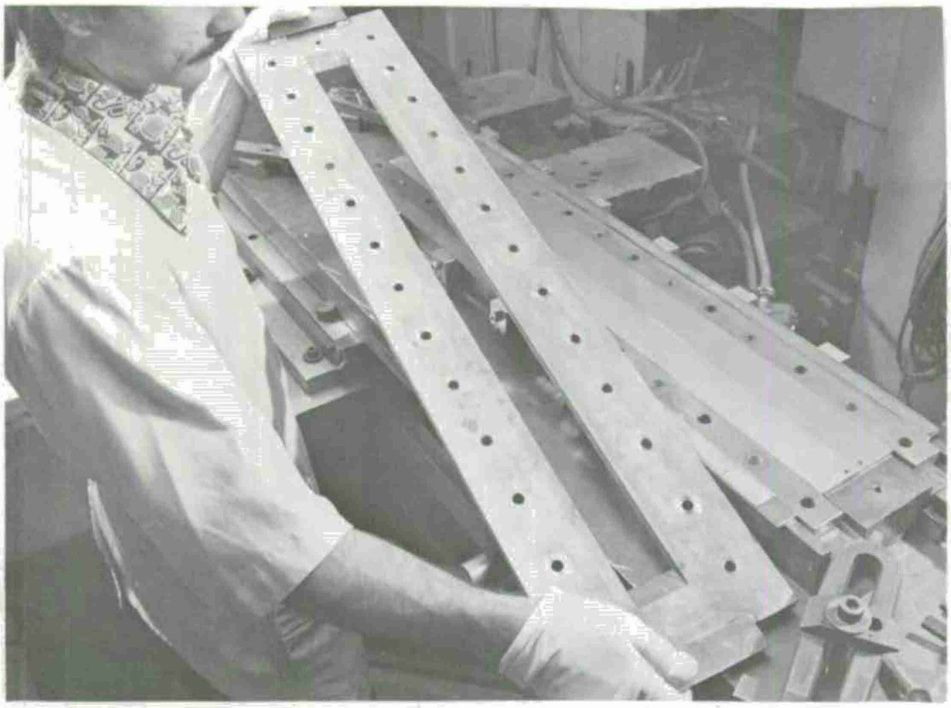

Figure 4. Placement of holddown plate.

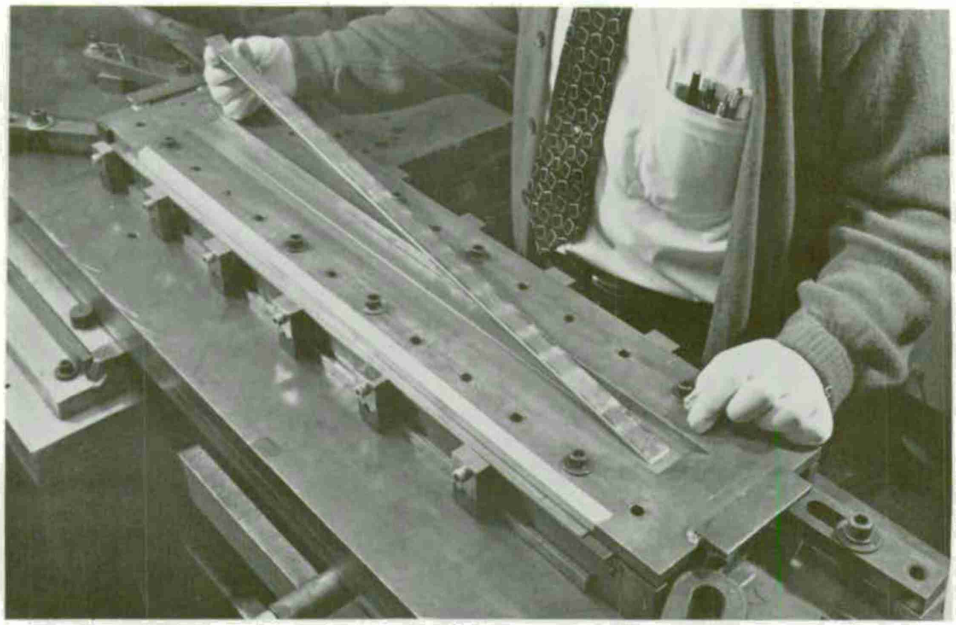

Figure 5. Positioning of thermal strip.

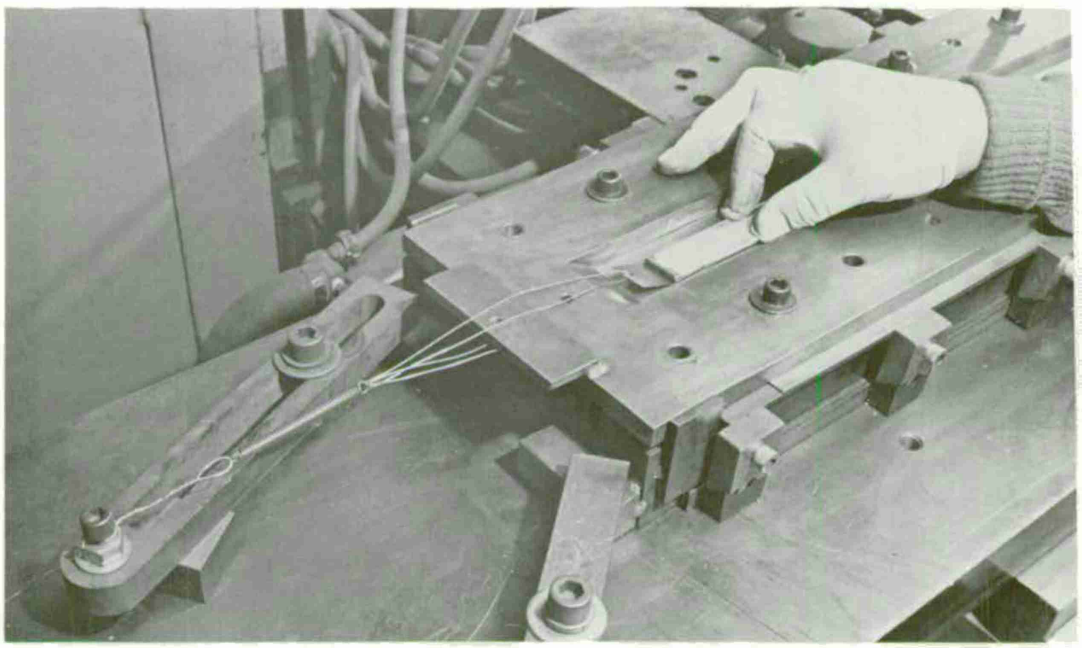

Figure 6. Attachment of spring load to foil strips.

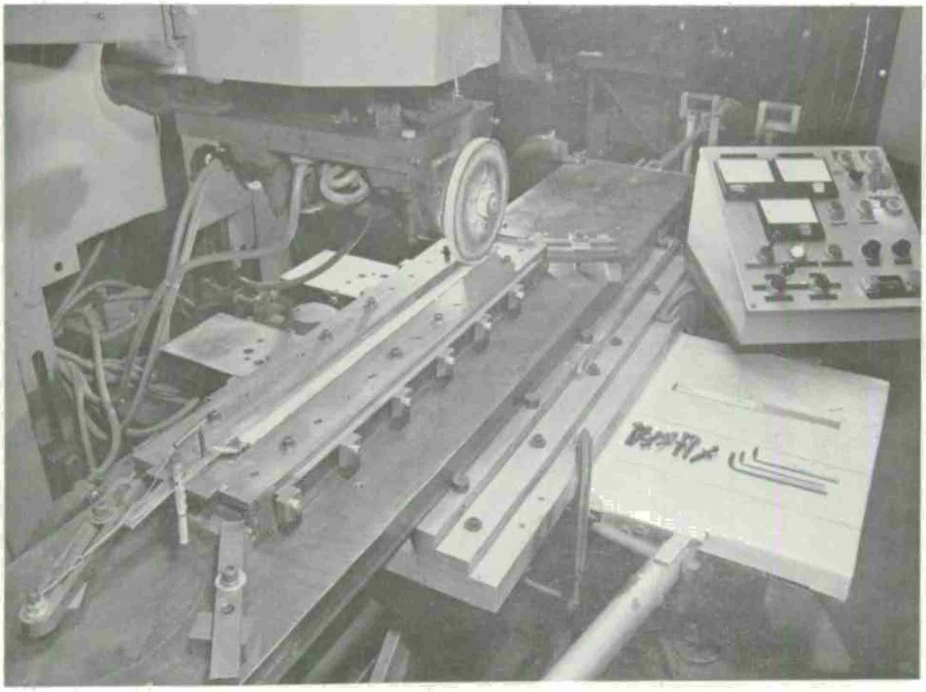

Figure 7. Completion of assembly for panel bonding in air.

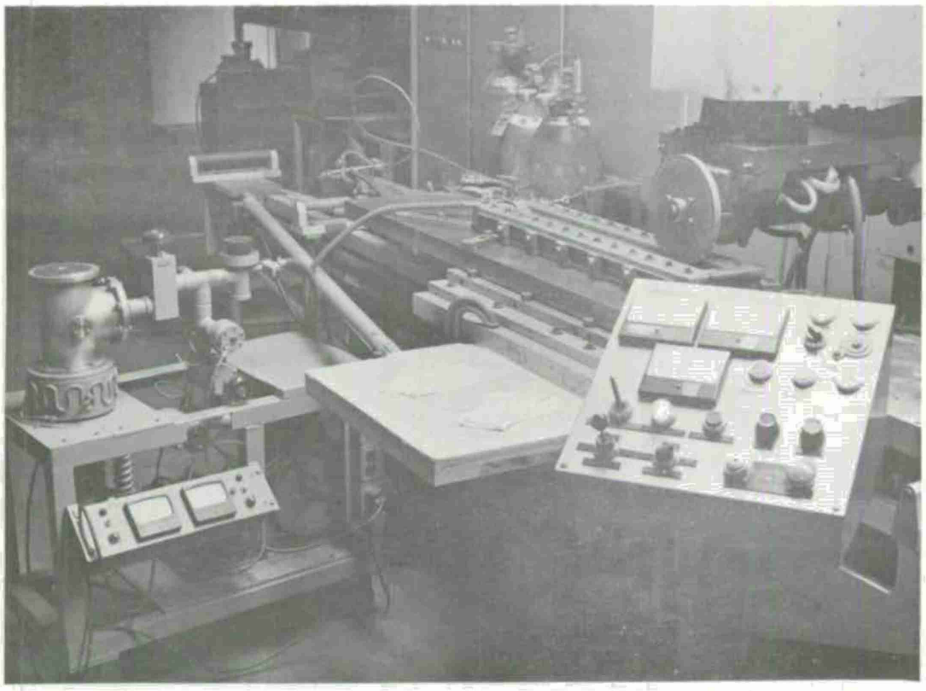

Figure 8. Set-up for vacuum bonding.

5. Bonding can then be accomplished after parameter settings are made on machine.

Figure 8 is presented to illustrate the external setup for bonding in vacuum conditions.

2.1.5 Heat Treatment

All test panels fabricated for this project were given a post-bond heat treatment. The purpose was to provide a near room-temperature equilibrium structure and to ensure panel flatness.

The heat treatment used was 1350° F ± 25° F, at temperature for 1 hour, in a vacuum furnace. Flatness was attained by a welded package of six bonded panels, interleafed and contained with 1/4 x 4 inch length CRS steel bar stock.

2.2 EVALUATION OF BONDED PANELS

The panels were subjected to various forms of mechanical and nondestructive testing and the joint regions were examined metallographically. Each of the evaluation techniques will be discussed separately.

2.2.1 Bend Tests

A schematic of the bend test fixture is shown in Figure 9. The 1.25 inch diameter punch subjects the specimen to a bend radius of 5 times the specimen thickness, which is approximately 9.25% outer fiber tensile strain. Specimens were 0.5-inch wide and tests were performed in both the "top-up" and "top-down" position. Top-up refers to positioning the specimen in the bend fixture so that the surface nearest the bonding wheel is on top and maximum outer fiber tensile strain occurs on the joint surface farthest from the bonding wheel. "Top-down" tests produce maximum outer fiber tensile strain on the joint surface nearest the bonding wheel. Testing in both positions provides a measure of joint quality through the thickness of the specimen.

The 5T bend tests were performed on all sections of panels containing variables and also on the "run-on" and "run-off" portions.

2.2.2 Tensile Tests

Tensile tests were performed using an Instron testing machine. Ultimate tensile strength, 0.2% offset yield strength, and 1 inch and 2 inch elongation were determined. Specimen configuration was chosen to simulate a service condition. The specimens were 0.5-inch wide with parallel sides. Specimen configuration is shown

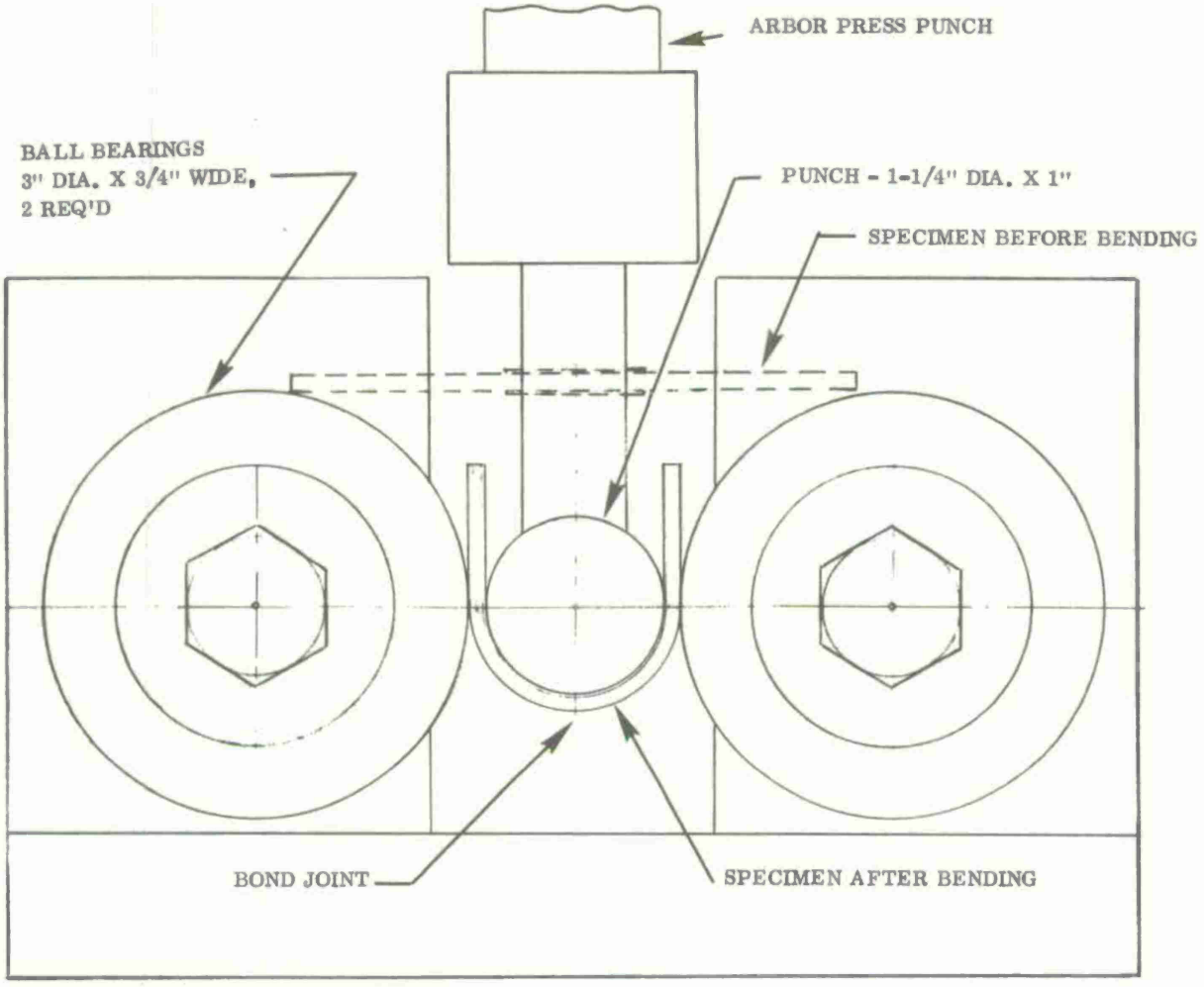

Figure 9. Schematic of bend test fixture.

in Figure 10. The 0.005 inch thick titanium foils on both sides of the joint were partially removed, by grinding, to simulate the condition of a finished spar. However, the joint area was still slightly thicker than the rest of the specimen. When failure occurred outside the joint area, the maximum stress on the joint was determined. One inch elongation provided a measure of ductility in the joint region and 2 inch elongation relates to ductility in the overall part.

2.2.3 Fatigue Tests

Resonant fatigue tests were performed on selected panels. The specimens were fabricated with a reduced cross section to induce failure at the joint. Specimen configuration is shown in Figure 11. Overall width is 0.5 inch and the reduced cross section is 0.25 inch. The specimens were rigidly mounted in a support block as a simple cantilever beam and vibrated at their resonant frequency by means of a Calidyne 1500 pound-force electro-dynamic shaker system. Specimen tip deflection

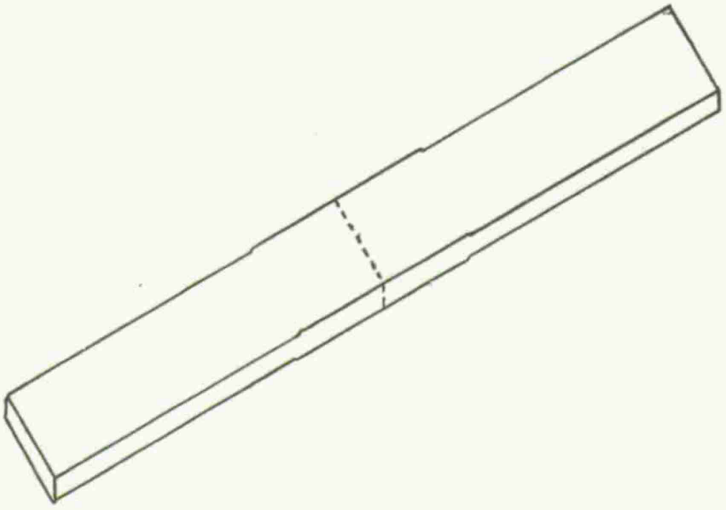

Figure 10. Configuration of tensile test specimen.

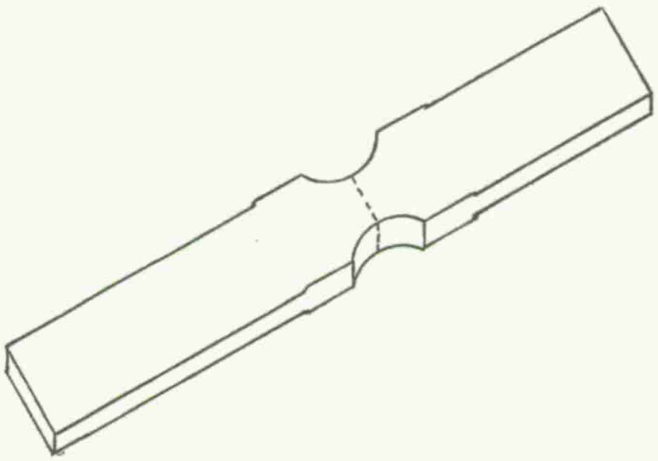

Figure 11. Configuration of resonant fatigue specimen.

was measured and controlled at 0.100 inch throughout the test. This deflection corresponds to 0.5% strain peak to peak and was chosen to produce failure in 10^4 to 10^7 cycles. The test setup with a fatigue test in progress is shown in Figure 12.

In addition to the bonded panels, a "standard" was also tested. The standard material referred to as CSDB processed, consisted of a panel which had been subjected to the standard diffusion bonding parameters plus post bond heat treatment, but did not contain a joint, i.e., instead of the normal 2 inch strips, a single 4 inch strip was used. This was done to insure that the standard specimens had the same processing and configuration as the specimens containing a joint.

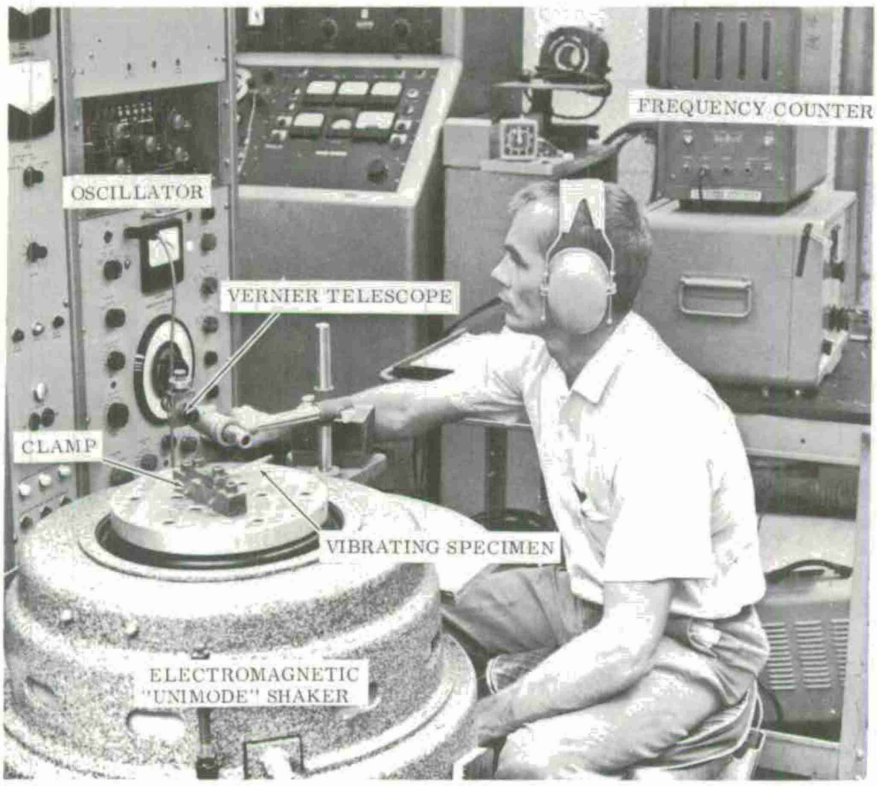

Figure 12. Resonant fatigue test apparatus.

2.2.4 Metallographic Examination

All of the panels were examined metallographically. Specimens were prepared using an etch-polish technique with Krolls etchant (2% HF, 3% HNO_3, 95% H_2O). Specimens were subsequently etched for up to 2 minutes with Krolls etchant. This is considered a very heavy etch for titanium alloys. However, generally the bond line was not apparent with this heavy etch, and an even stronger etch was required to locate the bond line. The composition of the stronger etchant, called CSDB etch, is 40% HNO_3, 10% HF and 50% H_2O.

Figure 13 shows examples of the microstructure revealed with the two etchants. In both cases, severe overetching was necessary to reveal the bond line. The bond line is apparent only because the indications are lined up. As can be seen in Figure 13, other areas in the general microstructure are more severely etched.

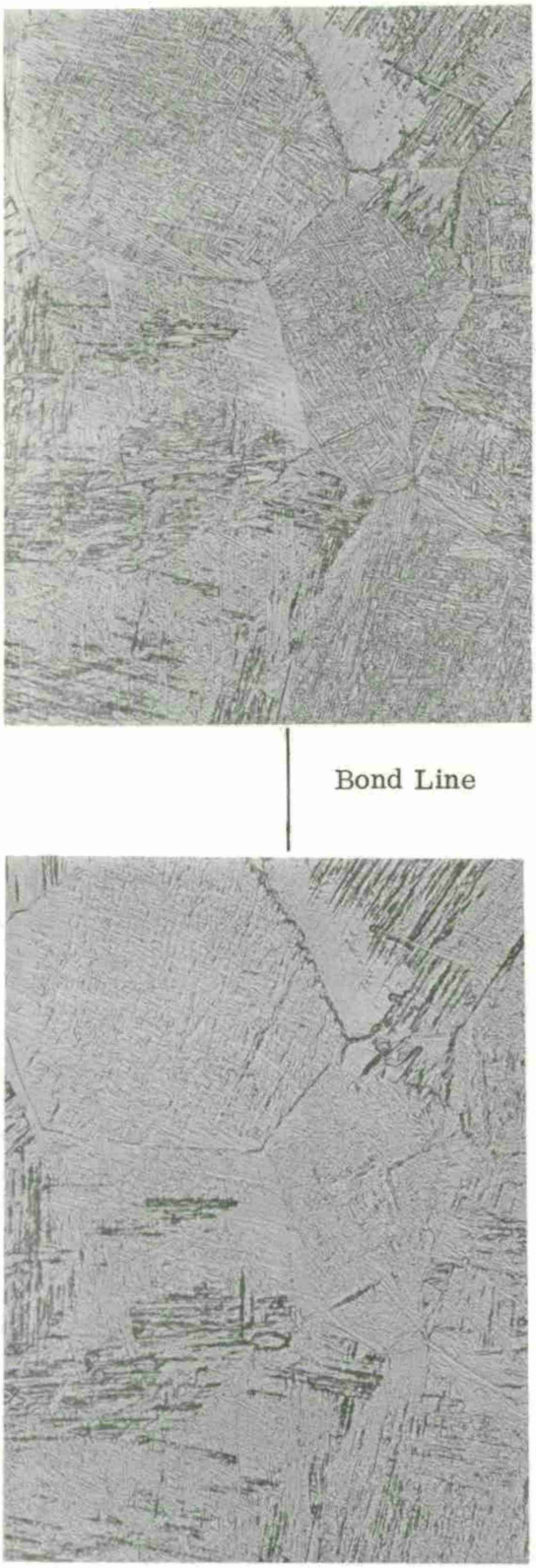

Etchant: 1 min Kroll's

Etchant: 2 min Kroll's
+ 4 sec CSDB.

Magnification: 200X

Figure 13. Example of etched microstructure of CSDB joints (note severe etching required to reveal bond line). Magnification: 200X

2.2.5 Nondestructive Testing

Various methods of nondestructive testing were used to examine the bonded panels. The specific techniques were x-radiography, dye penetrant inspection and ultrasonic inspection. In addition, the use of acoustic emission as a method of nondestructive testing for the bonded panels was evaluated.

X-radiography

The Radiographic Inspection was performed to MIL-STD-453 specification and to 1% sensitivity (approximately 0.001 inch in sheet thickness).

Dye Penetrant

Inspection performed per MIL-I-6866.

Ultrasonic

Inspection performed by International Harvester Manufacturing Services. The bonded panels were inspected using a 5 mhz immersion transducer at a 30° angle. The calibration procedure consisted of using a No. 1 flat bottom hole (0.0156 inch diameter) located 2 inches from the transducer and adjusting the height of the reflection from the No. 1 hole for a Category 16 on the computer readout.

Category 16 is the maximum indication size. A measure of the lower category sizes was obtained from a double bonded calibration plate supplied by Army Materials and Mechanics Research Center, Watertown, Massachusetts. Holes of specific sizes were eloxed in the plate prior to bonding. All holes were 0.0065 inch diameter, 0.006 inch deep and symmetrical about the 1/8 inch panel centerline. A variation in apparent void size was accomplished by placing a number of adjacent holes in a a specific location. The size of the voids after bonding had not been determined, but some reduction in size would be expected from the diffusion bonding process. A single hole corresponded to a Category No. 7.

The variation in category number with indication size is not linear. An example of the relationship for inclusions is shown in Figure 14. It is reported by International Harvester Manufacturing Services that a Category 16 for the CSDB panels would correspond to a Category 8 in Figure 14, and the shape of the curve is expected to be similar.

The panels were automatically scanned and number of counts in each category were given by computer printout. Additionally, the panels were scanned manually, and the highest category indications were physically located and marked on the panels.

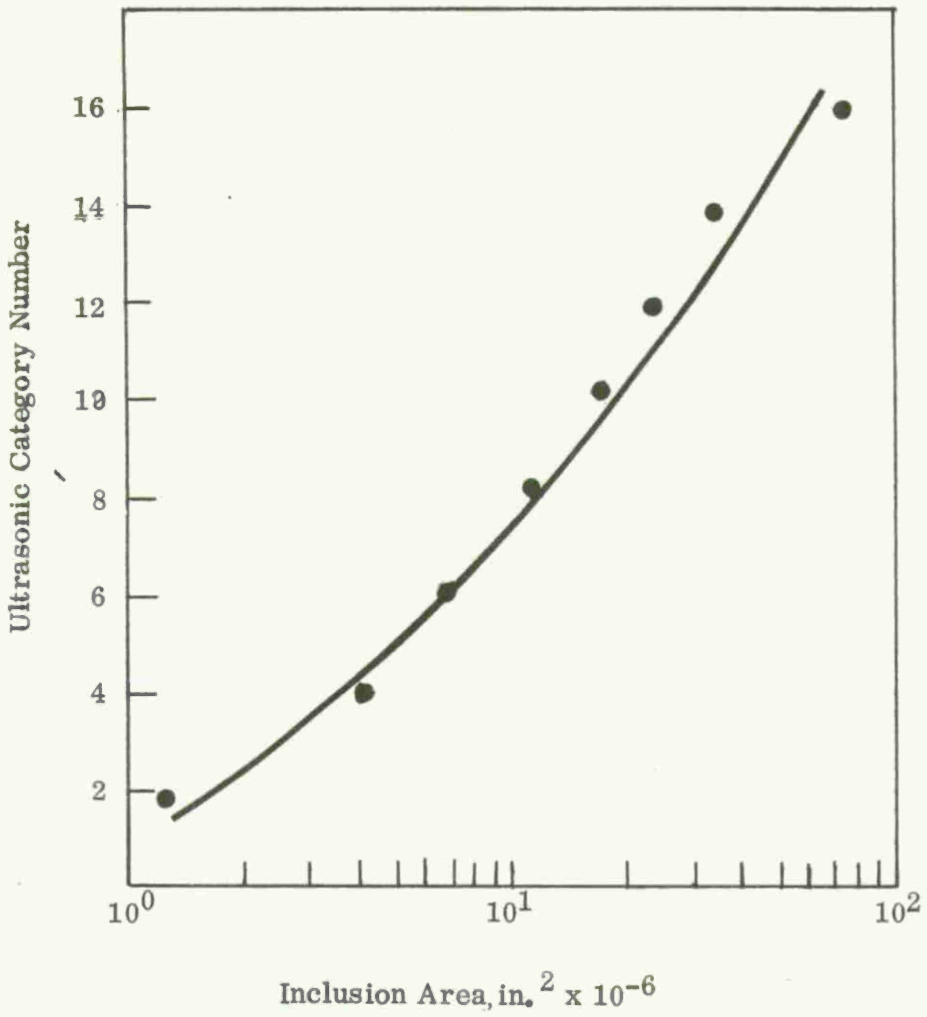

Figure 14. Ultrasonic inclusion category versus inclusion area as measured by light microscopy.

Acoustic Emission

An evaluation program was performed by Rohr Industries, Inc. The purpose of the program was to determine the feasibility of using acoustic emission as a nondestructive test technique for diffusion bonded panels. The details of the program will be discussed in Section 5.4 of this report.

2.2.6 Nomenclature

Analysis of bond quality was not only based on results of the mechanical tests and metallography but also by visual examination of the failed specimens. An abbreviated notation of the types of failure which occurred was adopted and will be used throughout the remainder of this report. A list of these symbols and their meaning is given below. Examples of the various types of failures are shown in Figures 15-17.

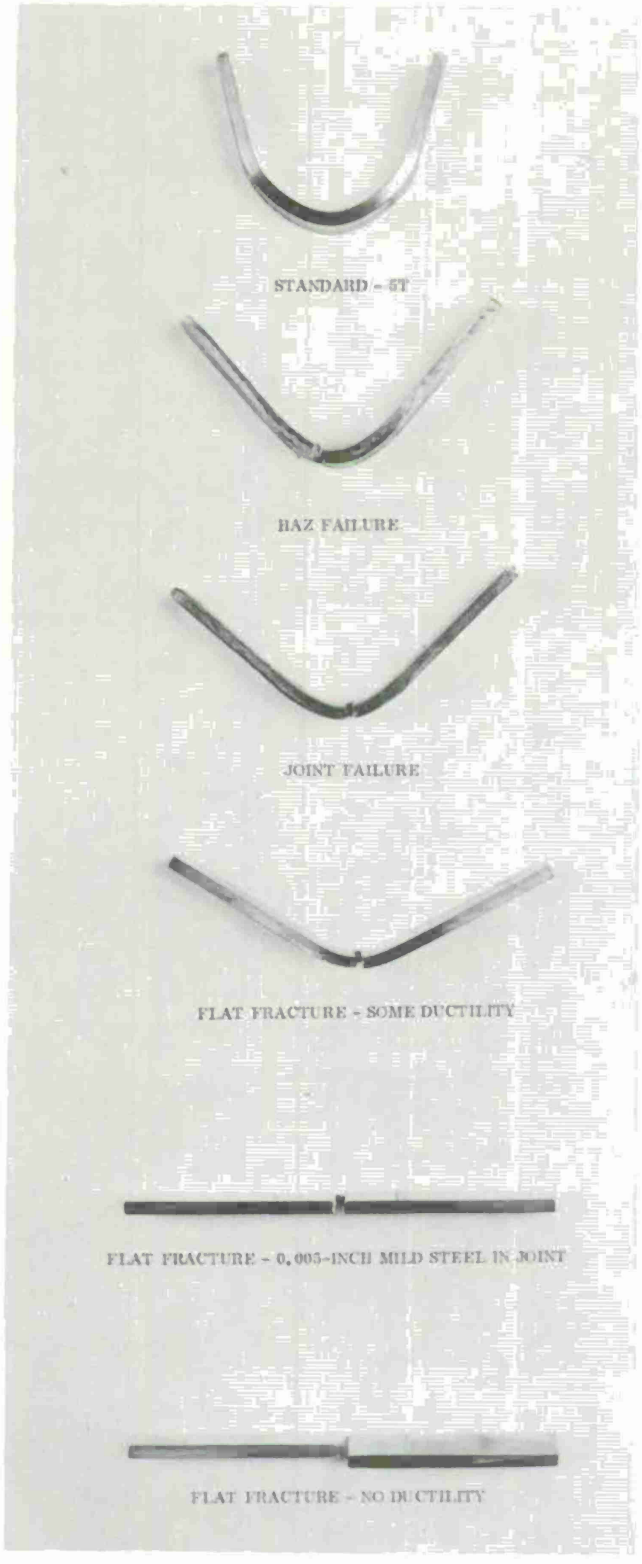

Figure 15. Examples of bend test results.

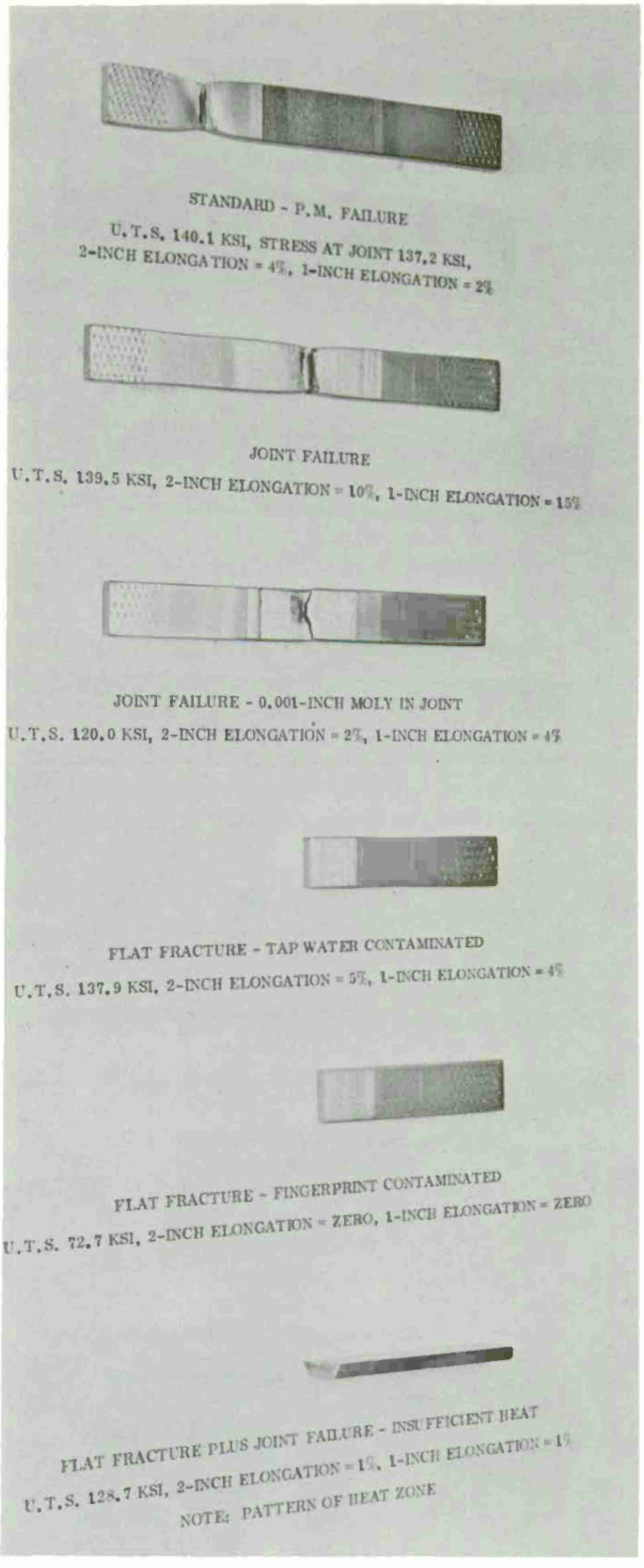

Figure 16. Examples of tensile test results.

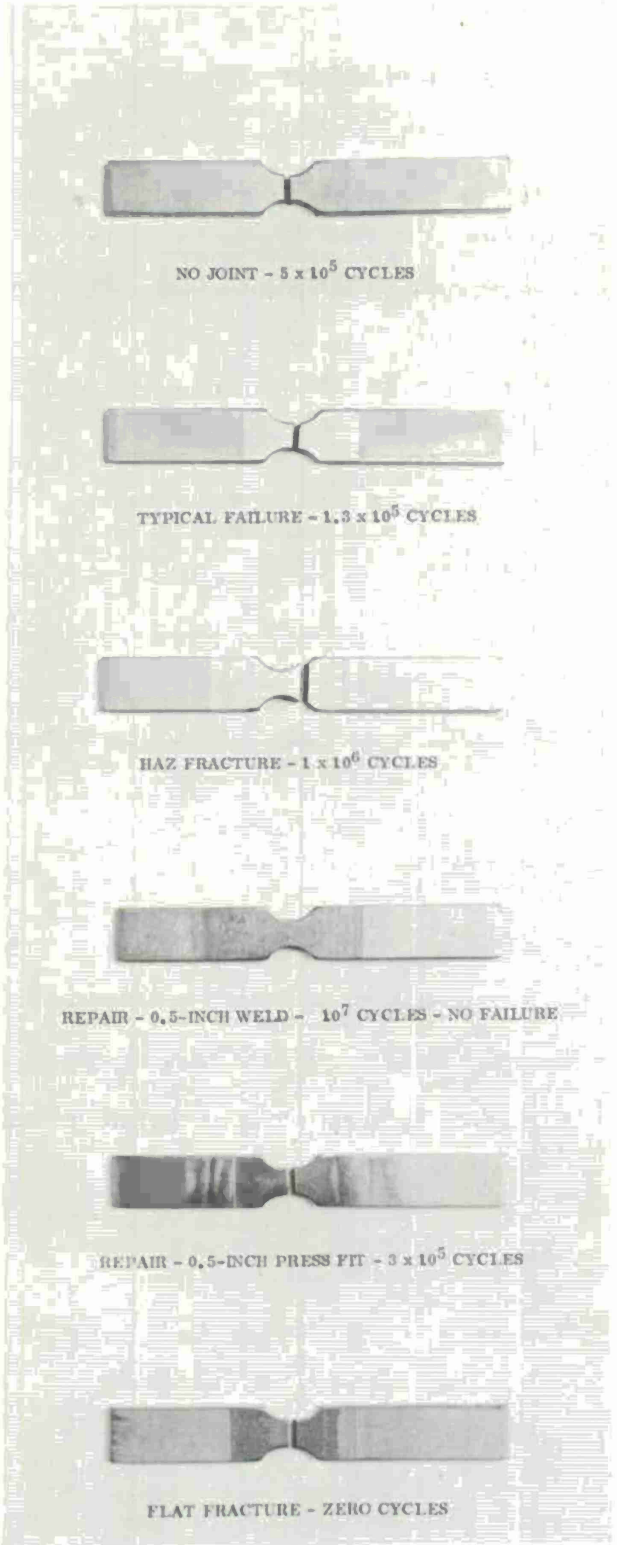

Figure 17. Examples of fatigue test results.

Bend Tests (Figure 15)

5T	Withstood 5T bend test without failure
HAZ	Failure occurred in heat affected zone
JZ	Parent metal type failure at joint region, i.e., grain pull out on both sides of joint plus ductility
FE	Failure initiated on edge of reinforcement foil (not shown in Figure 15)
FF	Failure at original bond line with no grain pull out (flat fracture) and limited ductility

Tensile Tests (Figure 16)

No Joint	Standard specimen/CSDB processed, 4 inch strip (see Section 2.2.3)
PM	Failure occurred in parent metal away from heat affected zone and joint area
JZ	Parent metal type failure occurring in the joint area
FF	Failure at original bond line with no grain pull out (flat fracture)

Resonant Fatigue Tests (Figure 17)

No Joint	Standard specimen/CSDB processed, 4 inch strip (see Section 2.2.3)
JZ	Parent metal type failure at joint
HAZ	Failure occurred in heat affected zone
FF	Failure at original bond line with no grain pull out

3

PARAMETRIC STUDY

The purpose of this phase of the program was to establish the degree of control necessary to achieve high quality diffusion bonded joints. Bonding parameters were varied as well as joint variables including fit-up, material preparation and contaminants.

Standard parameters for bonding were selected during the work on indirect variables based on prior experience plus the current work. These standards were used throughout the remainder of the program with the intent to adjust to new standard values, if warranted, at the completion of the direct variable portions of the parametric study. However, no change was necessary.

3.1 INDIRECT VARIABLES

The indirect variables with maximum effect on joint quality are wheel contour, wheel width, tool temperature, and atmosphere. These variables had been either set arbitrarily, although based on prior experience, or left uncontrolled in prior work on 10-foot spars. For example, tool temperature had not been controlled in the spar manufacture but it had been observed that the tooling became hotter as the end of the spar was approached, and, in turn, this had required a manual reduction in power setting to avoid surface pitting due to overheating.

Bonding Wheel

The configuration of the bonding wheel was investigated for its effect as an indirect variable on the diffusion bonding process. Basic considerations were wheel diameter, thickness and circumferential face configuration.

Four wheel parameters were used and are listed in the sequence tested:

Diameter	Thickness	Face Contour
9 inches	0.7 inch	12 inch radius face
11.5 inches	1.1 inch	Flat
8 inches	0.9 inch	Flat
9 inches	0.7 inch	Flat

Results of different wheel usage was judged on bond quality (5T bend tests), heat affected zone in the part, effect on thermal strips and part contour.

The first wheel has evolved as the standard for CSDB of joints other than butt joining and relatively good butt bonding results were obtained with this wheel. The major objection was that the 12-inch radius face forged the thermal strip to the same radius and transferred the radius to the heat-affected zone of the panel which decreased the panel thickness at the centerline. The radius face also allowed intermittent creeping of the foils under the thermal strip and a slightly varying width of heat-affected zone in the panel.

These problems led to the testing of the second wheel, 11.5-inch diameter by 1.1-inch wide. The aforementioned problems were eliminated but the wider wheel created an extremely wide heat zone at the panel top which decreased sharply through the thickness. Also, the mass of the wheel removed so much of the generated heat that the panel never attained uniform bonding temperatures. Only one panel was attempted with this wheel.

The third wheel, 8 inches in diameter by 0.9-inch in width, created only one major problem. An excessively wide heat-affected zone resulted from this wheel, however, a relatively good quality bond resulted.

Conclusions reached from the second and third wheel results indicated the wider wheels were not acceptable. There was a good indication that the flat face condition was an improvement over the original 12-inch radius face wheel. As a consequence, the fourth wheel configuration was created. This wheel was the same as the first, except the face was machined to a flat condition. The bonding parameters selected as standard for this wheel were: 11,200 amps current; 2200 lbs wheel force; and a speed of 3.75 inches per minute.

After an initial test panel, with no problems as a result of the wheel, all the remaining test panels were fabricated with the fourth wheel configuration.

Tool Temperature

Tool temperature control can be accomplished by two basic methods, variable amperage input control or tool temperature control with internal/external cooling.

Initial use of the water cooling tubes on this project bonding aid resulted in excessive cooling. Further use of these cooling tubes was abandoned and the tool temperature was maintained by the water cooled table upon which the tool was mounted.

Actual tool temperatures were taken during panel fabrication through the use of three thermocouples mounted on the bottom side of the back-up bar. A multi-point recorder

was used to record this information. The temperatures recorded were 1.165 inch below the bonded joint. The thermocouple was separated from the joint by the 0.006-inch titanium foil, 0.002-inch molybdenum foil, 0.032-inch Hastelloy X thermal barrier, 0.125-inch thermal strip and the 1-inch thick back-up bars. The temperatures were measured during the fabrication of the panels in the parametric study. Since the parameters ranged so far on each side of the standard, no specific temperature was established as optimum. There was, however, a significant range established. Bonding occurred when the back-up bar peak temperatures were as low as 500° F at the start position and as high as 700° F at the finish without detrimental effects on the part or thermal strip during a standard parameter run. Temperatures as high as 920° F were recorded. The highest acceptable temperature was in the 880° F range because higher temperatures than this usually resulted in melting the thermal strip under the bonding wheel. Poor joint quality due to lack of heat resulted when temperatures were below 500° F

Atmosphere

CSDB work on titanium alloys is normally performed in air. Evidence suggested that an inert gas, such as argon, would be trapped in the joint and when trapped would stabilize porosity to a greater extent than air. It was also considered that bonding in vacuum could reduce the porosity due to trapped gas in the joint.

Panels were fabricated using standard bonding conditions of current, wheel force and speed in atmospheres of argon and under 500 and 1000 microns of mercury air atmosphere. The mechanical test results for these panels plus a panel fabricated in air are shown in Table 1. Table 1 also includes test results for CSDB processed - no joint material (refer to Section 2.2.6 for nomenclature.) As can be seen, no failures occurred in 5T bend tests. There is some difference in yield strength between the 4 panels shown. The CSDB-processed material and the vacuum bonded panel have lower yield strengths and greater elongation than the panels bonded in air and argon. However, there is no appreciable difference in ultimate tensile strength between the 4 panels and the panel bonded in air is marginally better. The resonant fatigue results of the three bonded panels are within the range of values exhibited by CSDB processed material. The mechanical test results indicate there is no advantage to bonding in vacuum.

Photomicrographs of the joint area for the three bonding atmospheres are shown in Figure 18. The bond line is indicated. As mentioned previously, severe overetching of the microstructure is required to reveal the bond line. In all three examples, the heaviest bond line etching is shown. The bond line indications in the argon panel are generally larger and more numerous than the vacuum and air panels. This observation is consistent with the hypothesis that insoluble gas trapped in the

TABLE 1. EFFECT OF BONDING ATMOSPHERE ON JOINT QUALITY

	Bonded Panels					CSDB Processed No Joint
Atmosphere	Air	Argon	500 micron vacuum	1000 micron vacuum		Air
Bonding parameters (current, speed, force)	Std	Std	Std	Std		Std
5T Bend Tests						
Top up	5T	5T	5T	5T		-
Top down	5T	5T	5T	5T		-
Tensile Tests				#1	#2	
0.2% yield (ksi)	129.8	126.1	-	111.9	115.8	122.6[a]
Ultimate Tensile Strength (ksi)	140.1	137.0	-	137.0	138.4	137.9[a]
Maximum Stress at Joint (ksi)	137.2	135.4	-	135.0	133.1	138.5[a]
2-inch Elongation (%)	4.0	5.0	-	12.2	12.4	12.5[a]
1-inch Elongation (%)	2.0	2.0	-	7.1	3.5	13.3[a]
Location of Failure	PM	PM	-	PM	PM	HAZ[a]
Resonant Fatigue Tests						
Cycles to Failure at 0.100 in. Defl.	2×10^5	4×10^4	-	2.4×10^5		1×10^4 to[b] 5×10^6
Location of Failure	JZ-HAZ	JZ	-	JZ		HAZ

[a] Average of 3 specimens

[b] Five specimens used

Figure 18. Effect of bonding atmosphere on joint.
Magnification: 200X
Etchant: 2 min Kroll's
+
4 sec CSDB.

joint is responsible for the bond line indications which become visible with etching. Argon trapped in the joint cannot diffuse away as rapidly as oxygen and nitrogen. No significant difference in joint appearance was observed between the panels bonded in vacuum and air.

It is concluded from the above results that no advantage in joint quality is gained by bonding in vacuum, but that bonding in inert gas may be detrimental.

Conclusions

- A flat, 12-inch diameter, 0.7 inch thick wheel was judged best for this particular CSDB application, and used for bonding all of the panels discussed in subsequent sections.
- Tool temperatures above 500° but below 880° F were found to result in good joint quality for the specific tool design. The standard bonding parameters result in tool temperatures between 500 and 700° F. The temperature range for adequate bonding will have to be established on different tools on an individual basis.
- No improvement in joint quality resulted from bonding in vacuum or argon rather than air. Consequently, air atmosphere was used for bonding all of the panels discussed in following sections.

3.2 DIRECT VARIABLES

The direct variables are the actual machine settings for diffusion bonding, i.e., bonding current, wheel force and speed. These settings are dependent on the previously discussed indirect variables. For example, the wheel diameter, face contour and width influence current and force requirements because the "footprint" of the wheel will determine current density and pressure. In turn, the current density is one of the important factors controlling the temperature attained and the pressure is an important factor in determining if adequate forging is achieved. Consideration of such facts led to performing this "direct variable" portion of the program after the indirect variables (wheel configuration and atmosphere) were fixed. Standard conditions of current (I), force (F) and speed (S) were developed in the indirect variable investigation. For this phase of the investigation, values were chosen on either side of these standard parameters to develop a three-dimensional matrix of joint quality. The objective was to determine the sensitivity of joint quality to each of the three principal direct variables and if necessary, to select a new optimum value of each bonding parameter safely removed from values where joint quality begins to decrease. Joint quality was determined by 5T bend tests, tensile and resonant fatigue tests and metallographic examination.

An initial combination of low, standard and high values of the 3 bonding parameters was selected. Current was varied 3%, speed was varied 15% and force was varied +9% -8% from the standard values. In addition, selected combinations of extreme values were made to extend the three-dimensional matrix. Table 2 shows the results of mechanical property determinations for the range of direct variables selected (refer to Section 2.2.6 for nomenclature).

A series of 2-dimensional plots were made which show the mechanical property results as a function of two of the bonding parameters. Shading was used to indicate regions of equal joint quality based on bend test results.

Bend Test Results

Figure 19 shows the bend test results for direct variables. The upper entry for each combination of parameters is bend result with "Top up" and the lower entry is for "Top down." Figure 19a gives current versus wheel speed at the standard wheel force of 2200 lb. The standard current and speed parameter is also noted. The upper left portion of Figure 19a indicates the region beyond which surface melting (pitting) is expected. The different shaded regions correspond to variations in joint quality as assessed by the bend tests. The lightest shading (upper left) corresponds to the region of too much heat as evidenced by a heat affected zone failure. The next region corresponds to acceptable joint quality as evidenced by no bend failures. The third region corresponds to marginal joint quality and is evidenced by 50% flat fractures. The final region corresponds to 100% flat fracture due to inadequate heating. Marginal joint quality based on 5T bend tests occurs for both high-heat and low- heat bonding parameters. The cause of the low-heat failures is obvious in that insufficient heat is available to form a good butt joint. However, the cause for flat fracture in an overheat situation is not apparent. Increased oxidation due to the higher bonding temperature was suspected but no evidence of oxidation or alpha case was observed metallographically. The effect of oxidation on joint quality will be discussed further in Section 3.4 on Preparation and Contamination Variables. Figure 15 gives examples of each type of bend test failure. As can be seen, a quite large variation in current and speed at the standard bonding force can be tolerated with good joint quality (100% 5T bends).

Figure 19b shows bend test results for current and speed at the constant high wheel force. The higher wheel force produces less heat in the part for a given current and speed by decreasing the resistance at the wheel interface. Thus, the surface melting boundary is moved upward as shown. Again, the 4 regions of joint quality are given and the envelope for good joint quality is quite large.

						CSDB Processed No Joint
Bonding Parameters						
11,200A I (Std)	Std	,870	10,870	10,870	10,870	11,530
3.75 in./min S (Std)	3.19	td	4.31	3.19	Std	4.31
2200 lbs F (Std)	Std	025	2025	2400	2400	2400
5T Bend Tests						
Top up	5T	5T	5T	5T	5T	5T
Top down	HAZ	5T	5T	5T	5T	5T
Tensile Tests						
0.2% Yield (ksi)	132.8	15.8	132.8	127.5	131.6	134.0
Ultimate Tensile Strength (ksi)	138.4	14.1	141.5	139.7	140.7	140.2
Maximum Strength at Joint (ksi)	134.4	13.7	135.5	139.7	138.9	136.7
2-inch Elongation (%)	4.0	2.5	5.0	11.5	5.5	6.5
1-inch Elongation (%)	1.5	1.5	1.5	8.0	1.5	2.0
Location of Failure	PM	PM	PM	JZ	PM	PM
Resonant Fatigue Tests						
Cycles to Failure at 0.100 in. Defl.	1.3×10^5	2×10^5	1.3×10^5	1×10^6	3.2×10^5	2.6×10^5
Location of Failure	JZ	JZ	JZ	HAZ	JZ	JZ

						CSDB Processed No Joint
Bonding Parameters						
11,200A I(Std)	11,530	11,530	10,200	10,200	10,200	Std
3.75 in./min S (Std)	Std	4.31 43	2.63	3.19	Std	Std
2200 lbs F (Std)	2025	2025 1	Std	Std	Std	Std
5T Bend Tests						
Top up	FF	FF F	5T	FF	FF	-
Top down	5T	5T F	5T	5T	5T	-
Tensile Tests						
0.2% Yield (ksi)	132.9	131.4 .2	130.5	127.8	122.3	122.6[a]
Ultimate Tensile Strength (ksi)	142.4	137.4 .4	137.5	128.5	122.5	137.9[a]
Maximum Strength at Joint (ksi)	142.4	137.4 .0	132.9	128.5	122.5	138.5[a]
2-inch Elongation (%)	3.0	2.5 .0	5.5	1.5	1.5	12.5[a]
1-inch Elongation (%)	3.5	1.5 .5	0	1.0	1.0	13.3[a]
Location of Failure	PM	95% F M	PM	20% FF	50% FF	HAZ[a]
Resonant Fatigue Tests						
Cycles to Failure at 0.100 in. Defl	2.6×10^5	3.9×10^4	1.4×10^5	0	0	1×10^4 to[b] 5×10^6
Location of Failure	HAZ	JZ Z	JZ	JZ	FF	HAZ[b]

[a] Average of 3 specimens
[b] Five specimens tested

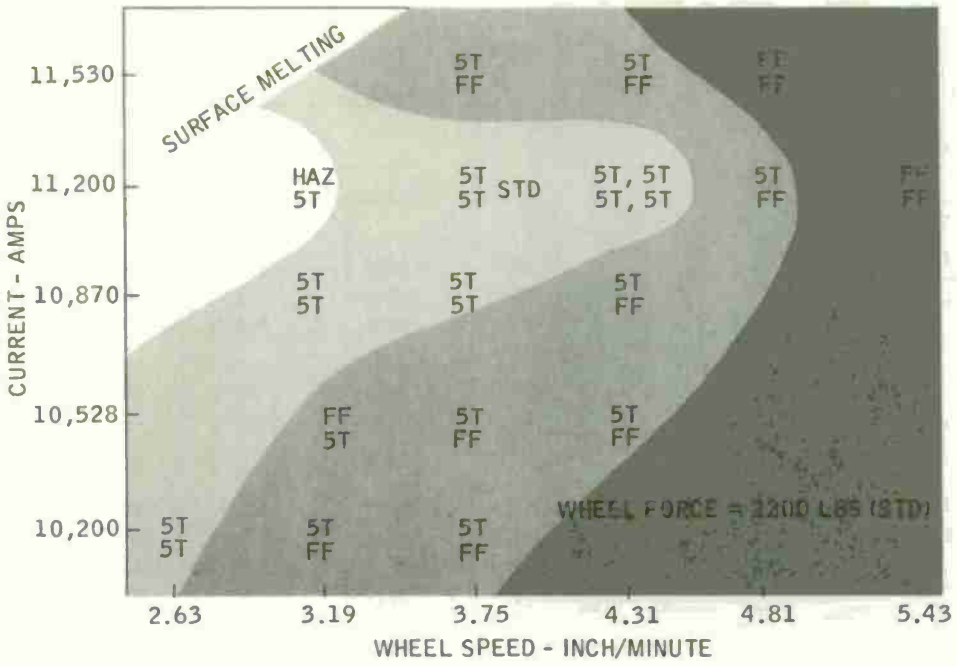

Figure 19a. Bend test results for various bonding parameters.

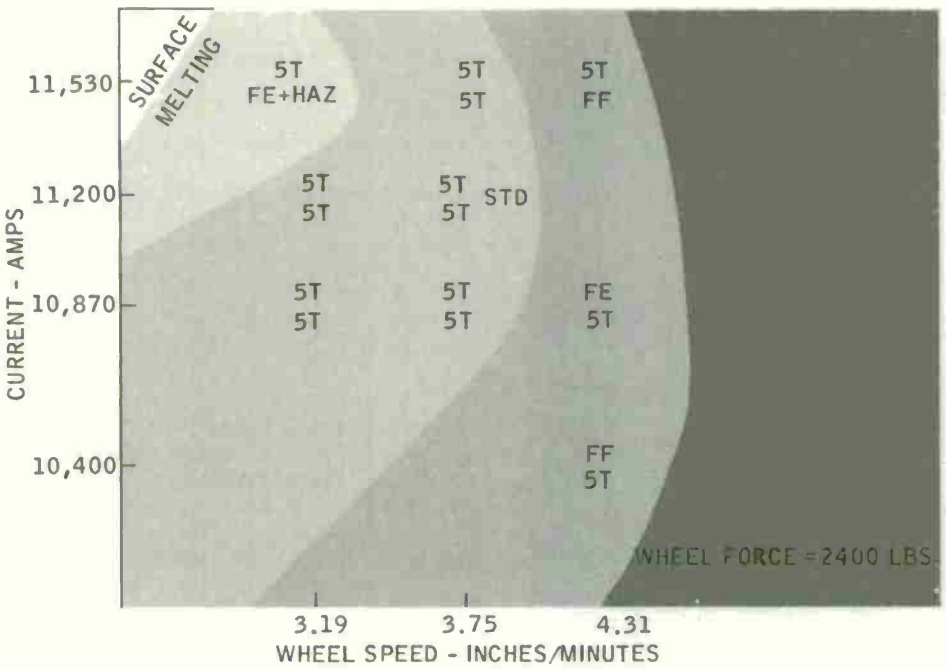

Figure 19b. Bend test results for various bonding parameters.

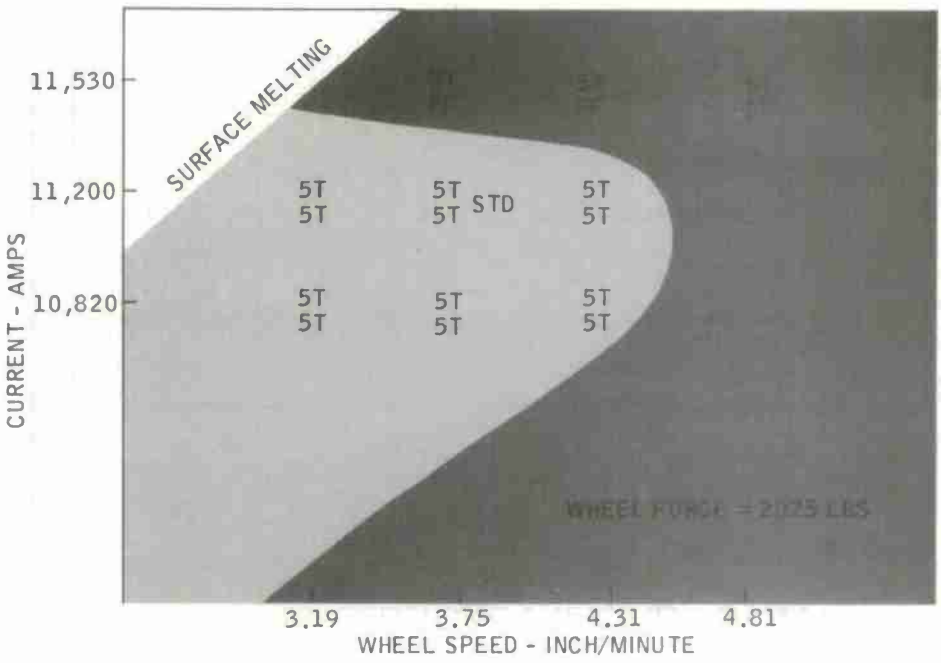

Figure 19c. Bend test results for various bonding parameters.

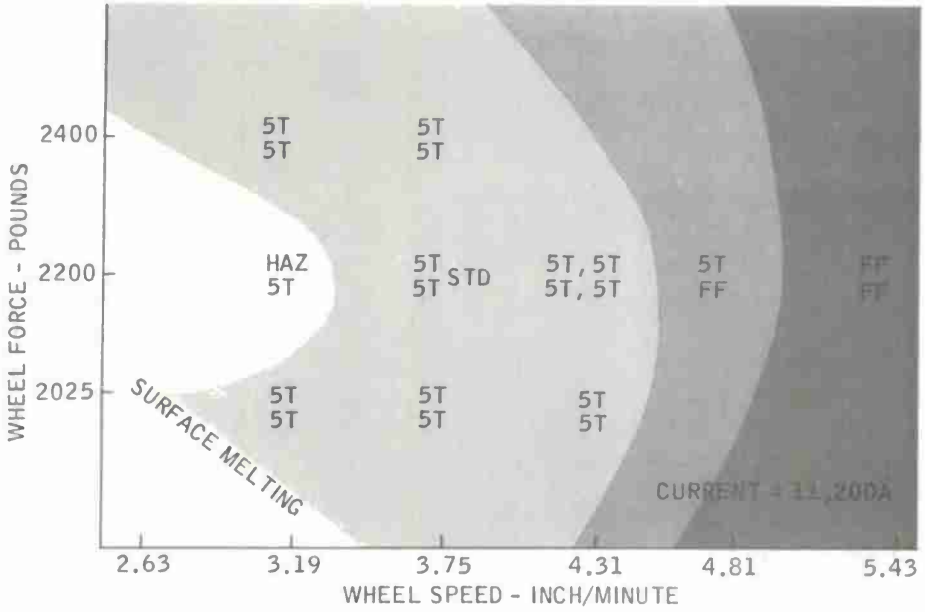

Figure 19d. Bend test results for various bonding parameters.

Figure 19c gives the bend test results for bonding at low wheel force. A low wheel force provides more resistance and thus more heat to the part than the standard conditions and moves the surface melting boundary down. Again, good joint quality occurs over a wide range of current and speed.

The bend test results for standard current and various wheel force and speed are shown in Figure 19d. In this case, the surface melting boundary occurs under low-pressure low-speed combinations. For the standard current, a large variation in wheel speed and pressure is possible for good joint quality.

A summary of the bonding parameter limits for good joint quality (100% bend test survivors) is shown in Figure 20. It is concluded that good joint quality is possible over a fairly wide range of bonding parameters.

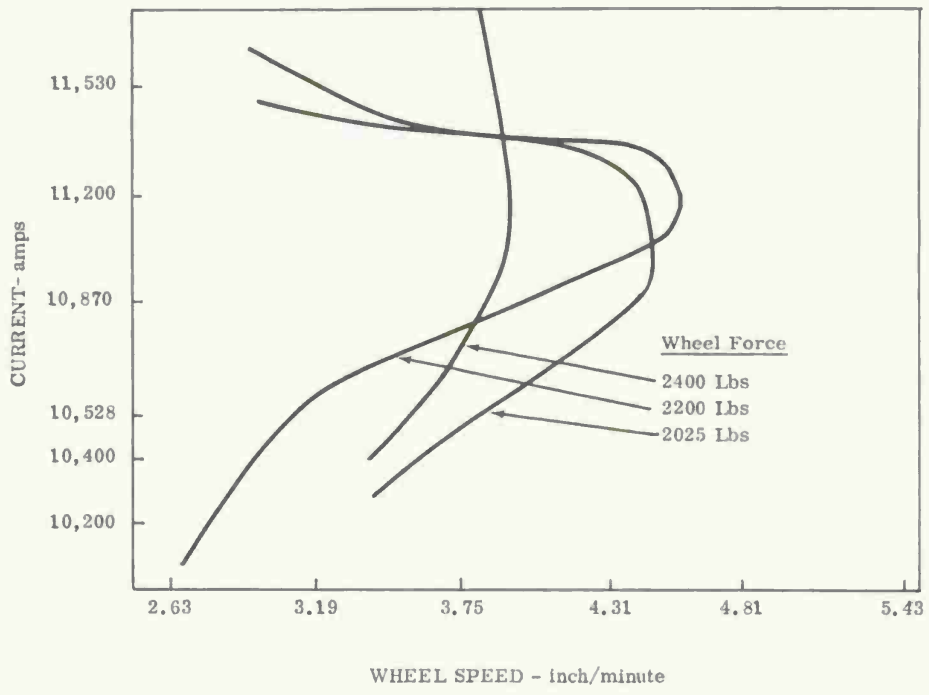

Figure 20. Bonding parameter limits based on one hundred percent 5T bend tests.

Tensile Test Results

A series of plots analagous to the bend test results are given for tensile tests in Figure 21(a-d). The tensile tests are not as critical a test of joint quality as the bend tests, and consequently the shaded regions are those from the bend test results for equivalent parameters. Since most of the tensile test failures occurred in the parent metal, (refer to Figure 16 and Table 1 for examples) the values given in Figure 21 are stress on the joint at failure. Table 1 gives the other details of the

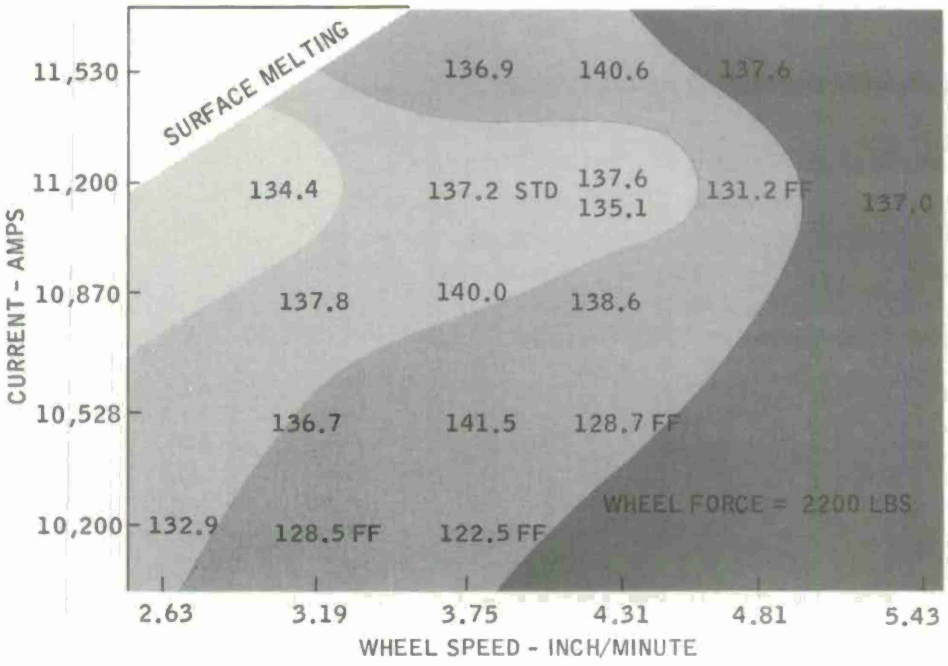

Figure 21a. Tensile test results for various bonding parameters. Values are stress on joint at failure, ksi.

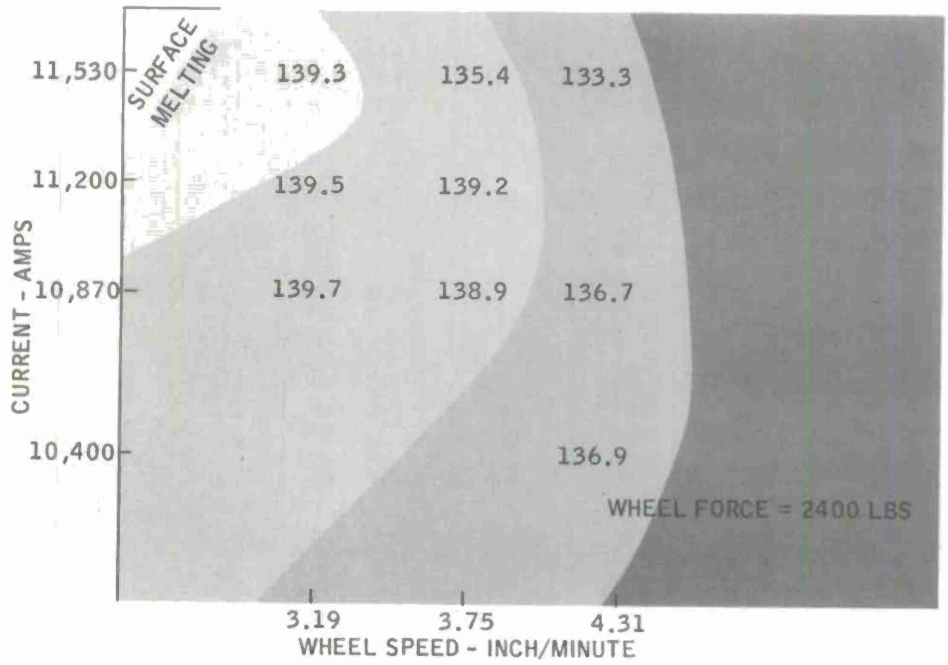

Figure 21b. Tensile test results for various bonding parameters. Values are stress on joint at failure, ksi.

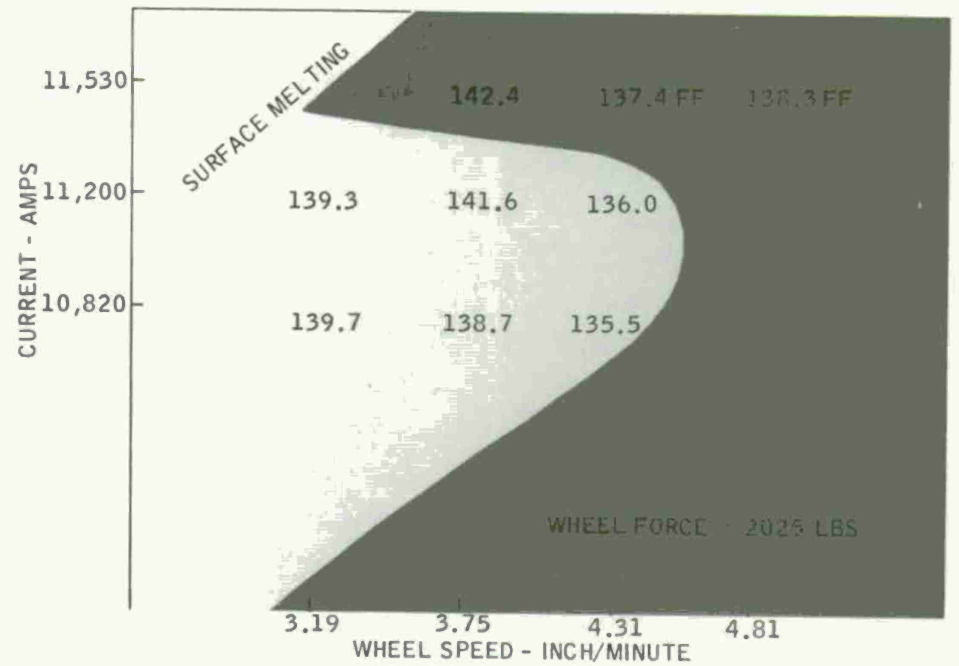

Figure 21c. Tensile test results for various bonding parameters. Values are stress on joint at failure, ksi.

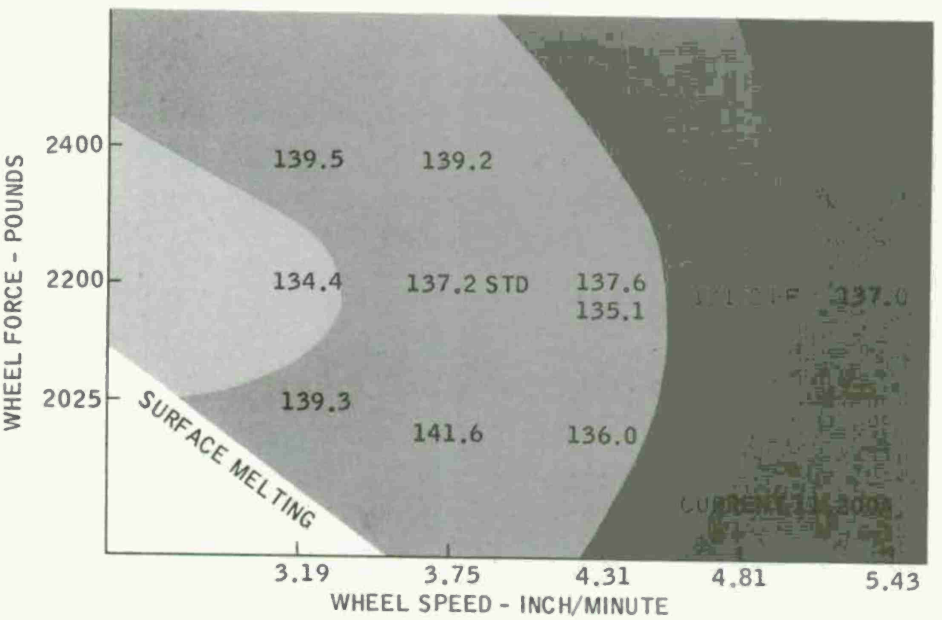

Figure 21d. Tensile test results for various bonding parameters. Values are stress on joint at failure, ksi.

tensile tests. The main observation from these results is that joints defined as marginal from bend tests do not show appreciable loss in tensile strength. Even specimens which exhibited flat fracture had ultimate tensile strengths greater than 120 ksi. Also, the flat fracture specimens did exhibit elongation on the order of 1% prior to failure.

There is a general correlation between bend test results and tensile behavior based on type of failure rather than absolute values, and the conclusion was reached that tensile tests are not as severe a test of joint quality as the bend test.

Resonant Fatigue Results

A series of plots analogous to the bend test results are given for the resonant fatigue test results in Figure 22 (a-d).. The values shown are the number of 10^4 cycles to failure for 0.100 inch deflection. The shaded areas correspond to those from the bend test results. The CSDB processed material which does not contain a joint was used as a standard for these tests. Five tests of this material gave results of 1.5, 8, 20, 50 and >500 x 10^4 cycles. All of the bonded panels, except three, failed within the span of the results for the CSDB processed material with no joint. There is a general correlation of cycles to failure with bend and tensile test results. The same panels which exhibited flat fracture in tension either exhibited flat fracture or failed on loading in resonant fatigue.

Metallography

Specimens from the entire matrix of bonding parameters were examined metallographically. All specimens were etched identically using the heavy etch discussed previously. Examples of the joint zone for various bonding parameters are shown in Figures 23-25. The three figures show respectively, good, marginal and inadequate quality joints based on mechanical tests. The mechanical properties, as well as bonding parameters, are given with each photomicrograph. A cursory comparison of the figures indicates that there is little apparent correlation between mechanical strength of the joints and severity of etching at the bond line. Grain growth across the bond line has occurred in all cases. Also, in all cases the region of heaviest etching along the bond line is shown, except for Figure 23a this corresponds to the bottom surface of the panel. Another visual evaluation of joint quality could be made from examination of the heat affected zone through the thickness of the panel. A direct correlation was found between shape of the heat affected zone and joint quality. This correlation is shown schematically in Figure 26. For good joint quality, the heat affected zone was approximately 1 inch wide throughout the thickness of the panel and symmetrical about the bond line. In the region of marginal joint quality, due to lack of heat, the heat affected zone was smaller on the bottom surface. This is consistent with the bonding parameter variation in that marginal bonding occurred as effective heat input was reduced. An example of the

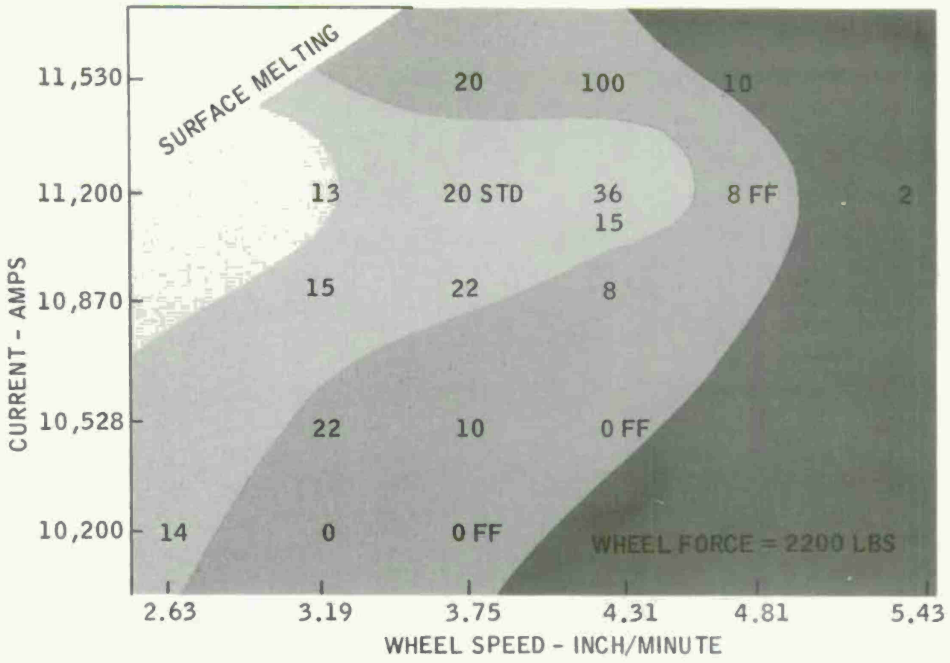

Figure 22a. Resonant fatigue results for various bonding parameters - cycles x 10^4 to failure for 0.100 in. deflection.

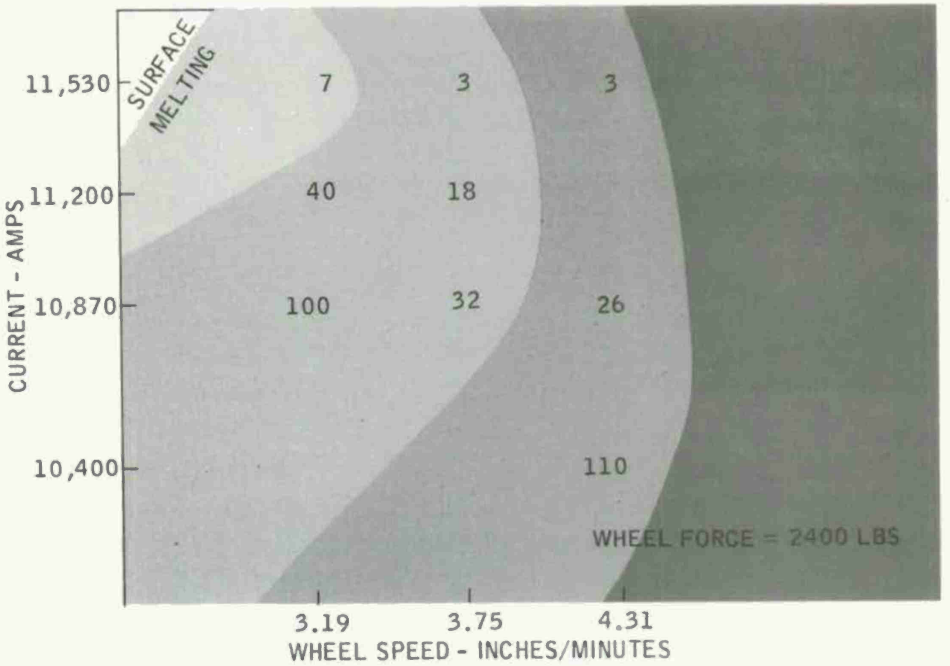

Figure 22b. Resonant fatigue results for various bonding parameters - cycles x 10^4 to failure for 0.100 in. deflection

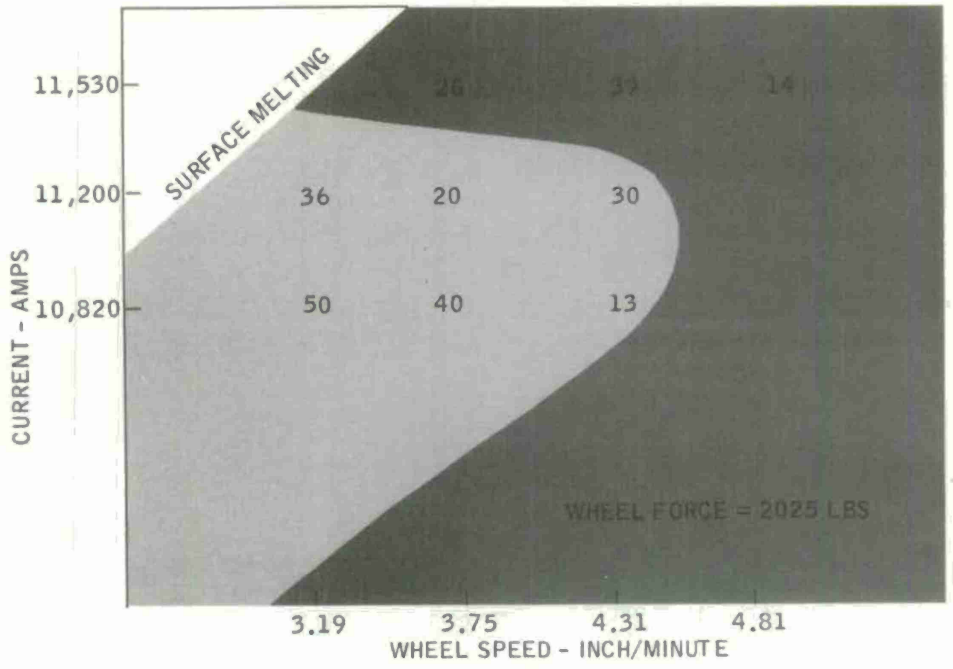

Figure 22c. Resonant fatigue results for various bonding parameters - cycles x 10^4 to failure for 0.100 in. deflection.

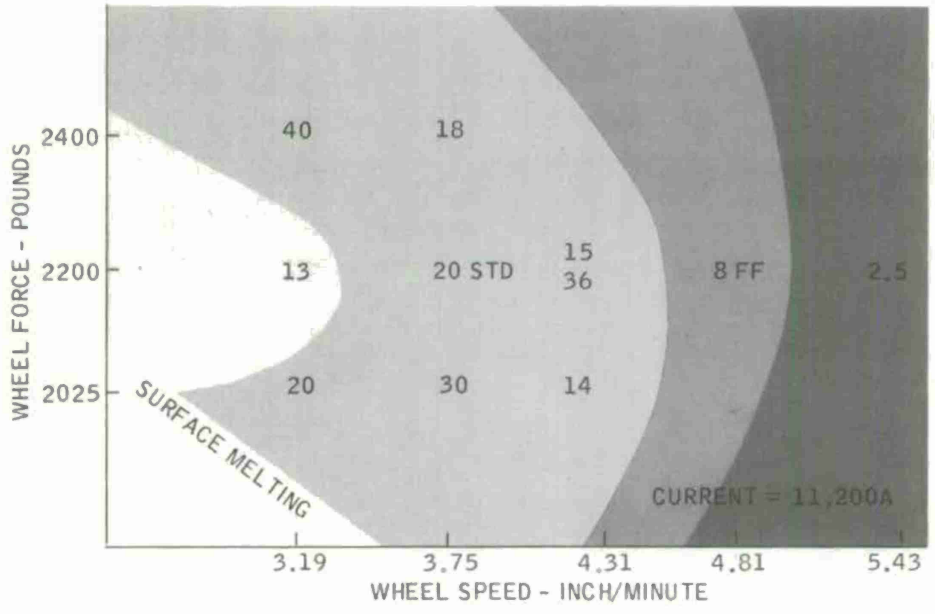

Figure 22d. Resonant fatigue results for various bonding parameters - cycles x 10^4 to failure for 0.100 in. deflection.

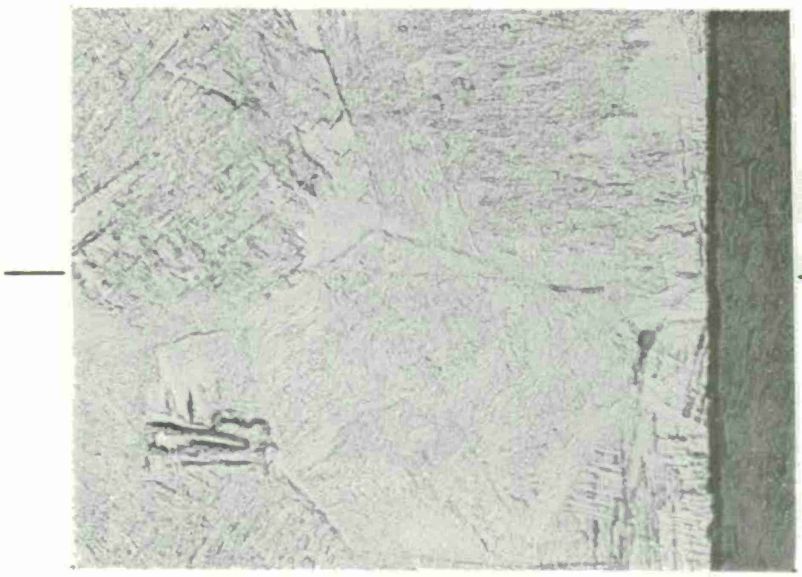

I = 11,200 amps (std)
S = 4.31 in./min
F = 2200 lbs (std)

5T, 5T bend
137 ksi UTS
4×10^5 cycles fatigue

Bond Line

a

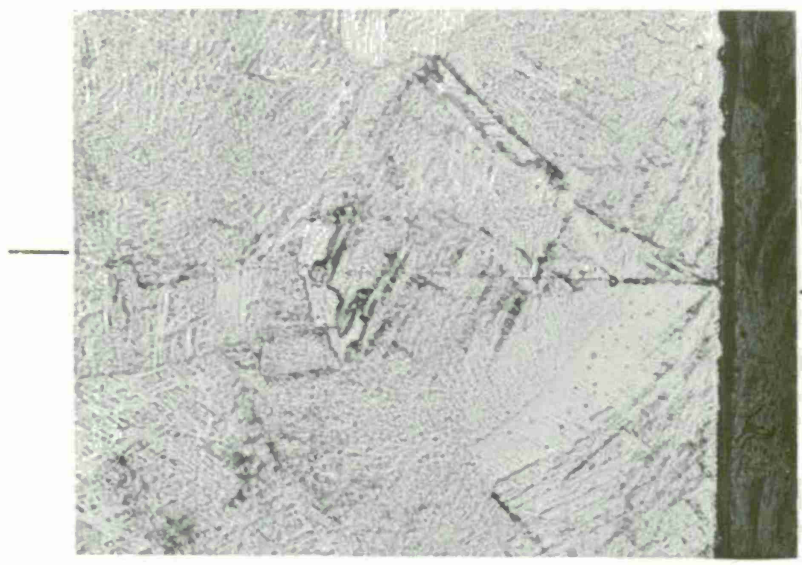

I = 11,200 amps (std)
S = 3.75 in./min (std)
F = 2025 lbs

5T, 5T bend
142 ksi UTS
3×10^5 cycles fatigue

Bond Line

b

Figure 23. Microstructure in joint region showing typical examples of good joint quality based on mechanical tests.
Etchant: 2 min Kroll's + 4 sec CSDB.
Magnification: 200X.

I = 11,530 amps
S = 4.31 in./min
F = 2200 lbs (std)

5T, FF bend
141 ksi UTS
1 x 10^6 cycles fatigue

Bond Line

a

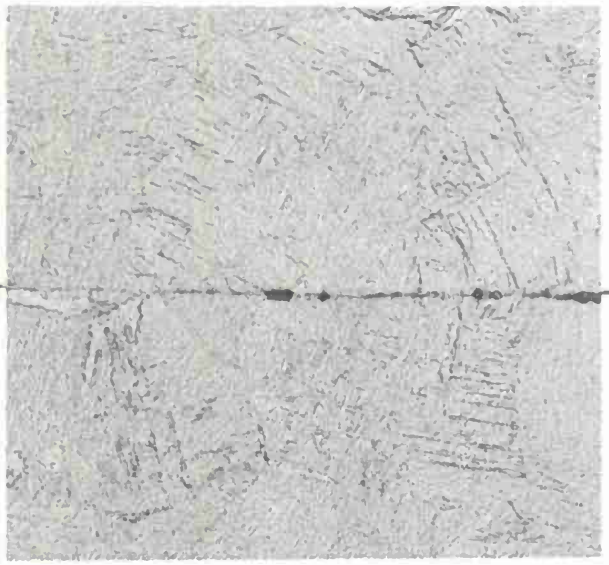

I = 11,530 amps
S = 4.81 in./min
F = 2025 lbs

5T, FF bend
138 ksi UTS-FF
1 x 10^5 cycles fatigue

Bond Line

b

Figure 24. Microstructure in joint region showing typical examples of marginal joint quality based on mechanical tests.
Etchant: 2 min Kroll's + 4 sec CSDB.
Magnification: 200X.

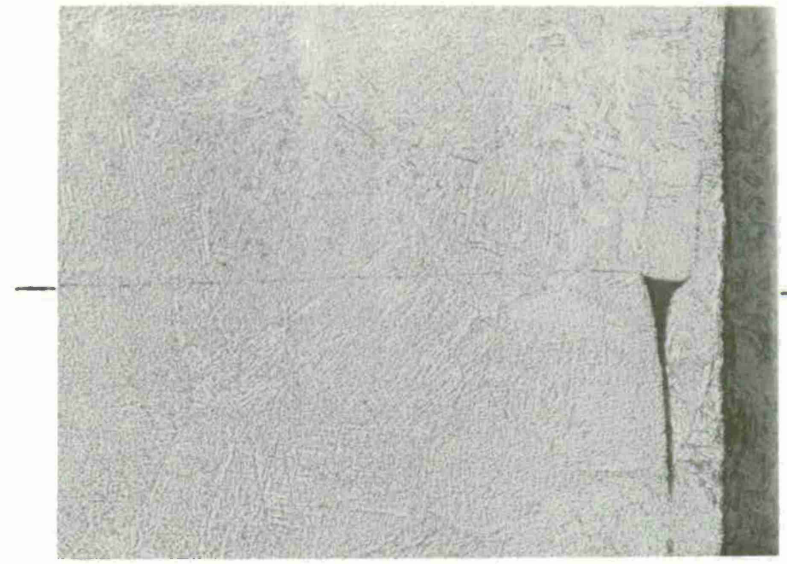

I = 11,200 amps (std)
S = 4.81 in./min
F = 2200 lbs (std)

5T, FF bend
131 ksi UTS-FF
8 x 10^4 cycles fatigue-F

Bond Line

a

I = 10,528 amps
S = 4.81 in./min
F = 2200 lbs (std)

5T, FF bend
128 ksi UTS-FF
0 cycles fatigue-FF

Bond Line

b

Figure 25. Microstructure in joint region showing typical examples of inadequate joint quality based on mechanical tests.
Etchant: 2 min Kroll's + 4 sec CSDB.
Magnification: 200X

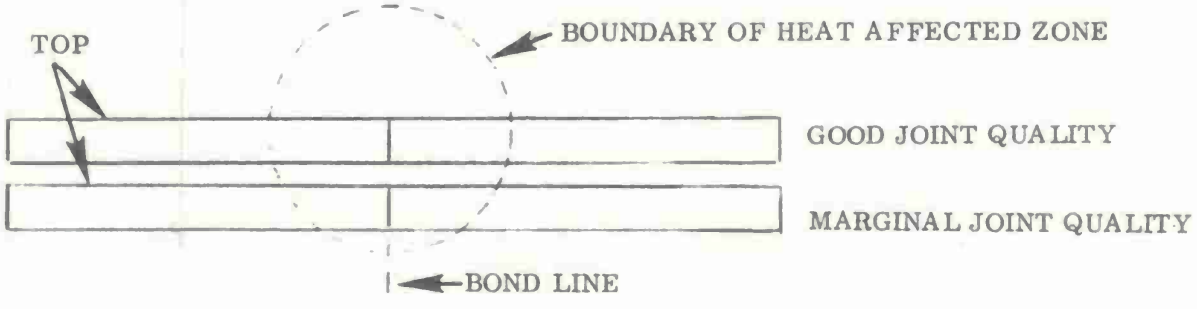

Figure 26. Schematic representation showing correlation of heat affected zone shape and joint quality based on direct bonding parameters.

heat affected zone is shown in Figure 27 for a tensile specimen that exhibited partial flat fracture. A uniform heat affected zone is a necessary, but not sufficient condition for good joint quality as will be discussed in the sections on geometric and contamination variables.

There are several variables which may affect joint strength in addition to specific bond line quality, particularly in the region of marginal joint quality. These variables will also be present in a Spar manufacturing process and for this reason were deliberately not controlled.

Since the as-received Ti-6Al-4V sheet varies in thickness along its length, a height difference in the joint region can occur in the prebond setup. Examples of this type of offset are shown in Figures 23a, 24a and is most marked in Figure 25a. When the bonding parameters are such that a high quality joint is produced the evidence of this offset is almost completely eliminated and strength of the joint is not appreciably affected (Figure 23a). However, as the bonding parameters are moved away from optimum, this offset may act as a stress riser to reduce strength or cause flat fracture in an otherwise high quality joint. This appears to be the case in Figure 25a. The etched bond line, although fairly continuous, does not contain any heavily etched regions or show lack of bonding (lack of grain growth) although flat fracture occurred in all test conditions.

Another potential variable involves amount of foil removal from the top and bottom surface of the panel. The mechanical test specimens were machined to simulate spar conditions, i.e., partial removal of the foil. Since the panels in this investigation are bowed after fabrication, complete foil removal occurred on some of the bottom surfaces.

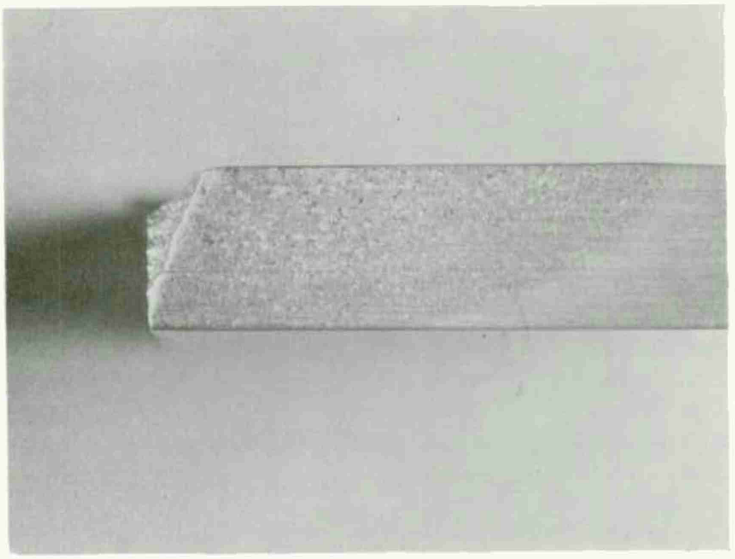

Figure 27. Heat affected zone in tensile coupon which exhibited flat fracture.

The foil in a good quality joint would add strength to the joint region due to increased cross section. However, for bonding conditions where insufficient heat and pressure were available to completely bond the foil to the part, voids such as those shown in Figure 24a could act as stress risers and effectively decrease the strength of the joint. An investigation to determine the effect of the foil on joint strength was not within the scope of this program.

It is clear that the bonding parameter boundaries between good and marginal joint quality are directly influenced by other variables. This will be discussed further in the sections on geometric and contamination variables.

Conclusions

- Good joint quality based on 100% 5T bend test survivors is produced within a large envelope of CSDB processing parameters. Variations of 6% current current, 30% speed and 18% wheel force could be tolerated.

- Marginal joints, based on 50% 5T bend test survivors, did not generally exhibit a reduction in tensile or resonant fatigue strength.

3.3 GEOMETRIC VARIABLES

Geometric variables result from several conditions, all of which cause some type of bond face misalignment. Among the causes for geometric variations are butt joint faces machined at an angle; inability of holding fixture to establish and maintain

position of butted parts; part thickness irregularities; and foreign objects under the bottom of the butted panels. Possible conditions were artifically created, panels were bonded and evaluated to determine the effect on joint quality.

The conditions studied included angularly machined faces that resulted in open joint gaps at the top or bottom of the joint and various offset conditions. Another variable placed in this category results from excessive cleaning. Test panel halves were over-etched to create rounded corners of the butt joint faces.

The top and bottom gaps were made by machining the butted faces at an angle which created gaps 0.005 inch wide.

Offset conditions, when one side of the butted panel half is out of plane with the other, were created by attaching various thickness spacers under one panel half. Four spacers, 0.005, 0.010, 0.020 and 0.040 inch in thickness, were used to establish the offset conditions.

Rounded corners were created by immersion in the hydrofluoric-nitric acid cleaning (etching) solution for various lengths of time. The time intervals used were 4 minutes, 8 minutes, and 16 minutes which resulted in three radius test conditions.

These artificial conditions are more extreme than would be expected in normal spar fabrication, and were selected to provide an assessment of maximum possible joint degradation.

Bonding was performed using standard conditions of 11,200 amp current, 3.75 in./min speed, and 2200 lbs force in an air atmosphere.

Mechanical Test Results

Bend and tensile test results for these panels are shown in Table 3. Refer to Section 2.2.6 for nomenclature. The data are arranged in order of apparent decreasing severity. A 0.005 inch notch at the bottom surface of the panel was the most severe condition. Although flat fracture occurred for both bend and tensile tests, tensile strength was 122 ksi. In all cases, no severe degradation in tensile properties occurred, and half of the conditions withstood 5T bend tests. The results of the mechanical tests indicate that quite severe mismatch of the detail parts can be tolerated without loss in joint quality. As mentioned previously, these conditions are more extreme than would be expected in a manufacturing operation. For example, offset conditions were simulated with various thickness spacers under one side of the panel. The existence of these spacers prevented any realignment which would normally occur during the bonding operation from wheel pressure.

TABLE 3. EFFECT OF GEOMETRIC VARIABLES AT JOINT IN ORDER OF DECREASING SEVERITY

	1	2	3	4	5	6	7	8		CSDB Processed No Joint
Geometry at joint	0.005" (Λ) notch bottom side	0.005" (V) notch top side	Offset with 0.005-0.010" Ti shims	Round corner (8 min. acid clean)	Round corner (4 min. acid clean)	Offset with 0.010-0.020" Ti shims	Offset with 0.020-0.040" Ti shims	Round Corner (18 min. acid clean)	Standard	No joint
Bonding parameters	Std	Std	Std	Std	Std	Std	Std	Std	Std	Std
5T bend test, top down	FF-JZ	FF	FF, FF	JZ	5T	5T, 5T	5T, 5T	5T	5T	5T
Tensile tests										
0.2% offset yield (ksi)	121.6	123.0	130.0	127.5	126.9	131.0	129.1	127.1	129.8	122.6[a]
Ultimate tensile stress (ksi)	121.6	136.9	137.2	141.6	140.0	136.8	135.9	140.0	140.1	137.9[a]
Stress at joint (ksi)	121.6	136.9	127.7	141.6	140.0	129.6	129.1	136.1	137.2	138.5[a]
2-inch elongation (%)	1.5	10.0	10.0	7.5	8.0	5.5	9.7	10.0	4.0	12.5[a]
1-inch elongation (%)	3.0	14.0	1.5	11.0	14.0	1.5	1.5	3.5	2.0	13.3[a]
Location of failure	FF	JZ	PM	JZ	JZ	PM	PM	PM	PM	HAZ[a]

[a] Average of 3 specimens

Metallography

Examples of the joint for the various geometric variables are shown in Figure 28(a-h) in the same order as Table 3. Figure 28a and 28b correspond to the notched panel. The dimension of the original notch is also given. It is interesting to note that the notched top surface was almost completely filled in during bonding while the bottom notch was only partially removed.

From the appearance of the joint in Figure 28c, it is not apparent why flat fractures were found (Table 3) for a joint offset by 0.005-0.010 inch. And, as discussed later, it is uncertain why this condition affected the joint more severely than greater offsets.

Based on appearance of the joint region, the rounded corner condition (Figure 28e and 28h) had little effect on joint quality.

The artificial offset condition resulted in a remarkably good bond, considering the severity of the mismatch. Figure 28g shows examples of the joint condition at the location of the 0.020 inch shim. Height of the offset at 150X is also given for comparison. In addition to the butt joint, the bonded Ti shims located 0.1 inch away from the joint are shown. Considerable forging of the material has occurred, as evidenced by the location of the bond line at the top of the panel.

Conclusions

- Quite severe geometric variations can be tolerated in pre-bond setup without markedly affecting finished joint quality.
- An open 0.005 inch notch at the bottom of the panel was the most severe condition.

3.4 PREPARATION AND CONTAMINATION VARIABLES

The principal variables in this group relate to cleaning method and bond surface contamination. The purpose of this phase of the investigation was to assess the effect of these conditions on joint quality to determine the degree of cleanliness and surface preparation necessary for a manufacturing operation. As with the geometric variables, excessive conditions were generally chosen.

The effect of chemical cleaning and storage was assessed by (1) cleaning in fresh acid, (2) cleaning in used acid (severely reduced etching rate), (3) cleaning in fresh acid +48 hour storage in plastic, (4) cleaning in Solar plant acid tanks (containing Ni, Fe, Si, etc.), and (5) final rinse in tap water.

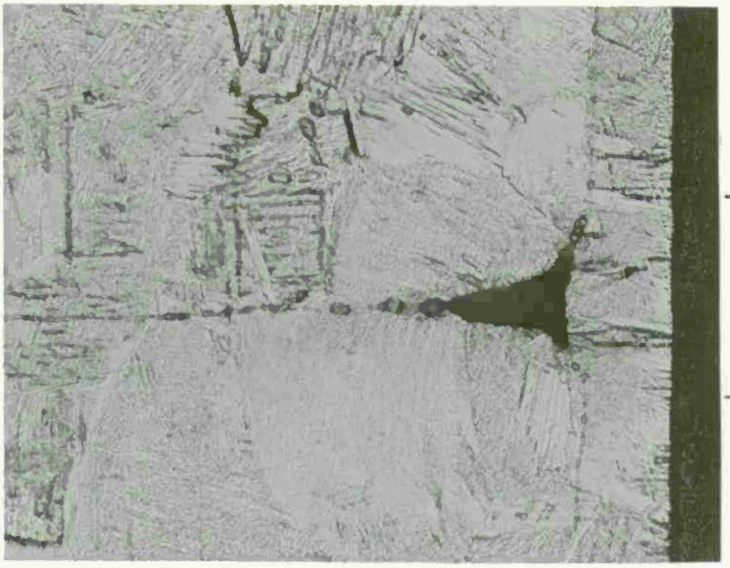

a) 0.005 inch notch (∧) bottom
Magnification: 200X

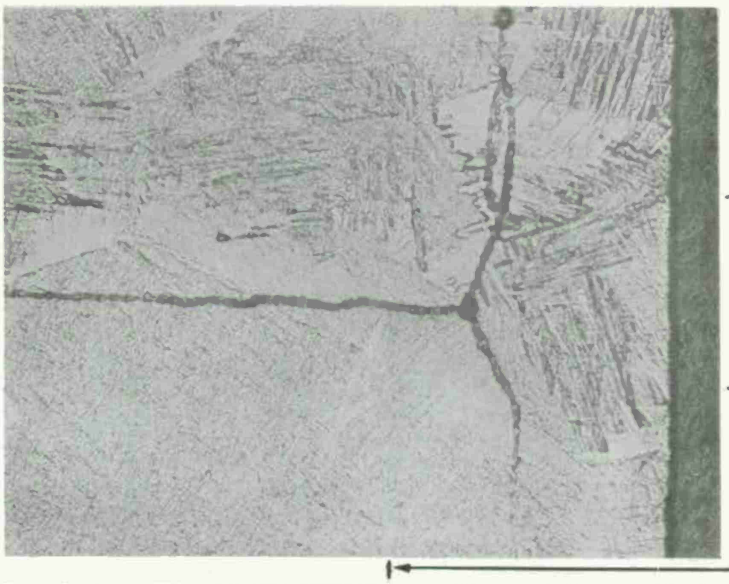

b) 0.005 inch notch (∨) top
Magnification: 200X

c) Offset with 0.005-0.010 inch Ti shims
Magnification: 150X

Figure 28. Effect of geometric variables on joint quality
Etchant: 2 min. Kroll's + 4 sec CSDB.
(Sheet 1 of 4)

Bond Line

d) Round corner (8 min acid clean)
Magnification: 200X

Bond Line

e) Round corner (4 min acid clean)
Magnification: 200X

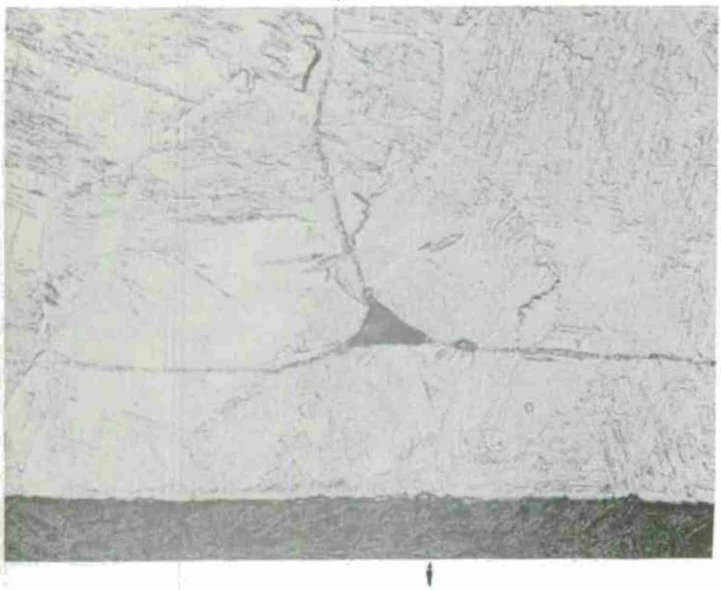

Bond Line

f) Offset with 0.010-0.020 inch Ti shims - bottom
Magnification: 150X

Figure 28. Effect of geometric variables on joint quality
Etchant: 2 min Kroll's + 4 sec CSDB
(Sheet 2 of 4)

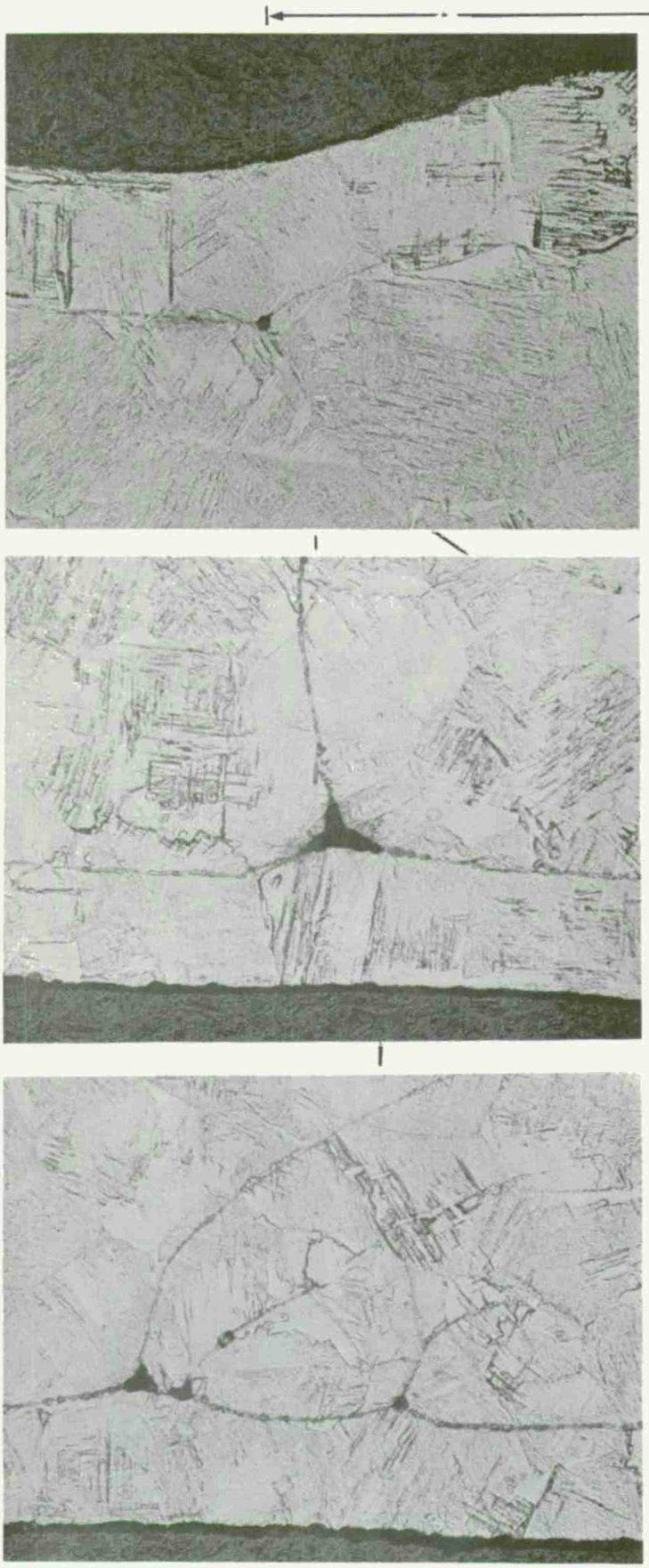

Figure 28. Effect of geometric variables on joint quality
Etchant: 2 min Kroll's + 4 sec CSDB.
(Sheet 3 of 4)

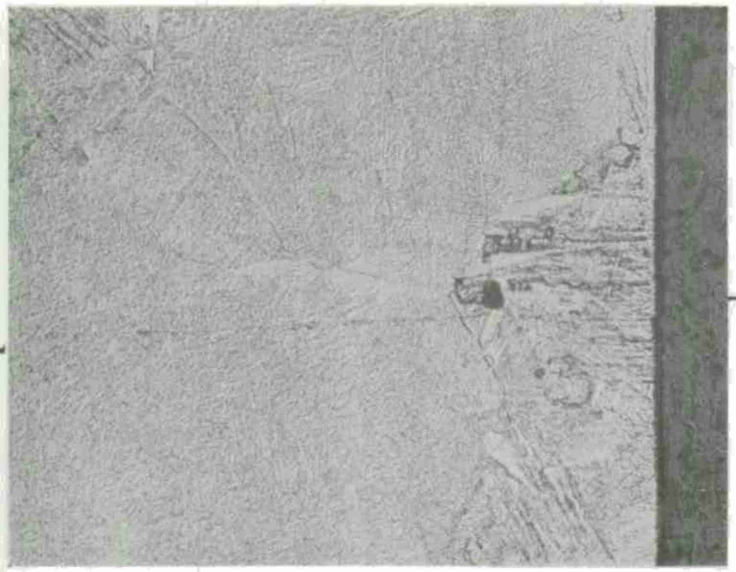

h) Round corner (18 min acid clean)
Magnification: 200X

Figure 28. Effect of geometric variables on joint quality. Etchant: 2 min Kroll's + 4 sec CSDB. (Sheet 4 of 4)

An important condition sometimes encountered with Ti-6Al-4V sheet is the presence of alpha case due to solution of oxygen. This condition may result from improper handling or inadequate cleanup of the sheet at the mill or during fabrication. Solar has found that high oxygen sheet (0.2% oxygen) does not diffusion bond as readily as the low oxygen sheet (0.1% oxygen) although both may be within acceptable limits for sheet stock. A recent report by J.A. Regalbuto, "Nondestructive Testing of Diffusion Bonded Titanium Alloys for Engine and Airframe Components," AFML Report No. TR-74-215, has shown that significant alpha case can be tolerated in press diffusion bonded Ti-6Al-4V. Such a degree of alpha case (e.g., that resulting from 6 hours air exposure at 1450° F) could not be tolerated in the fatigue-critical spar, but more importantly, the effect of mild alpha case on quality of diffusion bonded joints should be determined. The short time available for diffusion in the CSDB process (1-2 seconds) makes the process more sensitive to this effect than in press bonding where the standard cycle used by Regalbuto was six hours at 1700° F. To determine the effect of oxygen-contaminated surfaces on joint quality, panels were bonded which had been preoxidized for 5 minutes and 1 minute at 800° F. This is considered an extreme condition. The oxide was visible in both cases and would be detected prior to a manufacturing operation.

The principal sources of contamination by foreign material in the joint are expected to be: grinding media, metal chips and contaminants associated with the bonding process such as fingerprints, bonding wheel dust, and lint. Panels were fabricated containing the following contaminants at the bond line: 0.002 inch thick molybedenum foil, 0.001 inch thick molybdenum foil, 0.002 inch thick titanium foil, 0.005 inch mild steel, alumina grinding media, wheel dust (principally silver powder and molybdenum oxides), greasy fingerprints, and nylon and cotton thread.

Some of the conditions are shown in Figure 29 prior to bonding. The metal implants were 0.60 inch wide by 0.10 inch long and resistance spot tacked to one panel face for maintaining position. The location of the implants is shown in Figure 29. Some of these contaminants, particularly metal implants, also act as a geometric variable since they create a gap through the thickness of the panel.

The panels were bonded using the standard parameters of wheel force, speed and current. Joint quality was evaluated by mechanical tests and metallography.

Mechanical Test Results

Table 4 shows the mechanical test results in order of decreasing severity. Refer to Section 2.2.6 for nomenclature. Tensile strength of the panels contaminated with greasy fingerprints, lint, and steel chips is drastically reduced. It is interesting to note that these three panels are the only ones that exhibited strengths below approximately 120 ksi in this entire program.

Although flat fracture occurred in the preoxidized panels, no appreciable loss in tensile strength occurred.

Concerning the preparation variables, flat fracture occurred with plant acid cleaning and tap water rinse. The local tap water has a very high solids and mineral content. As mentioned previously, the plant acid is expected to contain impurities such as iron, nickel, chromium and silicon. The acid which had been used only to etch Ti-6Al-4V but had greatly reduced etching potential did not affect joint quality, nor did storage for 48 hours in plastic prior to bonding.

The molybdenum foil marginally reduced tensile properties and tensile failure occurred at the foil interface. However, specimens containing both 0.001 inch and 0.002 inch foil withstood 5T bend tests. The foils are placed in the center of the thickness of the sheet, that is at the neutral axis where their effect on bend strength will be minimal.

Bonding wheel dust and alumina grinding media had no apparent effect on joint quality based on mechanical test results.

Metallography

Examples of the microstructure in the joint region are shown in Figures 30-32 for the various preparation and contamination variables. Low magnification views are given to provide a comparison of overall joint quality. Observations of the bond line at high magnification will be presented in Section 4, where flat fracture characteristics are discussed. Figure 30 shows a comparison of joint quality resulting from variations in prebond preparation procedures. The standard overetching technique

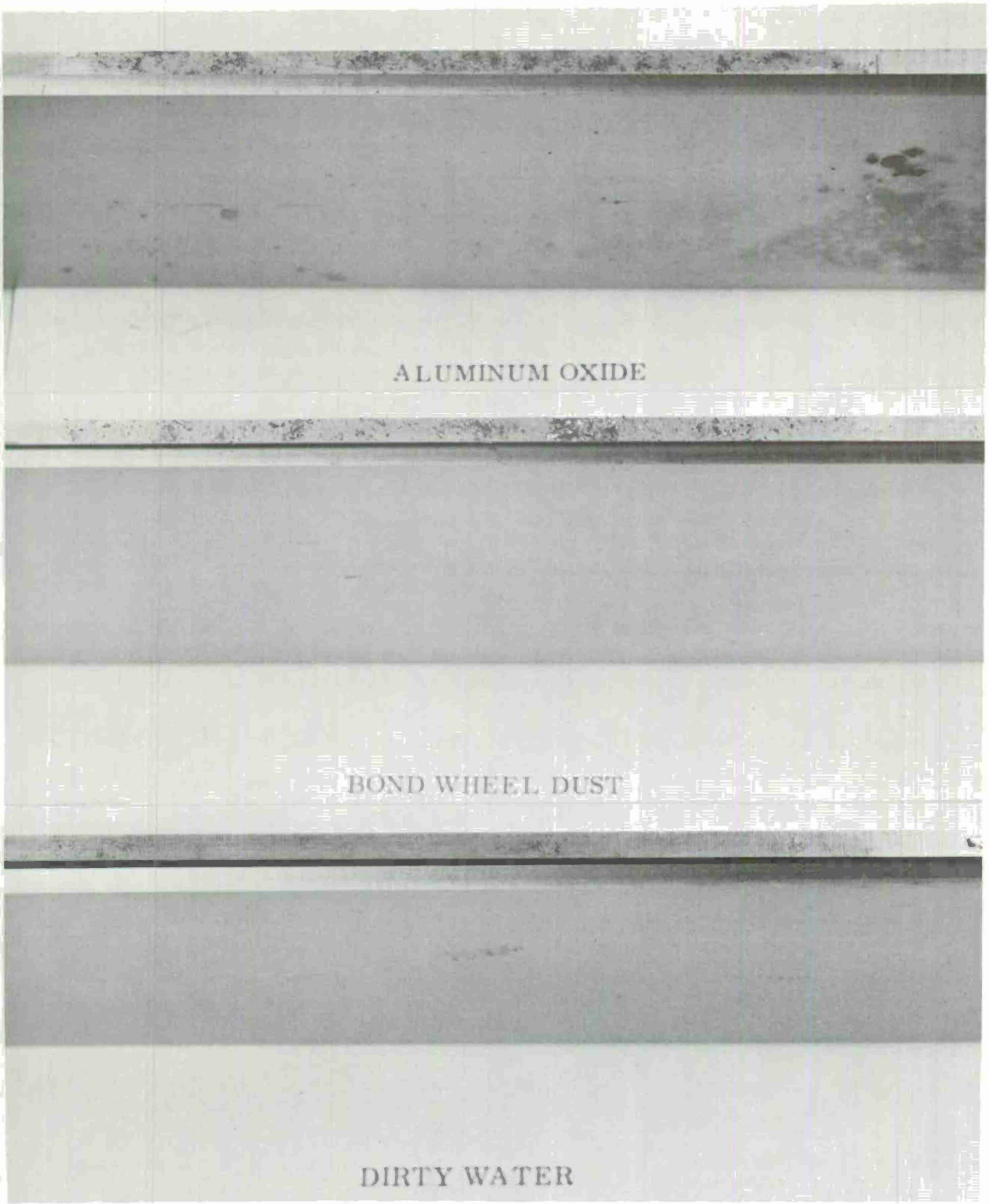

Figure 29. Contaminants at bond line prior to CSDB processing. (Sheet 1 of 2)

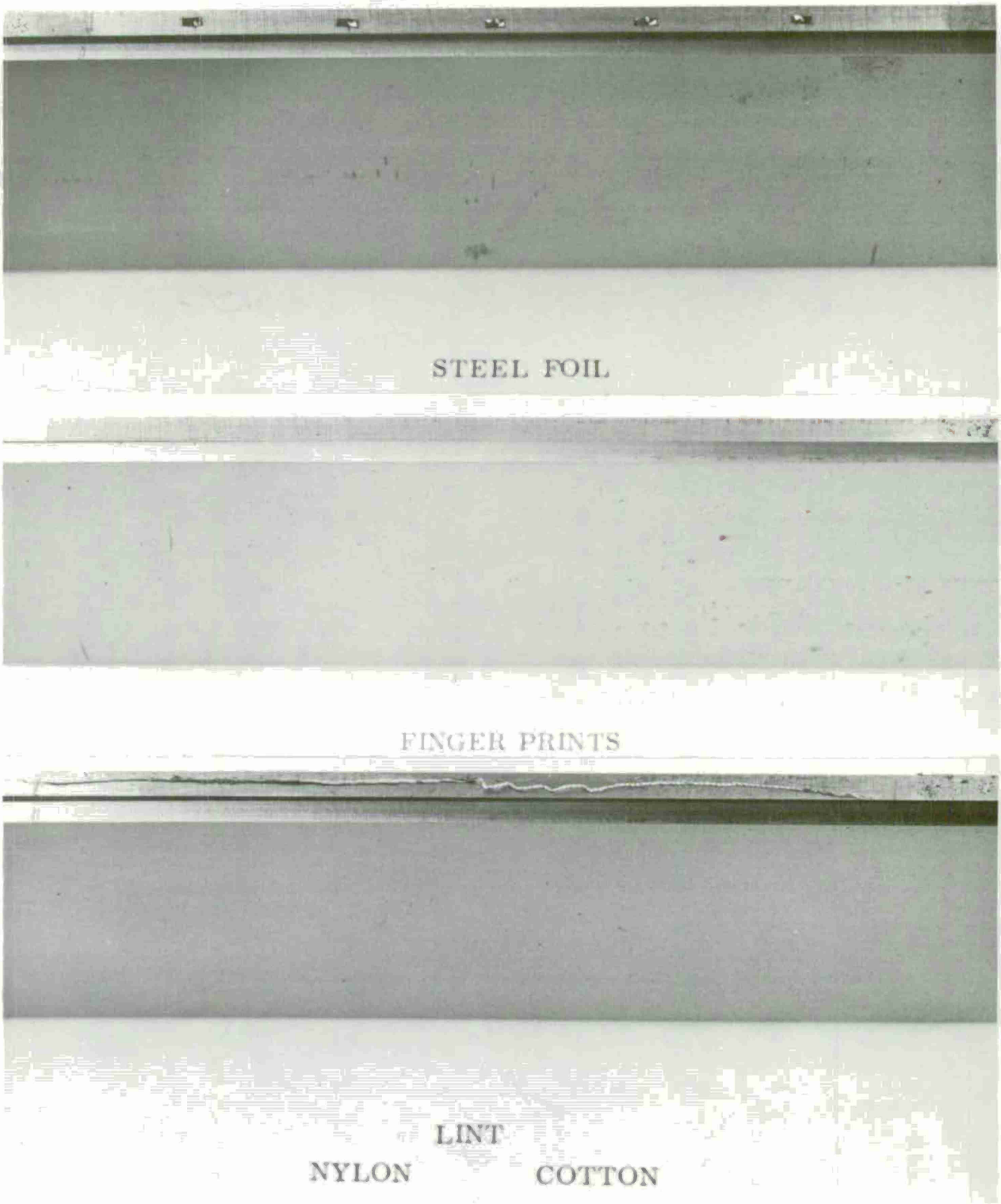

Figure 29. Contaminants at bond line prior to CSDB processing. (Sheet 2 of 2)

TABLE 4. EFFECT OF PREPARATION AND CONTAMINATION VARIABLES ON JOINT QUALITY IN ORDER OF DECREASING SEVERITY

	1	2	3	4	5	6	7	8	9	10	11	12	13	14	15		CSDB Processed No Joint
Contamination	Lint (cotton, nylon)	Finger-prints	0.005" steel	Plant acid	Pre-oxidized 5 min. @ 800° F	Pre-oxidized 1 min. @ 800° F	Tap water	0.001" Moly	0.002" Moly	Wheel dust Ag, MoO_3	Al_2O_3 grit	0.002" Ti	Acid (used) Ti-6Al-4V	New acid-stored 48 hrs in plastic	Acid (new)	Std	No Joint
Bonding parameters	Std	Std	Std	Std	Std	Std	Std	Std	Std	Std	Std	Std	Std	Std	Std	Std	Std
5T bend test, top down	FF-JZ	FF	FF	FF	FF	5T	5T	5T	5T	5T	5T	5T	5T	JZ	HAZ	5T	5T
Tensile tests																	
0.2% yield (ksi)	None	None	84.7	125.8	129.3	124.8	128.3	119.8	123.0	128.3	127.1	127.4	129.7	126.7	127.3	129.8	122.6[a]
Ultimate tensile stress (ksi)	66.87	72.65	84.7	137.1	139.6	135.8	137.9	119.8	128.3	136.9	139.3	137.7	136.3	138.2	139.5	140.1	137.9[a]
Stress at joint (ksi)	66.87	72.65	84.7	137.1	134.1	135.6	137.9	119.8	128.3	136.7	139.3	133.1	135.5	136.8	139.5	137.2	138.5[a]
2-inch elongation (%)	0.5	0	1.0	3.5	7.5	4.0	5.0	2.0	2.0	10.0	9.5	10.0	7.0	11.5	10.0	4.0	12.5[a]
1-inch elongation (%)	1.0	0	2.0	4.0	3.0	4.0	4.0	4.0	4.0	3.5	11.0	3.5	3.0	4.0	15.0	2.0	13.3[a]
Location of failure	FF	FF	FF through steel	FF	PM	FF	FF	FF-JZ	FF-JZ	PM	JZ	PM	PM	PM	JZ	PM	HAZ[a]

[a] Average of 3 specimens

Bond Line

a) Used acid (Ti-6Al-4V only)

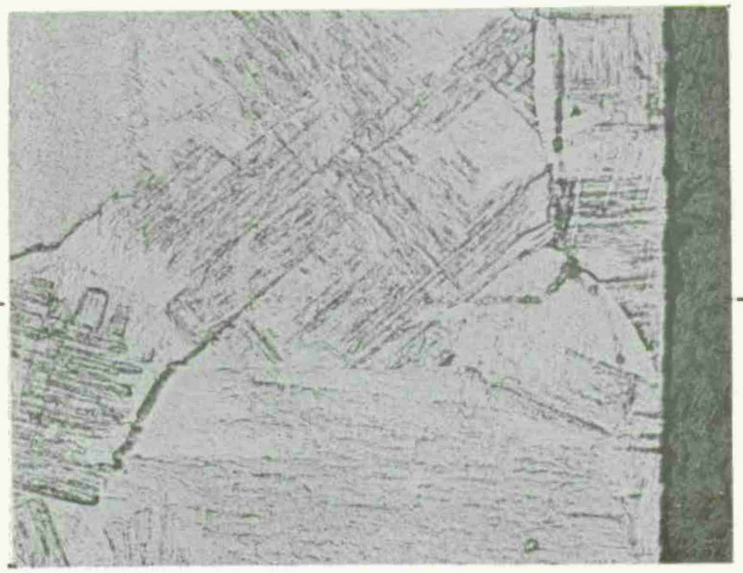

Bond Line

b) Stored 48 hrs prior to bonding

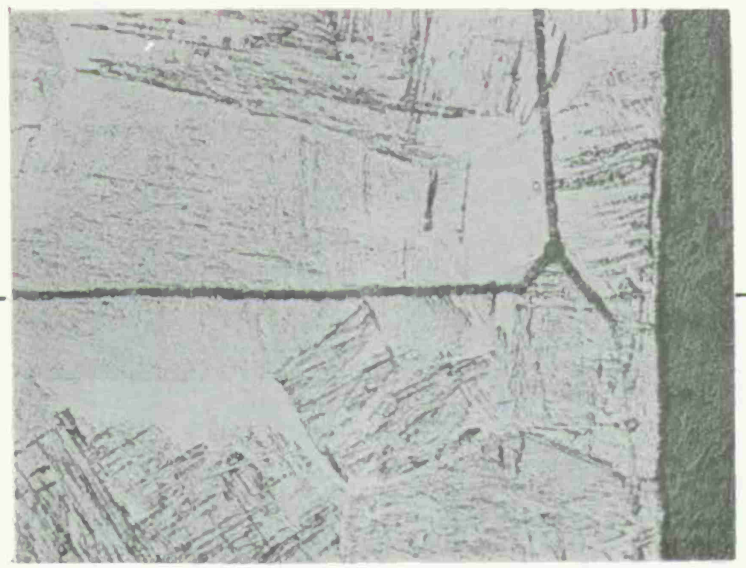

c) Plant acid

Bond Line

Figure 30. Effect of preparation variables on joint quality.
Etchant: 2 min Kroll's + 4 sec CSDB.
Magnification: 200X

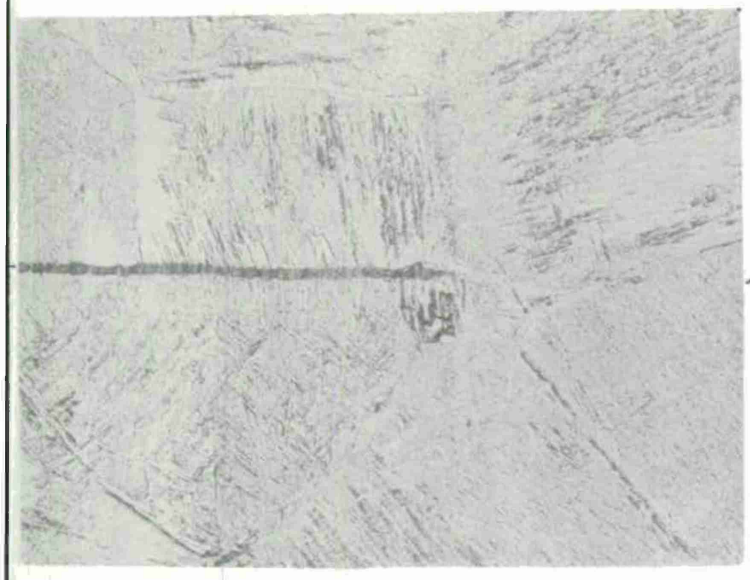

— Bond Line

a) Lint

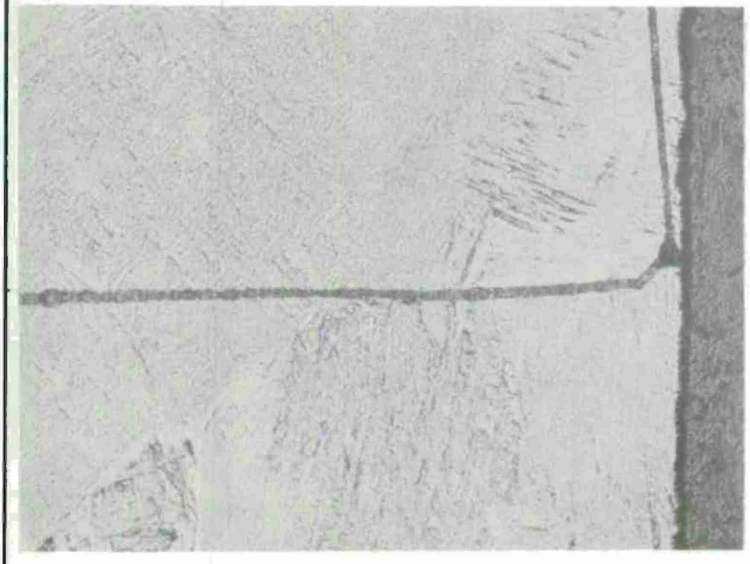

— Bond Line

b) Greasy fingerprints

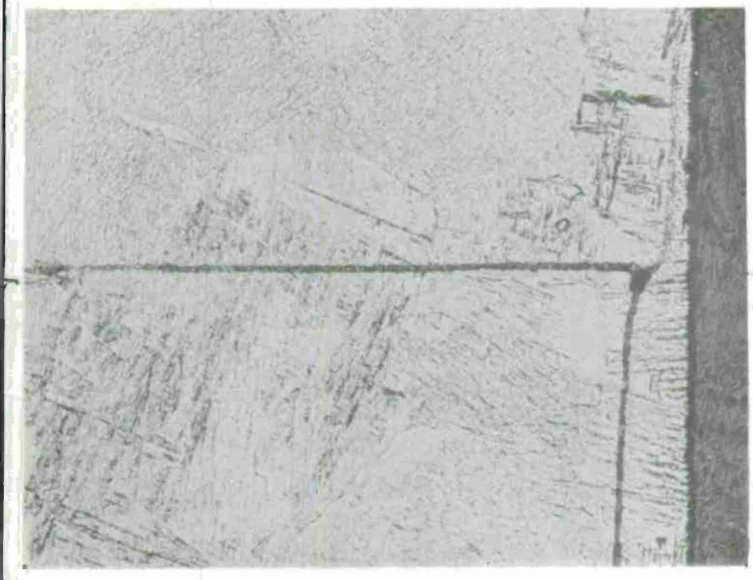

c) Tap water

— Bond Line

Figure 31. Effect of contaminants on joint quality. Etchant: 2 min Kroll's + 4 sec CSDB. Magnification: 200X (Sheet 1 of 2)

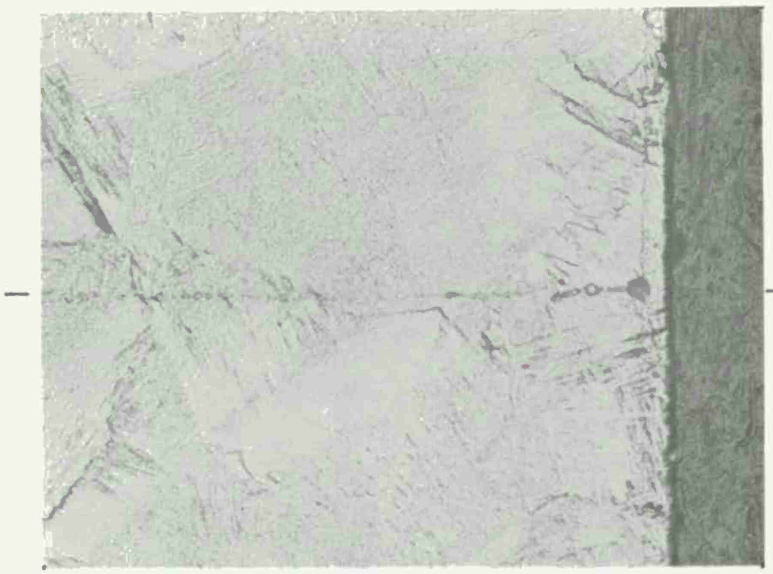

Bond Line

d) Al_2O_3 grinding media

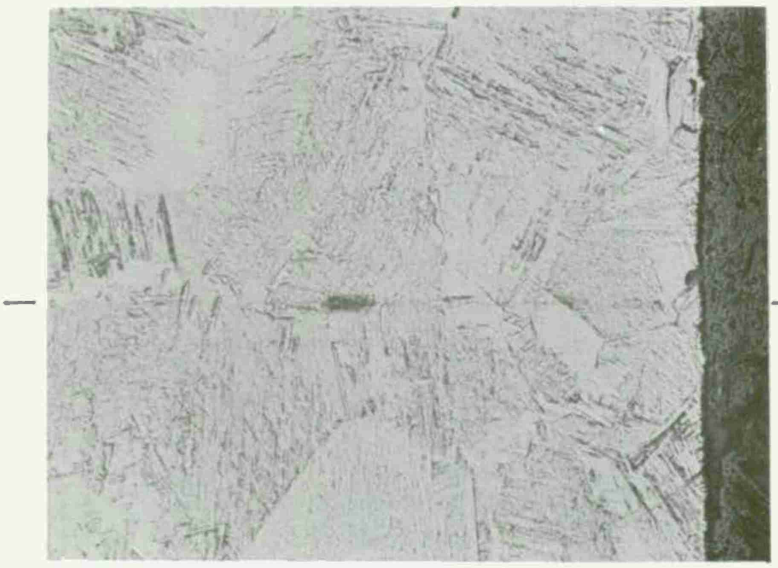

Bond Line

e) Dust from bonding wheel (Ag, Mo-oxides)

Figure 31. Effect of contaminants on joint quality. Etchant: 2 min Kroll's + 4 sec CSDB. Magnification: 200X. (Sheet 2 of 2)

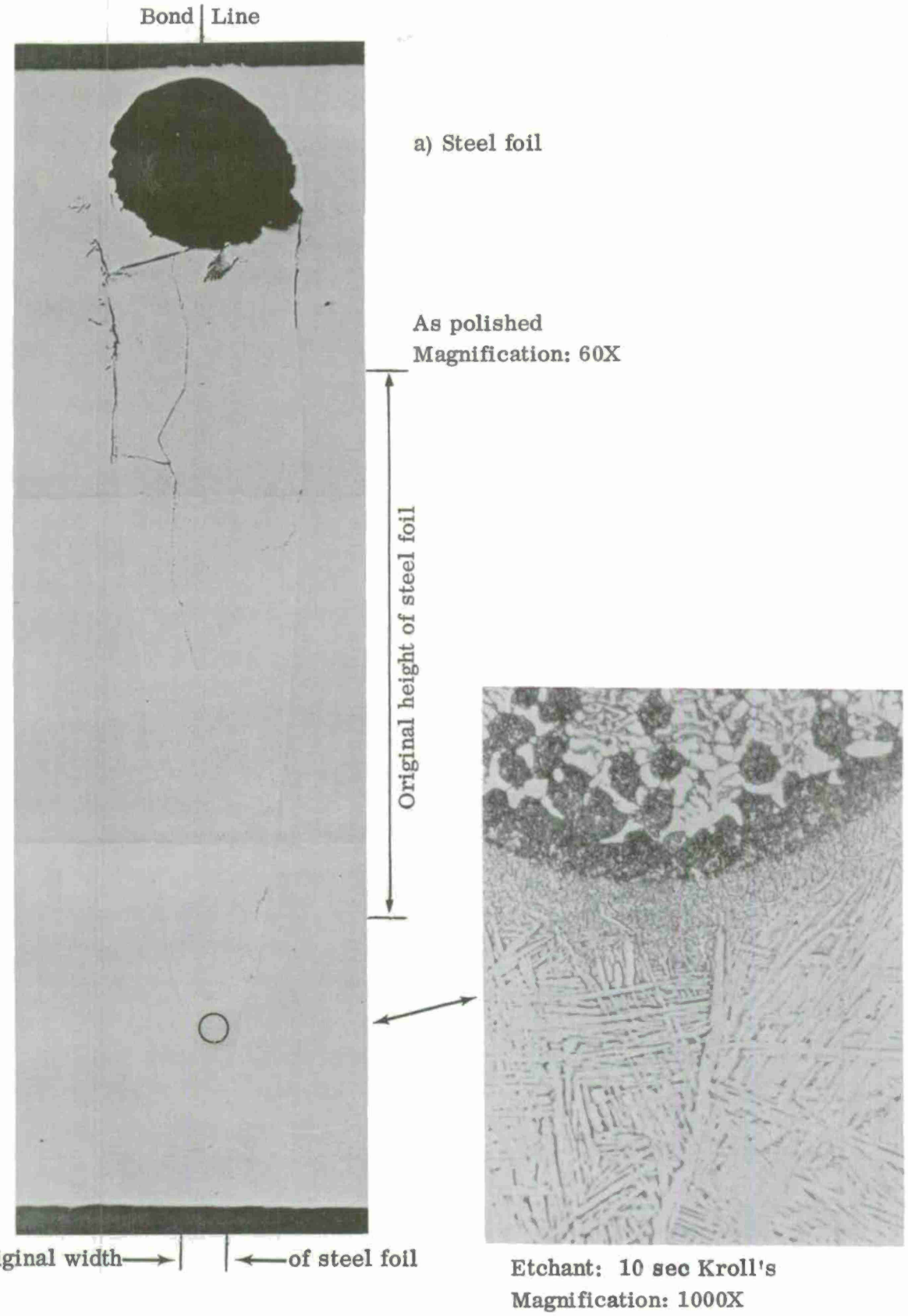

Figure 32. Effects of metal foil at bond line on joint quality. (Sheet 1 of 3)

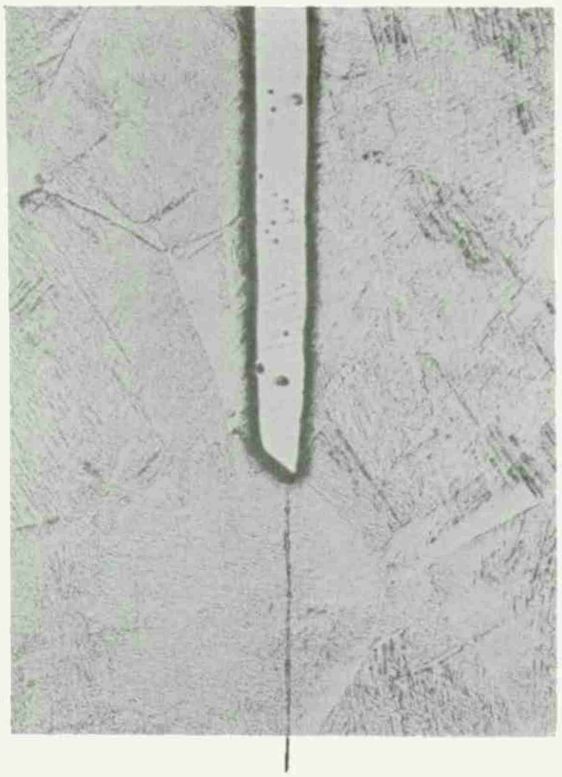

b) 0.002 inch thick molybdenum

Etchant: 2 min Kroll's + 4 sec CSDB.
Magnification: 200X

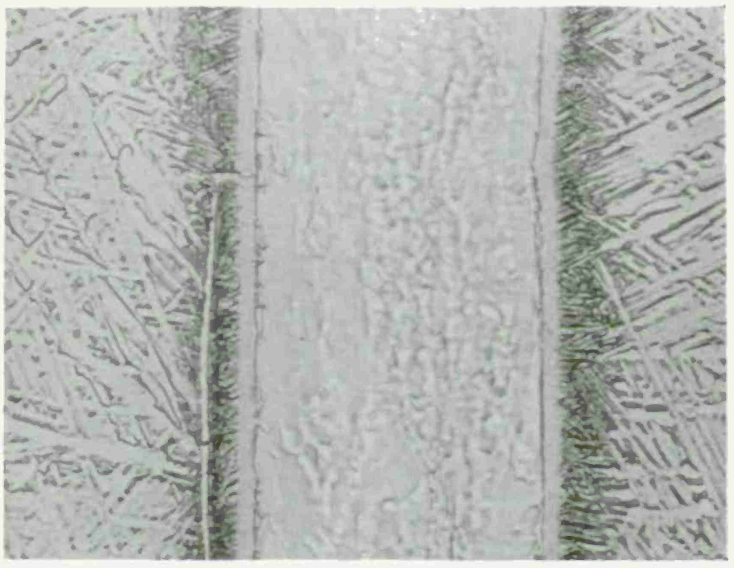

Etchant: 15 sec Kroll's + 10 sec Murakami
(10 K_3 Fe $(CN)_6$
10 KOH
100 H_2O)
Magnification: 1000X

Figure 32. Effects of metal foil at bond line on joint quality. (Sheet 2 of 3)

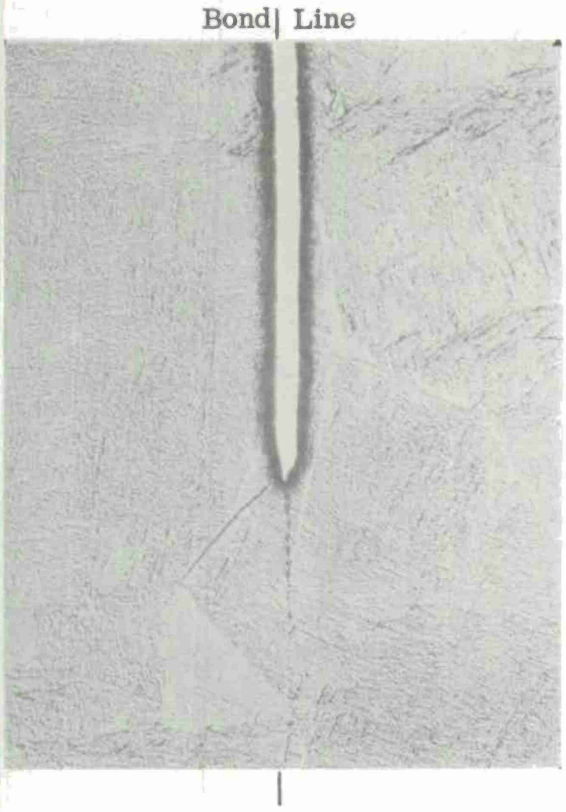

c) 0.001 inch thick molybdenum

Etchant: 2 min Kroll's + 4 sec CSDB.
Magnification: 200X

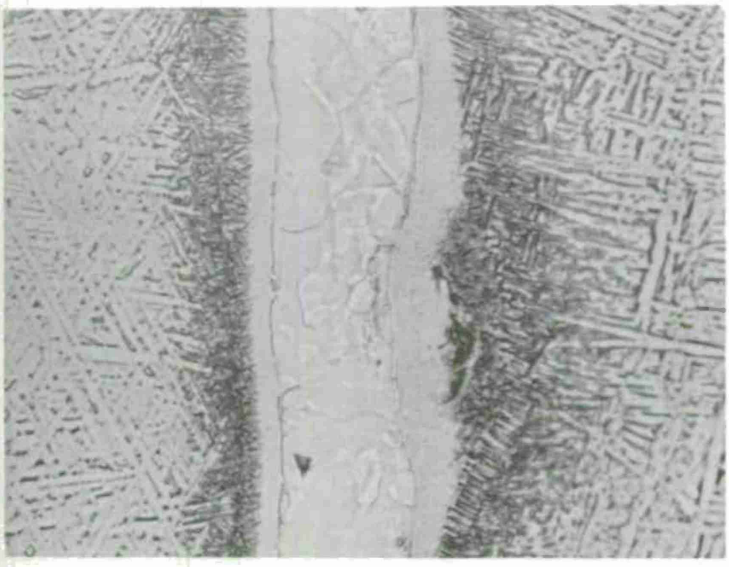

Etchant: 15 sec Kroll's + 10 sec Murakami
(10 K_3 Fe $(CN)_6$
10 KOH
100 H_2O)
Magnification: 1000X

Figure 32. Effects of metal foil at bond line on joint quality. (Sheet 3 of 3)

was necessary to reveal the bond line. The bond line indication for used acid and for the stored condition is much less severe than the plant acid condition which is consistent with mechanical test results since the panel cleaned in plant acid exhibited flat fracture in 5T bend tests and the others did not fail. No evidence of contaminants was observed metallographically.

The effect of various contaminants on joint quality is shown in Figure 31 in order of decreasing severity based on mechanical test results. Again, the overetched condition was necessary to reveal the bond line. Foreign particles in the bond line were not observed at these magnifications. There is a general correlation between etched bond line appearance and mechanical test results.

Metal implants in the bond line are shown in Figure 32. Considerable reaction occurred between the titanium and steel. Figure 32a shows the dimensions of the original steel foil in relation to the post bond condition. Considerable porosity and cracking also exists in the joint region. The appearance of this joint is consistent with the severely reduced tensile strength (Table 4). The tensile specimen failed at the joint through the steel and had a very brittle appearance in the reacted region.

Less reaction occurred with the Mo foil implants as can be seen in Figure 32 Band C. Also, no porosity or cracking was observed. Although the tensile failures occurred at the Mo-Ti interface, strength and ductility was not severely reduced.

Apparently, a steel chip in the bond line is a much more severe problem than molybdenum.

Conclusions

- A variety of contaminants can be tolerated in the bond line without affecting joint quality. However, lint, greasy fingerprints and steel chips severely degraded the joint.
- Joint quality was not affected by used acid (Ti-6Al-4V only) or 48 hour storage after cleaning. Acid used for general cleaning which contained impurities did not result in a good joint.

4

CHARACTERIZATION OF FLAT FRACTURES

One of the important tasks on this program was to characterize flat fractures so that this knowledge could assist in elimination of this type of failure. As discussed in the previous sections, it has been established that flat fracture surfaces show a flat, featureless appearance with little deformation revealed in the form of classic cup and cone fractures. All previous work had suggested that flat fracture results when the lined-up defects in the bond plane create stress concentrations producing fracture propagation from one defect to the next.

The view of the origin of these flaws accepted prior to the start of this program was as follows. During CSDB processing, a joint is formed by progressive merging of asperities on the two faying surfaces. Residual contamination and gas is trapped in the unbonded portion of the joint as it becomes sealed from the external environment. The air trapped in these voids expands as a result of heating. The final size of the void is determined when the internal pressure equals the forging pressure. However, solution of the principal gases, oxygen and nitrogen, in the titanium matrix is rapid at the typical bonding temperature, so that the equilibrium size decreases. All available data indicate that the noble gases in air (less than 1%) are not readily dissolved by the titanium. Hence, both residual surface contamination collected in depressions in the original surface, and the slow-to-dissolve noble gases, such as argon, may both contribute to stabilization of residual defects.

Further evidence from previous work at Solar and United Aircraft Research Laboratories (UARL) is that the defects are submicroscopic pores or inclusions less than 1000Å in size. Work at UARL was not able to detect any contaminant by electron microprobe studies, but this was not unexpected in view of the extremely small size.

The purpose of this phase of the investigation was to determine the cause and characteristics of flat fractures and recommend processing procedures to eliminate them. Several techniques were used for this purpose and they will be discussed separately.

4.1 EFFECT OF BONDING ATMOSPHERE ON JOINT

The effect of residual trapped gas on joint porosity was assessed by bonding in argon and vacuum.

A detailed discussion of the results is given in Section 3.1.3, Atmosphere Effects. Etching of the bond line was slightly heavier for the panel bonded in argon compared

with air and vacuum which is consistent with the hypothesis that noble gases are not readily dissolved in titanium. However, flat fracture was not observed, and there was no significant difference in strength between the panels. Further discussion on bonding atmosphere is given in Section 4.2, Heat Treatment.

Conclusions

- Bonding atmospheres of argon and vacuum have no significant effect on joint quality for processing parameters which produce a good quality joint in air.

4.2 HEAT TREATMENT

Stability of the submicroscopic defects was evaluated by vacuum heat treatment at 1600 and 2000° F for one hour. It was considered that analysis of the kinetics of removal at these temperatures would indicate if the rate is governed by solution of an interstitial (e.g., TiO), of a substitutional element (e.g., Mo or Fe), or of both (e.g., Al_2O_3). A second purpose was to determine whether heat treatment could be used to improve marginal joint quality.

Heat treatment was applied to panels made under the following conditions:

- Indirect Variables - Air, vacuum atmosphere
  - 1.1 inch flat wheel
- Direct Variables (processing parameters) - Several ranging from good quality joints to 100 percent flat fracture
- Contamination Variables - Greasy fingerprints
  Plant acid

Examples of the resulting microstructures are shown in Figures 33 to 36. Except for fingerprint contamination, a heavy overetch condition was necessary to reveal the bond line indications. For comparison purposes, the standard heavy etch was used for all the photomicrographs. In all cases, the area of heaviest etching is shown. No difference in bond line appearance was observed with the three heat treatments for a good quality joint (Figure 33). This indicates that the specie responsible for the etched indications is not readily soluble in the titanium matrix. In the absence of diffusion data, Table 5 lists some of the potential gaseous contaminants and their respective atomic sizes and solubilities in titanium. Small amounts of hydrogen, carbon, oxygen and nitrogen would be readily dissolved at both 1600 and 2000° F. These elements are considered interstitial due to their relatively small size compared with titanium atoms (1.46Å. Argon, sulfur and chlorine are expected to behave as substitutional elements and their solubility in titanium is probably quite low and consequently diffusion rates are expected to be very low. Compound formation

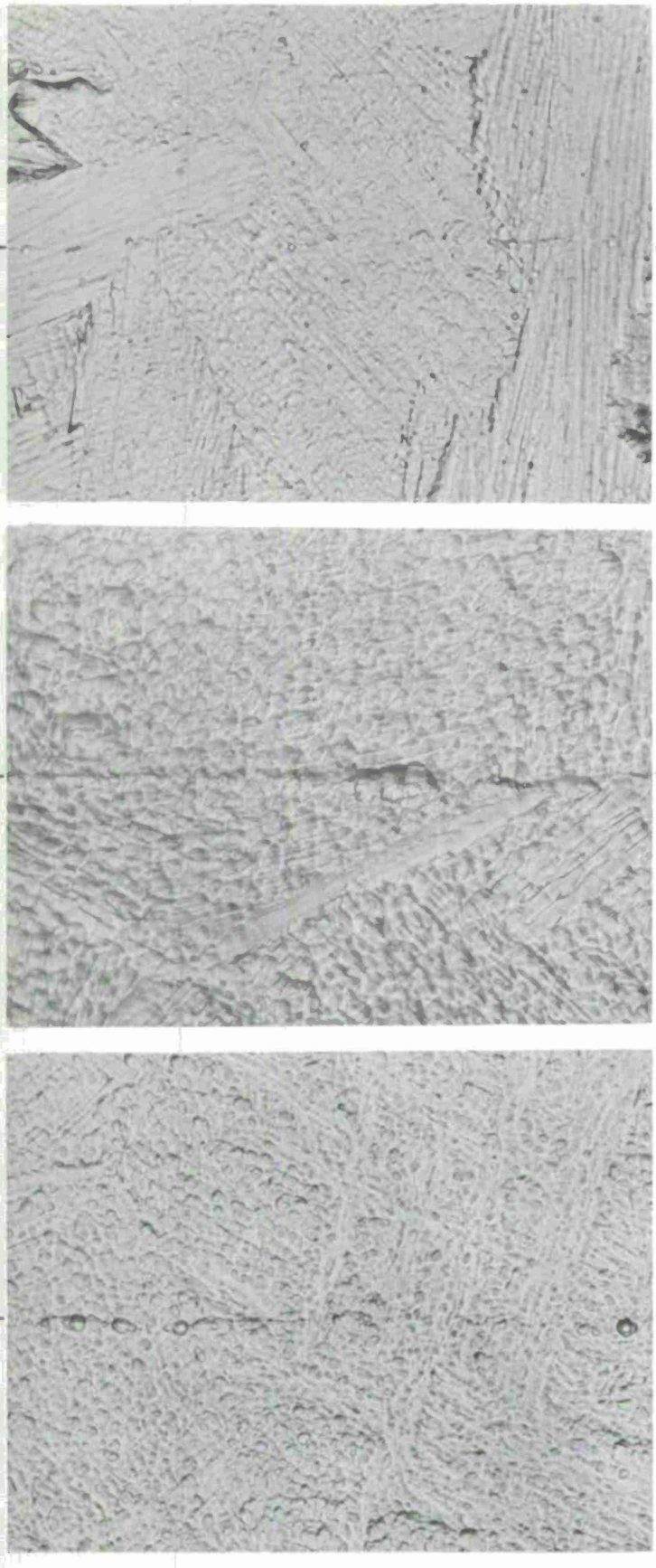

Figure 33. Effect of heat treatment on bond line indications for good quality joint. Etchant: 2 min Kroll's + 4 sec CSDB. Magnification: 1000X.

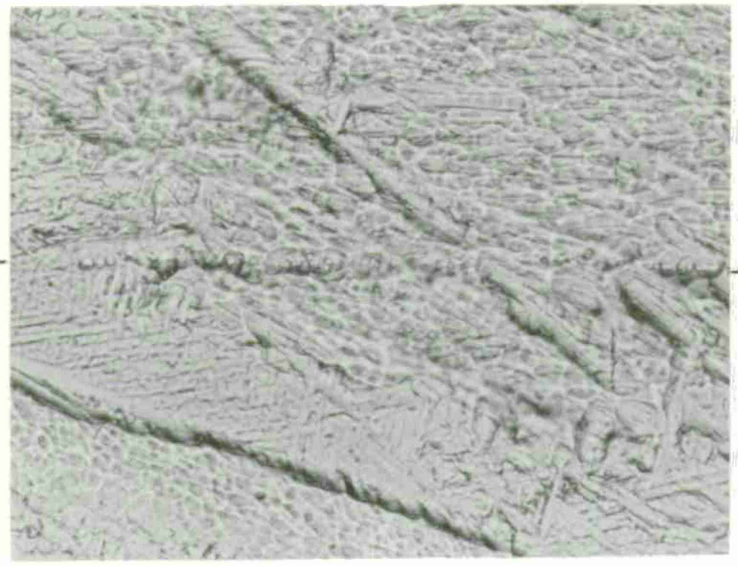

Bond Line

a) 1350° F

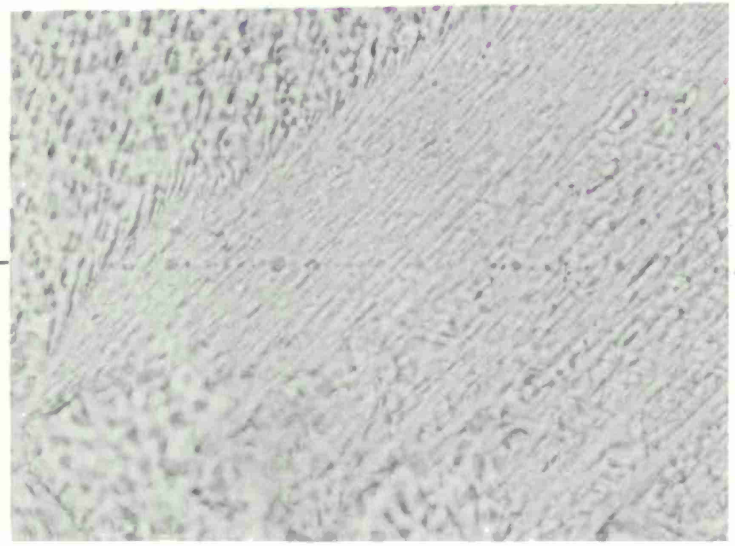

b) 1600° F

Bond Line

Figure 34. Effect of heat treatment on bond line indications for vacuum bonded panel. Etchant: 2 min Kroll's + 4 sec CSDB Magnification: 1000X.

c) 2000° F

Bond Line

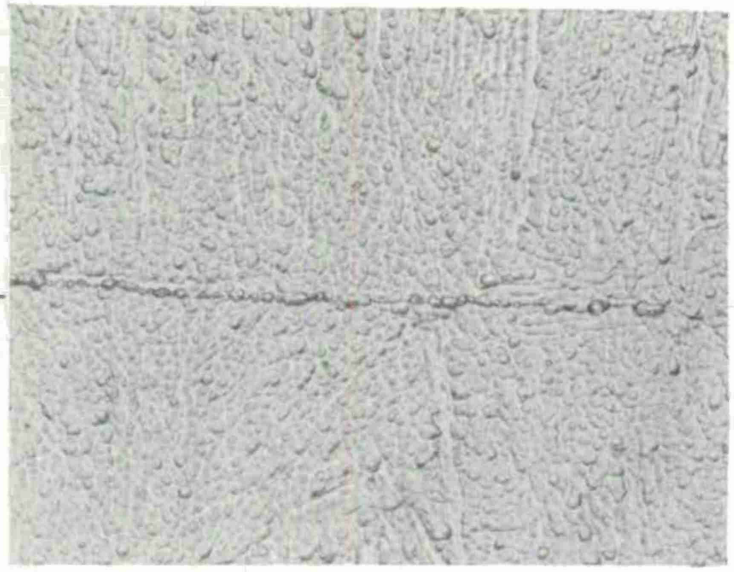

a) 1350° F

— Bond Line

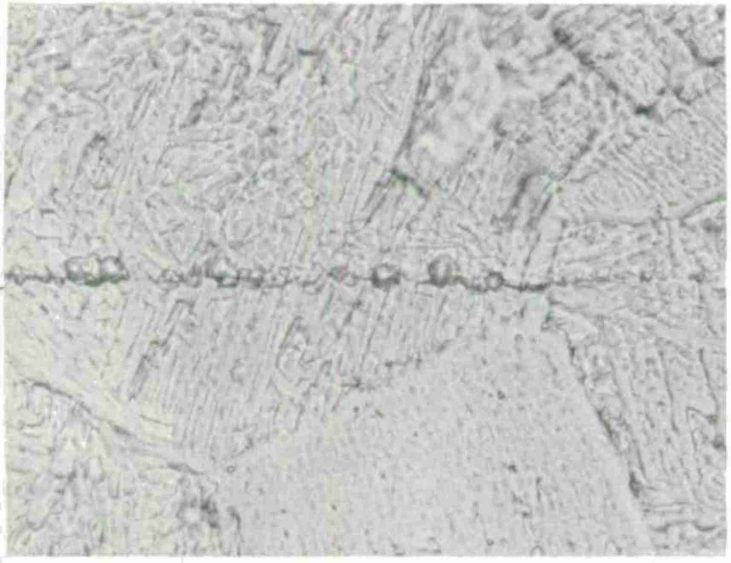

b) 1600° F

— Bond Line

Figure 35. Effect of heat treatment on bond line indications for process parameters resulting in poor joint quality. (flat fracture occurred for all mechanical tests)
Etchant: 2 min Kroll's + 4 sec CSDB.
Magnification: 1000X.

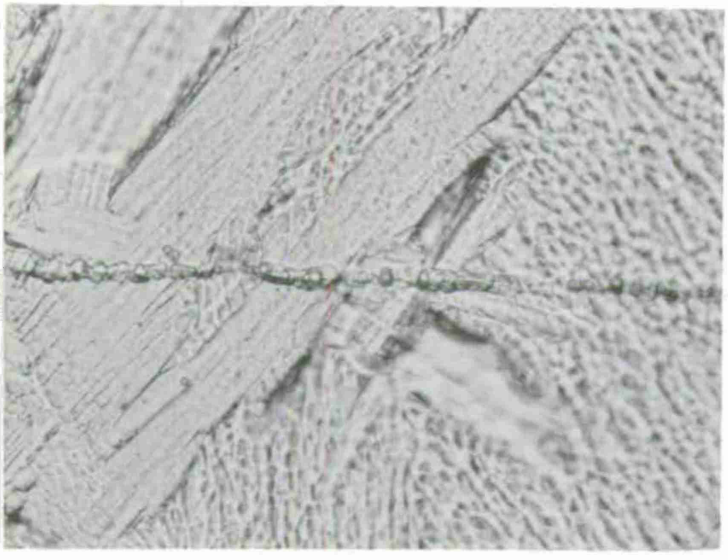

— Bond Line

c) 2000° F

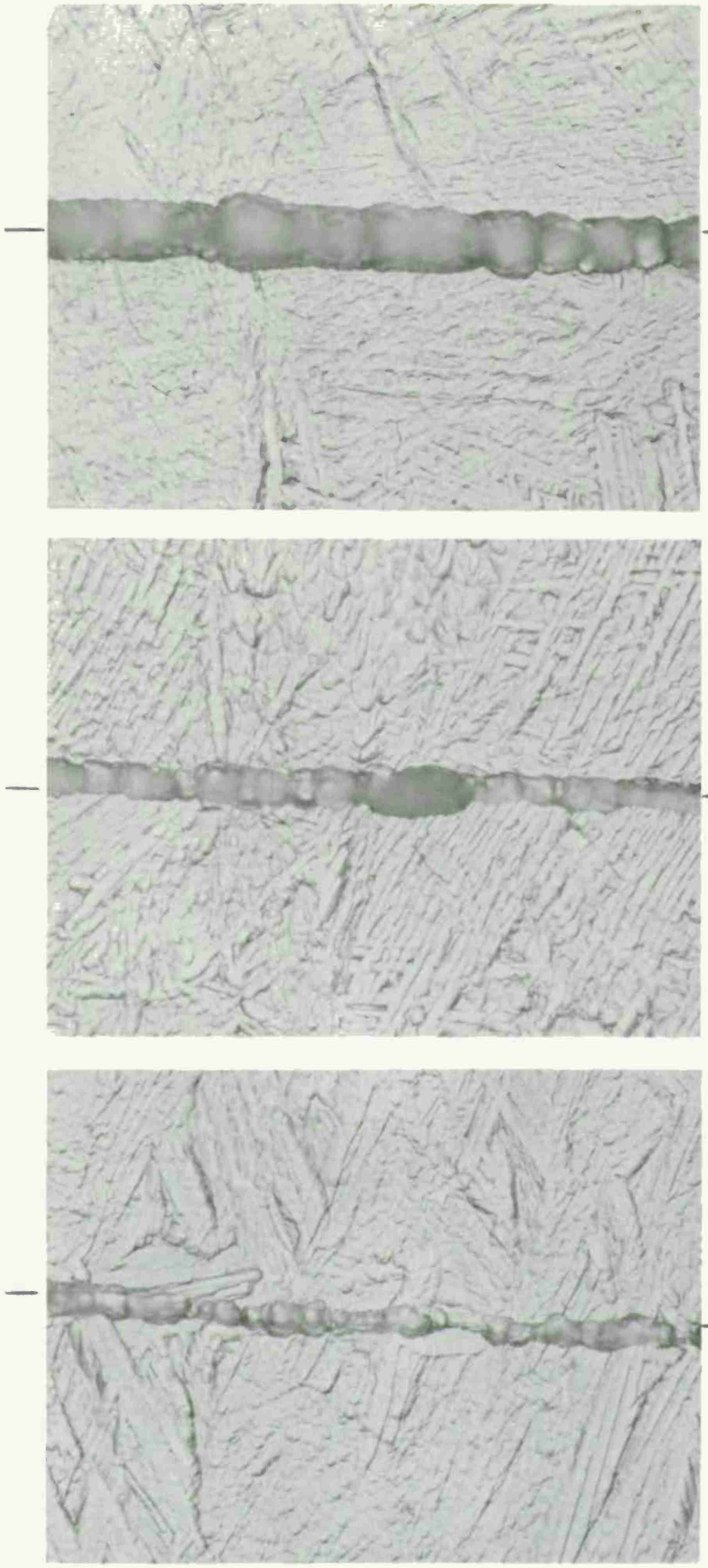

Figure 36. Effect of heat treatment on bond line indications for fingerprint contaminated panel.
Etchant: 2 min Kroll's + 4 sec CSDB.
Magnification: 1000X.

TABLE 5. ATOMIC RADII AND SOLUBILITY OF POTENTIAL CONTAMINANTS IN TITANIUM

	Atomic Radius Å	Solubility at 2000° F wt %
Hydrogen	0.46	0.25
Carbon	0.77	0.5
Oxygen	0.60	15
Nitrogen	0.71	6
Argon	1.91	-
Sulfur	1.04	0.009 - 0.0017
Chlorine	1.07	-

[1]Crystal Chemistry, R.C. Evans, Cambridge University Press, 1939, p 171.
[2]Constitution of Binary Alloys, M. Hanson, McGraw Hill, 1958.

would be most probable for chlorine and sulfur. Further discussion of inclusions in the bond line will be given in the section on scanning electron microscopy. From the above discussion, it is apparent that the most probable gaseous contaminant at the bond line is an inert gas, such as argon, which is a natural constituent of air. This is supported by the observation that no change in the bond line indications occurs for heat treatments up to 2000° F for good quality joints.

Additional support for this hypothesis is apparent from examination of the heat treated samples for the vacuum bonded panel (Figure 34). Again, there is no obvious difference between the etched bond line indications as a function of heat treatment. More important, however, is the observation that the size and number of the indications is less than that evident in the air bonded panel (Figure 33). The only difference in bonding procedure between the two panels was the bonding atmosphere and therefore, the size and number of indications should be a direct function of the amount of trapped gas.

Figure 35 shows a poor quality joint which failed by flat fracture in the mechanical tests. Again, there is no appreciable difference in the bond line indications for the three heat treatments. Although the size of the indications is essentially the same as for a good quality joint (Figure 33), the number of indication is much larger, giving an almost continuous decoration of the bond line. This observation suggests that the occurrence of flat fracture is not dependent on the size of indications of the bond line, but on their number. This particular panel was bonded using low-heat processing parameters.

The panel contaminated with greasy fingerprints did show improvement in bond quality with heat treatment (Figure 36). However, the joint quality would still be considered poor after one hour at 2000° F. It is possible that further annealing would result in increased quality. The major contaminants in this bond line are probably carbon and hydrogen resulting from decomposition of the grease, with minor amounts of chlorine and sulfur from perspiration. During CSDB processing, the time at temperature is only one to two seconds and it is probable that solution of the contaminants was not possible for this short period of time. However, the one hour heat treatments allowed solution of the rapidly diffusing species.

Conclusions

- No change in etched bond line indications occurred with heat treatments of 1600 and 2000° F for air and vacuum bonded panels as well as panels fabricated with various processing parameters which produced good, marginal (50% FF) and poor (100% FF) quality joints.
- For various processing parameters, the size of bond line indications is independent of joint quality, but number of indications along the bond line increases with decreasing joint quality.
- The panel contaminated with greasy fingerprints did show improvement in joint quality with heat treatment which indicates that rapidly diffusing species, such as hydrogen and carbon were principal contaminants.

4.3 SCANNING ELECTRON MICROSCOPY

Examination of the joints at high magnification was accomplished with a Cambridge scanning electron microscope. The microscope is equipped with an Ortec energy-dispersive x-ray analyzer. The unit is capable of detecting elements of atomic No. 11 (Na) and greater to a lower limit of 0.01 percent detectability in a one cubic micron volume. X-ray analysis was used to determine variations in composition at the bond line and to identify contaminants.

Two types of samples were examined. A comparison of the details of the fracture surfaces was made by examining resonant fatigue, bend test and tensile failures as follows:

Condition	Type of Failure
CSDB processed - no joint	Resonant fatigue - joint zone
Standard processing parameters	Resonant fatigue - joint zone
Low heat processing parameters	Resonant fatigue - flat fracture
Low heat processing parameters	Tensile - flat fracture
Al_2O_3 contaminant in joint	Tensile - joint zone
High heat processing parameters	Bend test - flat fracture
High heat processing parameters	Tensile - flat fracture
Greasy fingerprints in joint	Tensile - flat fracture
Plant acid cleaning	Resonant fatigue - flat fracture
Oxidized 5 minutes at 800° F	Bend test - flat fracture

In addition, specimens were fractured at the joint after machining to size for SEM examination. This technique was used to provide fresh fracture surfaces which did not contain cutting fluid residue so that any impurities detected would be directly attributable to as bonded joint contamination. The contaminant conditions for these specimens were lint, greasy fingerprints and plant acid, and all were flat fractures.

A comparison of the details of the various fracture surfaces revealed variations in degree rather than type of fracture. Examples of the structure are shown in

Figures 37 to 41. Figure 37 shows the surface of a resonant fatigue failure in a standard CSDB processed joint. The striations are typical of a ductile fatigue failure. There is no evidence of voids or impurity inclusions on the fracture surface.

Figure 38 shows a typical example of the CSDB processed-no joint fracture surface in the final overload region of a fatigue specimen. The equiaxed dimples are characteristic of a tensile failure in a ductile material. The size of the dimples is a measure of ductility and number of nucleation sites for failure. Dimple size increases with ductility. Figures 39 to 41 show examples of flat fracture surfaces and they are all characterized by a dimpled structure. However, the size of the dimples varies greatly. In effect, this means that a fracture which appears flat optically is not necessarily characteristic of poor bonding at the joint. This is consistent with the high tensile and resonant fatigue strengths of these flat fracture specimens (refer to Table 2).

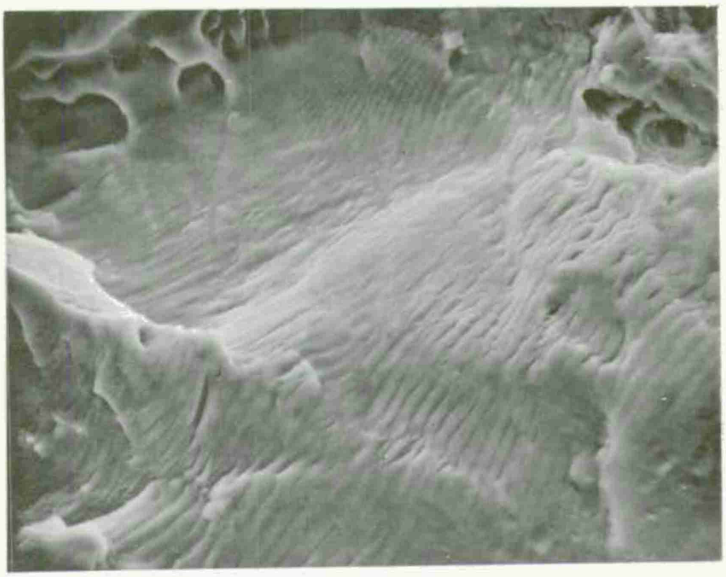

Figure 37. Resonant fatigue failure from standard processing parameters showing ductile fatigue striations.
Magnification: 1150X

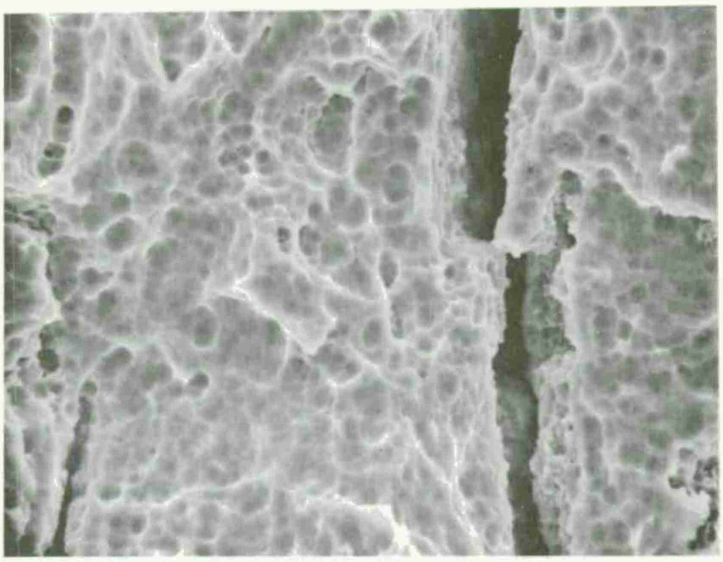

Figure 38. CSDB processed-no joint fracture surface showing dimpled structure characteristic of ductile overload failure.
Magnification: 1200X

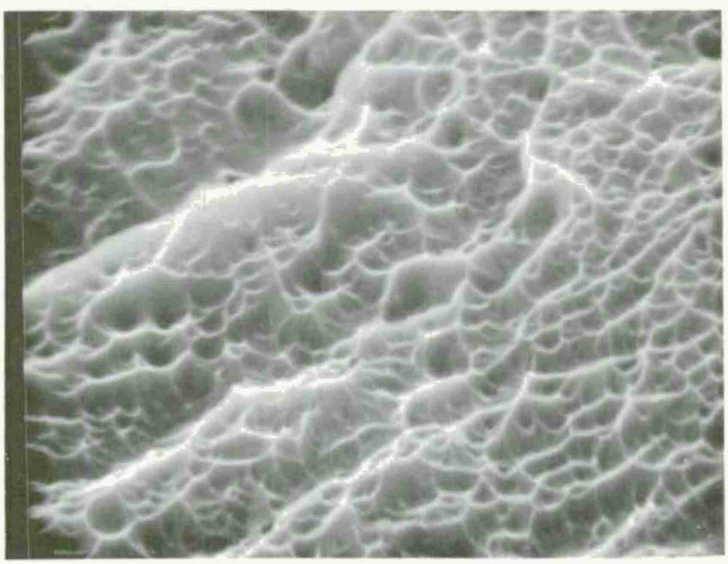

Figure 39. Bend test flat fracture surface from preoxidized joint showing dimpled structure characteristic of ductile overload failure.
Magnification: 10,000X.

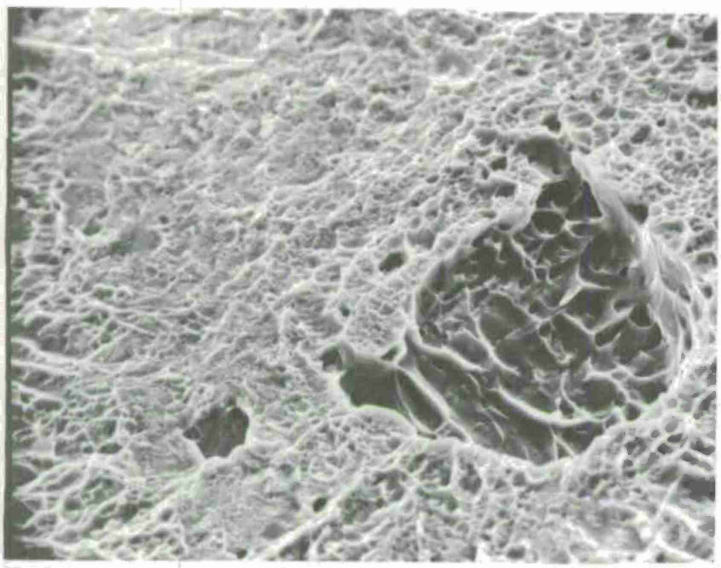

a) Dimpled structure characteristic of ductile overload. Note variation in dimple size.

Magnification: 1100X.

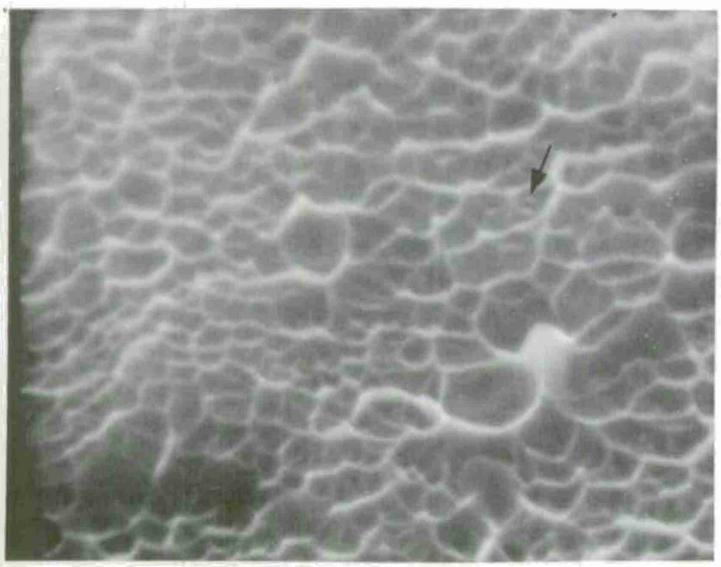

b) Higher magnification view of light region in a). Arrow indicates inclusion.

Magnification: 22,500X.

Figure 40. Tensile flat fracture surface from high-heat processing parameters.

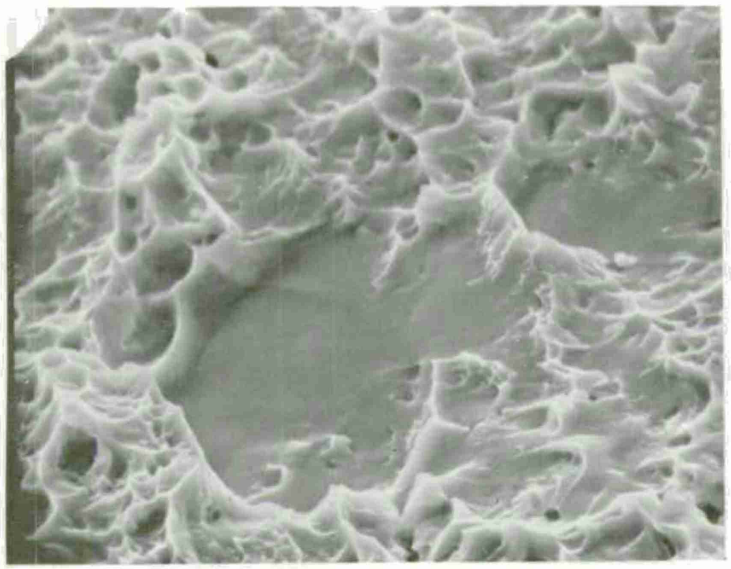

a) Dimpled structure characteristic of ductile overload surrounding flat featureless regions.

Magnification: 2000X

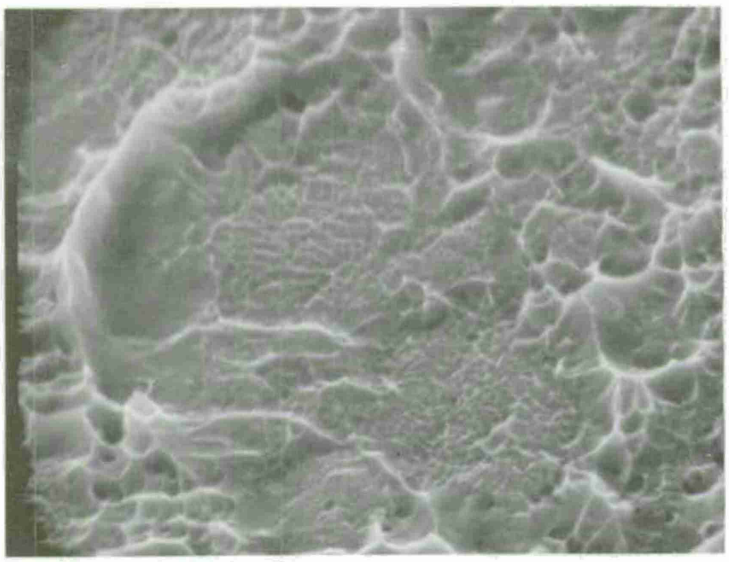

b) Dimpled structure characteristic of ductile overload. Note variation in dimple size.

Magnification: 4800X.

Figure 41. Tensile flat fracture surface from low-heat processing parameters.

The fracture surface of a preoxidized specimen (5 min at 800° F) is shown in Figure 39. The dimple size is quite small (on the order of 0.3μ or 3000Å diameter and indicates a relatively large number of nucleation sites available for fracture. (Dimple size for CSDB processed-no joint material is an order of magnitude larger.) However, there is no evidence of inclusions or voids in the bottom of the dimples to the limit of resolution of the photograph (~500Å).

A flat fracture surface resulting from high heat processing parameters is shown in Figure 40. A large variation in dimple size is evident in Figure 40a. The flat (light portion) is shown at higher magnification in Figure 40b. The dimple size is as small as 400Å. Occasional small particles are also observed as indicated by the arrow in Figure 40b. These particles are also on the order of 400Å and are too small to identify by x-ray analysis although an x-ray analysis of this region (indicated by arrow) did not detect any elements other than Ti, Al and V. These particles are only observed occasionally and consequently probably not responsible for the small dimple size.

An example of flat fracture resulting from low heat processing parameters is shown in Figure 41. Figure 41a shows the normal dimpled structure surrounding two flat-featureless regions. The lack of structure in these regions indicates lack of joint formation. However, surface diffusion has occurred as evidenced by the lack of machining marks or the etched surface produced by the cleaning process. There is a general absence of voids and inclusions in these areas also. This type of surface could have been produced in two ways. The heat and pressure of forging could have been insufficient to completely bond the two faying surfaces; or gas pressure build-up could have been sufficient to prevent bonding in these areas. A combination of the two processes is most likely. Figure 41b is similar to Figure 41a except that regions of very fine dimples replace the flat featureless region indicating that progressive bonding is occurring. This is not unexpected when the mechanics of diffusion bonding are considered, i.e., a bond is formed progressively between the largest asperities on the two faying surfaces. No evidence of voids or inclusions was found in these dimples.

The flat fracture surfaces produced by the contaminants lint and greasy fingerprints were characterized by voids. Figure 42 shows an example of the fingerprint contaminated panel. An unbonded region in the center of the photograph (Figure 42a) is surrounded by voids on the order of 1/2μ (5000Å) diameter. At higher magnification (Figure 42b) these voids are seen to contain particles which are relatively large (also on the order of 1/2μ diameter). An x-ray analysis of these particles did not detect any elements other than titanium, aluminum and vanadium. However, the elements carbon, nitrogen, oxygen and hydrogen are below the detectable limits of

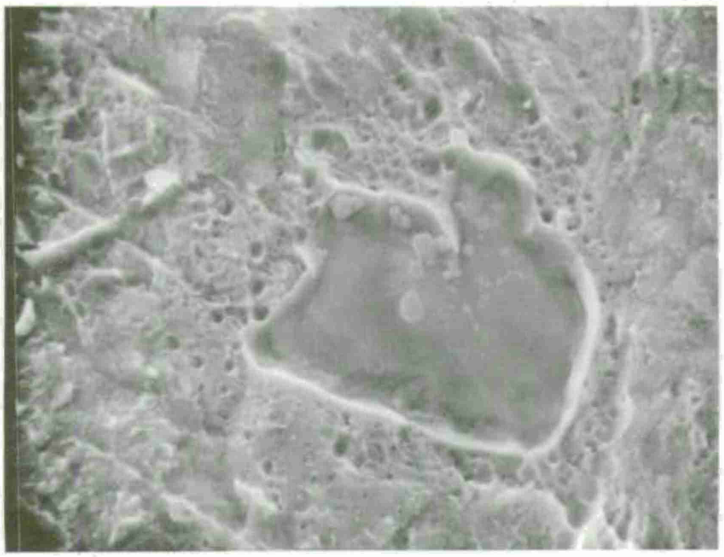

a) Unbonded region (center) surrounded by voids.

Magnification: 2400X.

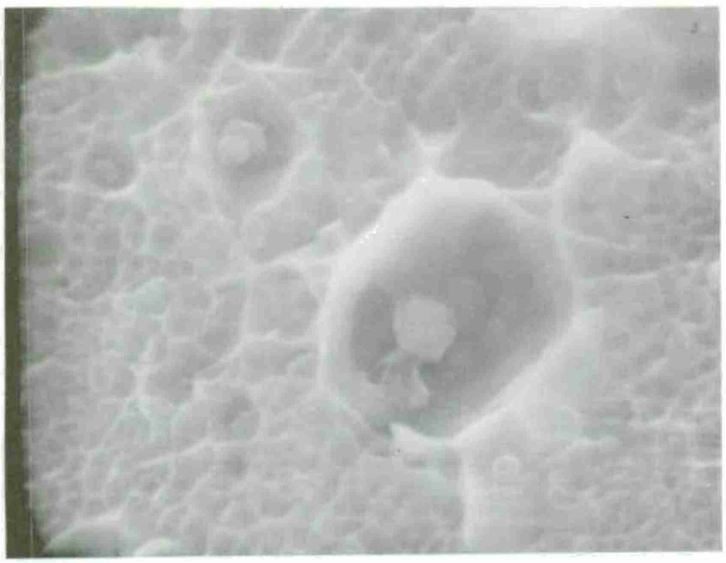

b) Voids and dimples containing precipitates.

Magnification: 12,000X.

Figure 42. Flat fracture surface from greasy fingerprint contaminated panel.

the analyzer. Most importantly sulfur and chlorine, two elements normally associated with fingerprints were not detected. It is probable that the inclusions are carbides, oxides or nitrides of the titanium alloy constituents. This is consistent with the heat treatment results, in that the fingerprint contaminated panel was the only one that showed improvement in joint quality with the high temperature anneals, and carbon, nitrogen and oxygen are expected to diffuse rapidly at these temperatures.

An example of the type of x-ray analyses performed on these specimens is given in Table 6. The corresponding areas are given in Figure 43. A computerized program is used to register x-ray counts per second and enables calculations of relative elemental amounts. The example given is for a plant acid cleaned panel. Particles one and two are probably oxides, carbides or nitrides since the heavy metal totals add up to approximately 50 percent. Small amounts of iron and manganese were present in particle one. Relative amounts of titanium, aluminum and vanadium on the flat fracture surface were about the same as the parent metal. The panel cleaned in plant acid showed the only evidence of foreign elements in the detectable range of the x-ray analyzer.

Conclusions

- Generally, fractures at the bond line which appear flat visually show good bonding at high magnification.
- Sites at the bond line which produce flat fracture could not be identified, but are <200Å (limit of resolution of microscope).
- X-ray analysis of flat fractures did not detect any foreign elements except in the plant acid cleaned panel. However, the limit of detection is atomic number 11 (Na) and greater.

TABLE 6. RELATIVE PERCENTAGE OF HEAVY ELEMENTS BASED ON X-RAY ANALYSIS OF REGIONS SHOWN IN FIGURE 43

	Ti	Al	V	Cu	Cr	Mn	Fe	Ni	Other Elements
Standard - parent metal fracture surface (x-ray counts per second)	859.4	47.4	127.0	0.6	4.1	0.7	2.3	1.1	- -
Percent from mill analysis	~90	5.8	4.0	-	-	-	0.12	-	- -
Percent based on total	-	-	-	0.05	0.4	0.07	-	0.1	- -
			Relative Percent Based on Standard						
Particle 1 - Figure 43	10	37	0.4	0.05	6	4	0.6	0.2	- -
Particle 2 - Figure 43	42	3	2	-	0.09	0.08	0.2	0.04	Trace amounts of S, Cl and Ca
General bond line (Region 3 - Figure 43)	95	4	4	-	0.3	0.06	0.17	0.1	- -
General bond line (Region 4 - Figure 43)	94	5	4	-	0.4	0.1	0.15	0.05	- -

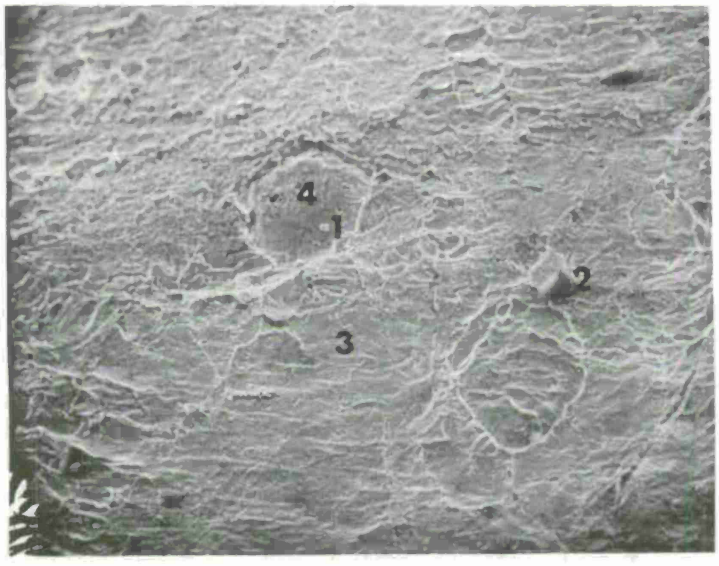

Figure 43. Flat fracture surface resulting from plant acid cleaning. Numbers correspond to x-ray analysis in Table 6. Magnification: 200X.

5

NONDESTRUCTIVE INSPECTION

This phase of the program was primarily directed to application of previously used NDT methods to the joints. These methods were: dye-penetrant, x-radiography, and ultrasonic inspection. Application of these methods provided a basis for comparison with earlier work on the spars. At the same time, the availability of a variety of joints with known defects suggested that new inspection methods should be evaluated for consideration for future development.

The specific methods are discussed below.

5.1 DYE PENETRANT INSPECTION

The inspection was performed per MIL-I-6866. The initial justification for dye penetrant tests was to assess the closure of the simple butt joint of the surface. However, when foil strips were introduced, the dye was no longer accessible to the butt joint. A limited number of samples were subjected to this inspection technique and in all cases the only indications detected were located at the outer edge of the foil and were not related to joint quality, but more to post bond clean-up procedures.

It is recommended that this nondestructive inspection technique be eliminated from consideration for spar manufacture.

5.2 X-RADIOGRAPHY

Radiographic inspection was performed to MIL-STD-453 specification and to one percent sensitivity (approximately 0.001-inch in panel thickness). In the initial stages of the program, all panels were examined radiographically. Exposure times and angle were varied to optimize examination of the butt joint. However, no indications were detected and usually, the joint was not visible. Blanket examination of the panels was discontinued. Selected panels were examined and included various contaminants in the joint, geometric variables, indications detected by ultrasonic inspection and the repair panel.

The molybdenum and iron joint implants (see Section 3.4) were visible with radiographic inspection. However, the panels contaminated with greasy fingerprints which exhibited inferior strength and flat fracture (Table 4) did not contain any

discontinuities detectable by x-radiography. Furthermore, none of the other contaminated joints revealed any indications nor could the ultrasonic indications be located by x-radiography.

It is concluded that x-radiography is useful only for detecting gross defects such as molybdenum and iron foil and cannot be used as the sole nondestructive inspection technique to determine joint quality.

5.3 ULTRASONIC INSPECTION

All of the panels from the parametric study portion of the program were subjected to ultrasonic inspection. A discussion of the specific technique used is given in Section 2.2.5, Experimental Methods - Nondestructive Testing. In areas where indications were located, joint quality was determined by bend tests, tensile tests or metallographic examination and correlated with properties of the remaining panel.

As discussed in Section 2, a computer printout was provided for the panels which gave the total number of counts in each category and the percentage for that category. The panels were also manually scanned and the highest category indications were located physically and marked. A computer printout and manual scan was provided for each of the panels fabricated with various processing parameters (direct variables). However, the panels containing geometric and contamination variables were only scanned manually due to equipment malfunction. The highest category indications were located physically and their magnitude was reported to be of the same order as that exhibited by the direct variable panels.

It is not practical to include all of the computer printouts in this report, particularly since the results are quite repetitious. A selection of the ultrasonic inspection results for good, marginal and poor joint quality is given in Figures 44 through 54. The figures are given in approximate order of increasing indication size. Also included in the figures are the bonding parameters, mechanical test results for the panel, the number and magnitude of indications located in the major categories and metallography or mechanical properties of the indications. The ultrasonic scans are for sections approximately 8 inches long.

There is a general correlation between joint quality determined by mechanical tests and the number and magnitude of ultrasonic indications. As discussed in Section 2.2.5, Category 16 corresponds to a 0.0156 inch diameter hole and Category 7 corresponds to 0.0065 inch diameter eloxed hole prior to diffusion bonding.

Metallographic examination of areas containing ultrasonic indications shows a reasonable correlation between severity of bond line etching and category number (refer to Figures 45-47, 49 and 51). The most obvious exception is shown in Figure 51 where the indication corresponds to Category 9 and the bond line etching

Bonding Parameters	Mechanical Properties
I = 10,870A	5T, 5T bend
S = 3.19 in./min	140.5 ksi UTS
F = 2200 lbs (std)	1.5×10^5 cycles fatigue

CATEG	COUNT	FREQ	P. FACT.	PROD
1	179	.0375	.0	.0002
2	4472	.9381	.3	.2814
3	115	.0241	.7	.0169
4	1	.0002	1.2	.0003
5				
6				
7				
8				
9				
10				
11				
12				
13				
14				
15				
16				
TOTAL	4767			

No indications located manually.

Figure 44. Ultrasonic inspection of CSDB panel.

as light. However, etching at the foil interface is relatively severe and could possibly account for the high reading. Figure 46 shows a Category 4 ultrasonic indication in the as-polished condition. This particular panel was fabricated with low heat processing parameters. The appearance of the bond line suggests incomplete bonding and illustrates one of the problems associated with nondestructive evaluative of joint quality. That is, the voids are minor individually, but when lined up on the bond line, constitute a weak joint.

The effect of the larger category ultrasonic indications were evaluated mechanically. The results are shown in Figures 48 and 50 through 54. The results are consistent with mechanical tests of the bulk panel. For example, compare Figure 53 and 54 which both contain Category 10 indications. The specimens were examined visually after testing, but no evidence of specific indications was found.

The results of the ultrasonic inspection indicate that it is a promising nondestructive evaluation technique. However, a definitive program is needed to correlate the magnitude of the indications with artificial defects of known size and configuration.

Bonding Parameters

I = 11,200A (std)
S = 3.19 in./min
F = 2400 lbs

Mechanical Properties

5T, 5T bend
141.9 ksi UTS
43 x 10^5 cycles fatigue

CATEG	COUNT	FREQ	P. FACT.	PROD
1	86	.0153	.0	.0000
2	4825	.8566	.3	.2570
3	577	.1024	.7	.0717
4	145	.0257	1.2	.0309
5				
6				
7				
8				
9				
10				
11				
12				
13				
14				
15				
16				
TOTAL	5633			

Two indications located manually corresponding to Category 3 and 4.

Area of ultrasonic indication - Category 3 or 4.
Etchant: 2 min Kroll's + 4 sec CSDB.
Magnification: 200X.

Figure 45. Ultrasonic inspection of CSDB panel.

Bonding Parameters
I = 10,870A
S = 4.31 in./min
F = 2200 lbs (std)

Mechanical Properties
5T, FF bend
141.4 ksi UTS
8.2×10^4 cycles fatigue

CATEG	COUNT	FREQ	P. FACT.	PROD
1				
2	348	.0652	.3	.0196
3	959	.1798	.7	.1259
4	4027	.7550	1.2	.9060
5				
6				
7				
8				
9				
10				
11				
12				
13				
14				
15				
16				
TOTAL	5334			

Two indications located manually corresponding to Category 4.

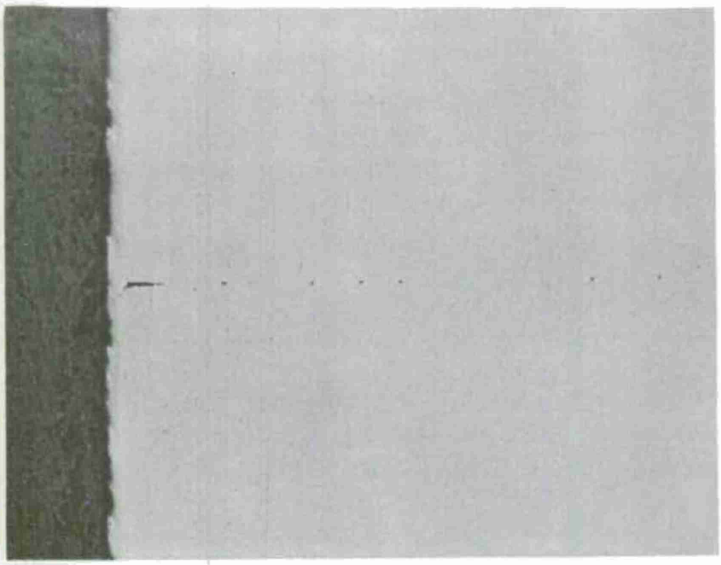

Area of ultrasonic indication - Category 4.
As-polished.
Magnification: 200X.

Figure 46. Ultrasonic inspection of CSDB panel.

Bonding Parameters
I = 10,200 A
S = 4.31 in./min
F = 2400 lbs

Mechanical Properties
FF, 5T bend
140.1 ksi UTS
1.1×10^6 cycles fatigue

CATEG	COUNT	FREQ	P. FACT.	PROD
1				
2	326	.0646	.3	.0194
3	779	.1544	.7	.1081
4	3775	.7481	1.2	.8977
5	166	.0329	1.8	.0592
6				
7				
8				
9				
10				
11				
12				
13				
14				
15				
16				
TOTAL	5046			

Two indications located manually corresponding to Category 4 and 5.

Area of ultrasonic indication - Category 4 or 5.
Etchant: 2 min Kroll's + 4 sec CSDB.
Magnification: 200X.

Figure 47. Ultrasonic inspection of CSDB panel.

Bonding Parameters	Mechanical Properties
I = 11,200A (std)	5T, FF bend
S = 4.81 in./min	131.2 ksi UTS-FF
F = 2200 lbs (std)	8 x 10^4 cycles fatigue - FF

CATEG	COUNT	FREQ	P. FACT.	PROD
1	23	.0044	.0	.0000
2	1436	.2745	.3	.0824
3	1115	.2132	.7	.1492
4	2445	.4674	1.2	.5609
5	207	.0396	1.8	.0712
6	5	.0010	2.6	.0025
7				
8				
9				
10				
11				
12				
13				
14				
15				
16				
TOTAL	5231			

Three indications located manually corresponding to Categories 5 and 6. Indications survived 5T bend tests.

Figure 48. Ultrasonic inspection of CSDB panel.

This correlation would be accomplished by comparison of mechanical properties, metallography and other nondestructive inspection techniques such as X-radiography for spar configuration joints. In this regard, it must be pointed out that the defects associated with the CSDB process (1-2 seconds under temperature and pressure) differ markedly from those associated with press bonding (6-24 hours under temperature and pressure).

Bonding Parameters
I = 11,200A (std)
S = 4.31 in./min
F = 2025 lbs

Mechanical Properties
5T, 5T bend
140.2 ksi UTS
1.4×10^5 cycles fatigue

CATEG	COUNT	FREQ	P. FACT.	PROD
1				
2	517	.1099	.3	.0330
3	1950	.4145	.7	.2901
4	958	.2036	1.2	.2443
5	823	.1749	1.8	.3149
6	295	.0627	2.6	.1630
7	162	.0344	3.5	.1205
8				
9				
10				
11				
12				
13				
14				
15				
16				
TOTAL	4705			

One indication located manually corresponding to Category 7.

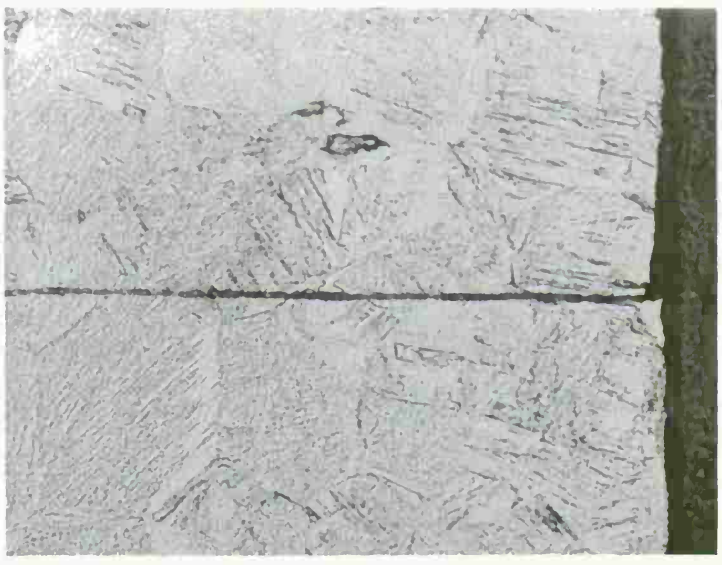

Area of ultrasonic indication - Category 7.
Etchant: 2 min Kroll's + 4 sec CSDB.
Magnification: 200X.

Figure 49. Ultrasonic inspection of CSDB panel.

Bonding Parameters
I = 10,870A
S = 3.19 in./min
F = 2400 lbs

Mechanical Properties
5T, 5T bend
140.0 ksi UTS
1 x 10^6 cycles fatigue

CATEG	COUNT	FREQ	P. FACT.	PROD
1				
2	42	.0086	.3	.0026
3	1542	.3156	.7	.2209
4	576	.1179	1.2	.1415
5	684	.1400	1.8	.2520
6	704	.1441	2.6	.3746
7	1253	.2564	3.5	.8976
8				
9	85	.0174	6.2	.1079
10				
11				
12				
13				
14				
15				
16				

TOTAL	4886			

Two indications located manually corresponding to Categories 7 and 9.

Tensile Properties at Indications

	1	2
0.2% yield (ksi)	129.0	128.6
UTS (ksi)	141.4	140.6
2 inch elongation (%)	11.5	8.7
1 inch elongation (%)	13.5	9.8
Location of failure	JZ	JZ

Figure 50. Ultrasonic inspection of CSDB panel.

Bonding Parameters
I = 10,870A
S = 3.75 in./min (std)
F = 2200 lbs (std)

Mechanical Properties
5T, 5T bend
143.6 ksi UTS
2.2×10^6 cycles fatigue

CATEG	COUNT	FREQ	P. FACT.	PROD
1				
2				
3	209	.0407	.7	.0285
4	1049	.2043	1.2	.2451
5	1546	.3011	1.8	.5419
6	931	.1813	2.6	.4714
7	1018	.1982	3.5	.6939
8				
9	382	.0744	6.2	.4612
10				
11				
12				
13				
14				
15				
16				
TOTAL	5135			

Three indications located manually corresponding to Category 9.

Area of ultrasonic indication - Category 9.
Etchant: 2 min Kroll's + 4 sec CSDB.
Magnification: 200X.

Figure 51. Ultrasonic inspection of CSDB panel.

Bonding Parameters	Mechanical Properties
I = 10,200A	5T, 5T bend
S = 2.63 in./min	137.5 ksi UTS
F = 2200 lbs (std)	1.4×10^5 cycles fatigue

CATLG	COUNT	FREQ	P. FACT.	PROD
1				
2				
3	97	.0144	.7	.0101
4	468	.0696	1.2	.0835
5	763	.1131	1.7	.2035
6	4351	.6473	2.6	1.6829
7	494	.0735	3.5	.2572
8	122	.0181	4.7	.0853
9	194	.0289	6.2	.1789
10	236	.0351	8.0	.2809
11				
12				
13				
14				
15				
16				
TOTAL	6722			

Three indications located manually corresponding to Categories 9 and 10. Material at indications survived 5T bend tests.

Figure 52. Ultrasonic inspection of CSDB panel.

Bonding Parameters
I - 11,530A
S = 4.31 in./min
F = 2200 lbs (std)

Mechanical Properties
FF, 5T bend
140.6 ksi UTS
1 x 10^6 cycles fatigue

CATEG	COUNT	FREQ	P. FACT.	PROD
1				
2				
3	17	.0035	.7	.0024
4	125	.0256	1.2	.0308
5	797	.1634	1.8	.2942
6	2797	.5735	2.6	1.4911
7	506	.1038	3.5	.3631
8	143	.0293	4.7	.1378
9	405	.0830	6.2	.5149
10	87	.0178	8.0	.1427
11				
12				
13				
14				
15				
16				
TOTAL	4877			

Two indications located manually corresponding to Categories 9 and 10.

Mechanical Properties at Indications

	1	2
5T bend	5T	
0.2% yield (ksi)		136.5
UTS (ksi)		146.4
2 inch elongation (%)		5.0
1 inch elongation (%)		2.0
Location of failure		PM

Figure 53. Ultrasonic inspection of CSDB panel.

Bonding Parameters
I - 10,200A
S = 3.75 in./min (std)
F = 2200 lbs (std)

Mechanical Properties
FF, 5T bend
122.5 ksi UTS-FF
0 cycles fatigue - FF

CATEG	COUNT	FREQ	P. FACT.	PROD
1				
2				
3				
4	36	.0051	1.2	.0061
5	204	.0286	1.8	.0516
6	3306	.4642	2.6	1.2069
7	1317	.1849	3.5	.6472
8	443	.0622	4.7	.2923
9	1153	.1619	6.2	1.0037
10	663	.0931	8.0	.7447
11				
12				
13				
14				
15				
16				
TOTAL	7122			

Two indications located manually corresponding to Category 10.

Tensile Properties at Indications

	1	2
0.2% yield (ksi)	--	--
UTS (ksi)	119.3	97.2
2 inch elongation (%)	0.8	0.5
1 inch elongation (%)	1.5	0.8
Location of failure	FF	FF

Figure 54. Ultrasonic inspection of CSDB panel.

5.4 ACOUSTIC EMISSION

The potential of using acoustic emission as a nondestructive inspection technique for diffusion bonded spars was evaluated.

The work of Regalbuto of General Dynamics has shown that acoustic emission is a useful technique for testing joints. In his work, the emission was measured during a tensile test of a bar cut from a press diffusion bonded block. The latter does not qualify as a nondestructive method. However, under certain conditions, acoustic emission is believed to be a promising method for examination of butt joints in spars. For example, internal pressurization could provide a means for producing an acoustic emission signature.

Rohr Industries, Inc., San Diego, California performed a feasibility study on the use of acoustic emission technique for nondestructive evaluation of diffusion bonded butt joints. The primary purpose was to determine practicality and reliability of the technique and define the problems involved in effective use of such a technique for a spar configuration.

Rohr currently uses acoustic emission for nondestructive evaluation of brazed and diffusion bonded structural honeycomb sandwich. The method makes use of a scheduled test load applied to honey comb sandwich which causes acoustic emission. The signature is used to estimate joint quality parameters such as ultimate strength and room temperature creep. Estimates of joint quality are based on a comparison of an acoustic emission signature of the test piece with predetermined standards.

The Rohr report "Acoustic Emission Techniques for Diffusion Bonded Titanium" is given in Appendix A. Three types of loading were used to produce an acoustic emission signature. Thermal loading and cantilever beam loading were used because of their applicability to production hardware. Tensile loading was used to produce a signature which could be correlated with a stress-strain curve. Due to panel configuration, it was not possible to evaluate pressurization as a loading method.

The results indicated that acoustic emission has potential for nodestructive evaluation of CSDB processed spars and that a program to develop a specific technique is recommended.

6

REPAIR TECHNIQUES

6.1 TYPICAL DEFECTS AND REPAIR TECHNIQUES

The necessity for repairs in a CSDB joint must be considered. The high forging pressure makes voids unlikely. It is, however, conceivable that an inclusion could be contained in the joint. In addition, incomplete forging or sheet stock geometry (e.g., inadequate thickness, notched or rounded sheet edge) could leave residual voids. There is also the possibility that surface damage could occur. Because of these possibilities, two types of repair techniques were examined, one for surface damage and one for inclusions or voids.

6.2 PROPOSED REPAIR METHODS

To establish and evaluate repair techniques, a series of different size holes, 1/8 inch, 1/4 inch and 1/2 inch diameter were drilled and reamed through a standard panel to simulate the removal of voids or inclusions. Surface damage was simulated by 1/8 inch, 1/4 inch and 1/2 inch diameter drill points into the surface of the panel, approximately 1/16 inch deep. Figure 55 shows the panel before repair.

Each of the through holes was filled with a press-fit plug extending 0.005 inch to 0.020 inch on each side of panel. One plug in each size was TIG welded into place on the top surface of the panel. Each of the drill point surface damage areas were overfilled with TIG welded titanium filler wire, one of which was ground flush with the surface.

The panel was then placed back in the panel bonding aid, without titanium foil added, but using 1/16 inch by 1 inch wide molybdenum thermal strips and subjected to the standard CSDB parameters. In addition to the repair panel, a panel was fabricated with two standard CSDB passes to evaluate the effect of altered microstructure on joint quality.

6.3 EVALUATION OF REPAIRS METHODS

Visual inspection of the repair panel showed almost no evidence of plugs on the top side and very little on the panel back side. No evidence showed for any of the drill point weld filled areas.

Photographic evidence of the 1/2 inch diameter plugs on the back side of the panel (most conspicuous example) is shown in Figure 56.

Figure 55. Panel prepared to evaluate repair techniques.

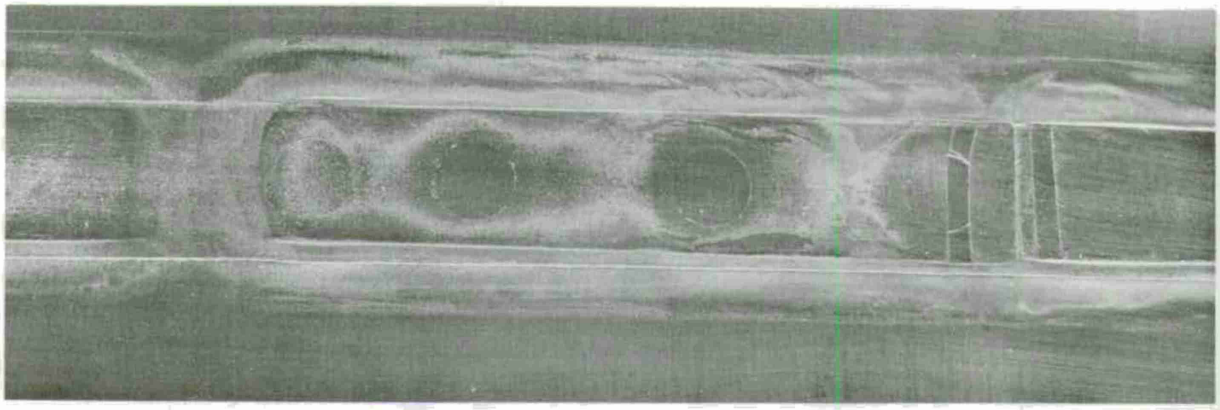

Figure 56. Section of repair panel after second bonding showing location of one-half inch diameter plugs.

Radiographic inspection of the repair panel did not reveal any indications along the bond line or associated with repair regions.

Mechanical properties of the repair regions are given in Table 7. Also included in the table are the properties of the panel subjected to two standard CSDB passes and the CSDB processed-no joint material. The bend and tensile specimens were fabricated with the plugs or drill points in the center of the section. Since the resonant fatigue specimens are fabricated with a reduced cross section to induce failure along the bond line, the weld repairs were located such that both bond line and repair material were in the reduced cross section.

The bend specimens containing repairs failed either in the HAZ away from the repair or around the repair interface. However, tensile strengths of all repair areas were high and failure in all cases occurred away from the joint and heat affected zone in parent material. The resonant fatigue results are within the range exhibited by CSDB processed-no joint material.

TABLE 7. EFFECT OF REPAIR TECHNIQUES ON JOINT QUALITY

	Repair Panel							Std. Panel Bonded Twice	CSDB Processed No Joint
Condition	1/8 in. plug	1/4 in. plug	1/2 in. plug	1/8 in. drill pt.	1/4 in. drill pt.	1/2 in. drill pt.	no repair	Std	no joint
Bonding Parameters	Std 2 passes	Std 2 passes	Std 2 passes	Std 2 passes	Std 2 passes	Std 2 passes	Std 2 passes	Std 2 passes	Std
4T Bend Tests									
Top up	-	JZ-around plug	-	HAZ	HAZ	-	4T, JZ	4T	-
Top down	JZ-around plug	-	JZ	-	HAZ	-	4T, JZ	JZ	-
Tensile Tests									
0.2% yield (ksi)	133.1	131.8	121.2	-	-	129.1	-	128.3	122.6[a]
Ultimate Tensile Strength (ksi)	139.0	138.8	140.0	-	-	141.1	-	139.6	137.9[a]
Maximum Stress at Joint (ksi)	127.1	128.2	132.4	-	-	140.9	-	138.5	138.5[a]
2% Elongation	3.5	2.5	3.5	-	-	7.5	-	11.5	12.5[a]
1% Elongation	1.0	1.5	1.5	-	-	5.5	-	5.0	13.3[a]
Location of Failure	PM	PM	PM	-	-	PM	-	PM	HAZ
Resonant Fatigue									
Cycles to Failure at 0.100 in. Defl.	2×10^5	1.6×10^5	3×10^5	4×10^5	-	$>10^7$	-	-	1×10^4 to[b] $>5 \times 10^6$
Location of Failure	HAZ	JZ-through plug	JZ-through plug	HAZ	-	did not fail	-	-	HAZ[b]

[a] Average of 3 specimens
[b] Five specimens tested

Examples of the microstructure in the repair areas are shown in Figures 57 and 58. The location of the plugs was apparent from grain structure differences as shown in Figure 58a. As can be seen in the photomic rographs, a good to moderate quality joint was formed at the plug-panel interface. Grain growth across the bond line was noted throughout the section and the special overetching method was required to reveal any indication of the bond line. An example of the joint region in the panel bonded twice is given in Figure 59. The only noticeable difference in structure from a single pass panel is an increase in grain size.

6.4 CONCLUSIONS AND RECOMMENDATIONS

Effective repair techniques applicable to full scale spars have been demonstrated. However, a parametric study of second pass bonding parameters will be necessary to optimize repair procedures.

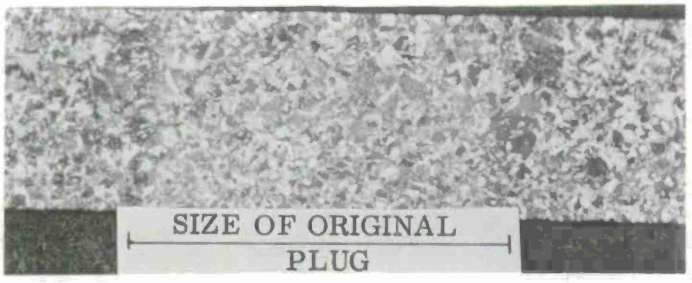

a) Magnification: 8X.

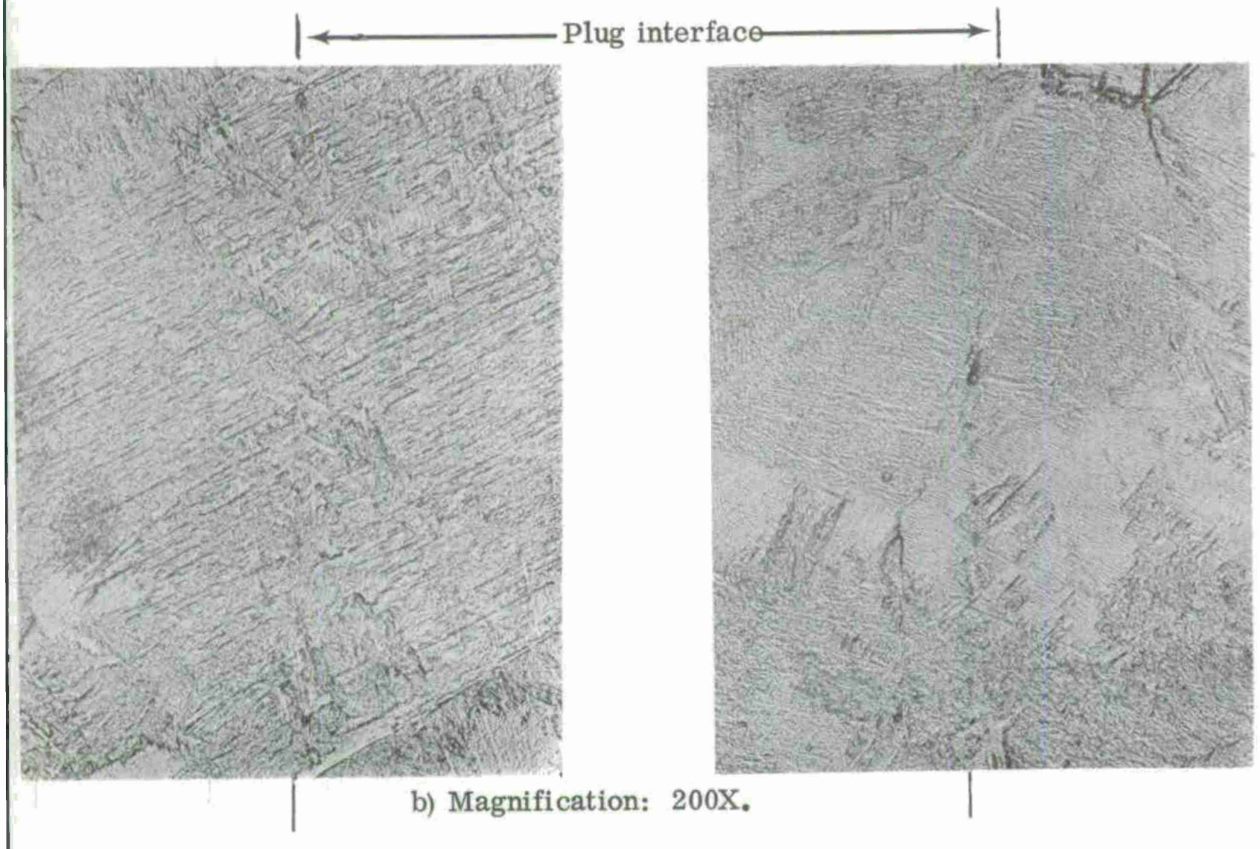

b) Magnification: 200X.

Figure 57. Microstructure of repair section containing 0.25 inch diameter plug. Etchant: 2 min Kroll's + 4 sec CSDB.

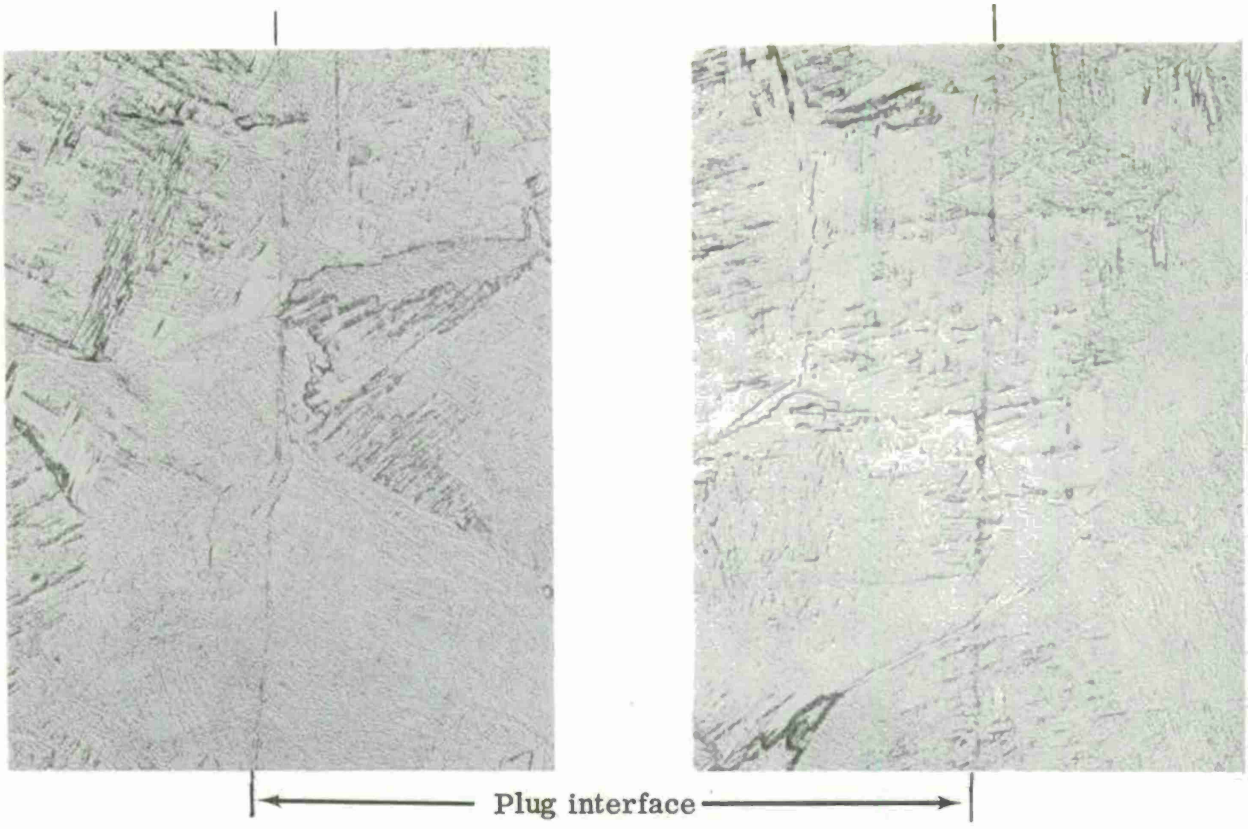

Figure 58. Microstructure of repair section containing 0.50 inch diameter plug. Etchant: 2 min Kroll's + 4 sec CSDB. Magnification: 200X.

Figure 59. Microstructure of joint region after two standard CSDB operations. Etchant: 2 min Kroll's + 4 sec CSDB. Magnification: 200X.

7

RECOMMENDATIONS FOR FUTURE WORK

The principal and most immediate work to follow this program is expected to be application of the CSDB process to full size UTTAS helicopter rotor spars. The recommendations for future work will be directed first, to this immediate short range objective, and, second to longer range objectives.

7.1 RECOMMENDATIONS FOR WORK TO APPLY CSDB TO UTTAS SPARS

The first butt joints made by CSDB used two opposed wheels on each side of the sheets. This symmetrical condition provided uniform heating through the joint. Access to one side of the joint by a wheel is not possible with the spar. Instead, internal tooling is used with a wheel on the outside. Earlier work on nine foot sections of spars revealed two problems related to the tooling: (1) heating-up of the tooling along the length, eventually requiring a reduction in power input; and (2) excessive heat loss on lower side so that bond quality was poorer on the inside. The second problem has been solved to a great extent by the work on this program, particularly by minimizing and controlling the heat flow from the backup bar (see Figure 2). The length affect could not be studied on this program with three foot long tools. However, the temperature distribution in the joint is dependent on the tooling mass, configuration and other factors. Differences resulting from the tooling for a spar and the tooling used on this program will require repetition of some of the studies, but these will be aided very considerably by the identification of the relative importance of each processing factor resulting from this program.

Specific recommendations for work to support application to the spar include studies of:

- Use of 1-1/4 inch wide molybdenum foil to separate steel thermal strip and titanium to eliminate occasional pits that result from steel titanium contact and interaction.
- Use of unalloyed titanium foil instead of Ti-6Al-4V foil. The low flow strength of the unalloyed titanium will aid flow to accommodate differences in sheet thickness and to fill in the V-notch resulting from poor fit-up.
- Consistency of bond quality along panel. Perform a minimum of 20 bend tests along 30 inch panel to assess consistency.

- Repair techniques. Establish repair methods for butt joints.
- Acoustic emission for quality assurance. More work is recommended to evaluate this technique for inspection of spars.
- Use of molybdenum for reuseable thermal strips. Results on the repair of panels on this program showed that molybdenum thermal strips could forge the sheet plus thicker inserts to a uniform gage. Also, the strips did not deform and could be used again.
- Develop relation between well characterized defects, ultrasonic inspection signature and mechanical properties.

7.2 RECOMMENDATIONS FOR FUTURE WORK ON CSDB OF BUTT JOINTS

Recommendations for general, long range work to advance the reliability of CSDB butt joints and to advance the applications of this joining method include:

- Investigate origin of fracture dimples by higher resolution electron microscopy.
- Investigate new approaches to identify flat fractures by nondestructive methods.
- Generation of design data for CSDB butt joints.

APPENDIX A

ACOUSTIC EMISSION TECHNIQUES FOR DIFFUSION BONDED TITANIUM

MODEL	CONTRACT NO.	DATE
	DAA-646-75-C-0040	6-24-75

RHR-75-246

ENGINEERING

TECHNICAL NOTE NO. 863-280

ACOUSTIC EMISSION TECHNIQUES FOR DIFFUSION BONDED TITANIUM

Prepared by: D. Weir

D. B. Weir
Structures Engineer, Senior

Approved: I. Holehouse

I. Holehouse
Technology Staff Engineer

Checked by:

Approved: F. Hom

F. Hom, Manager
Development Engineering

REVISIONS

DATE	REV.BY.	REVISIONS AND PAGES AFFECTED	REMARKS

ROHR INDUSTRIES, INC.
Chula Vista, California 92012

SUMMARY

The program objective was to evaluate the feasibility of using Acoustic Emission (AE) techniques for the nondestructive evaluation (NDE) of diffusion bonded joints made in the titanium alloy Ti-6Al-4V by a Solar International Diffusion Bonding Machine.

Feasibility requirements and suitable production test methods were identified. Representative laboratory test methods were selected and evaluated including thermal loading, cantilever beam and tensile coupon. Eighteen test specimens were made. Six were used to develop test techniques and twelve; including six control and six diffusion bonded, were used to evaluate the techniques. Reasonable correspondence between specimen stress and acoustic emission was observed for the tensile coupon but additional evaluation cycles (i.e., programmed variations of test method, test specimen and joint strength quality criteria) are needed to demonstrate feasibility.

CONTENTS

FIGURES

1/ INTRODUCTION

Solar International is currently engaged in the development of a machine which can be used to make diffusion bonded joints in titanium. The machine is especially suited to making longitudinal joints in tubular sections such as might be used for a helicopter rotor blade.

As a part of the development program, a prototype machine has been built and is being used to establish manufacturing and processing parameters. In this regard, bonded joints are made using variations in manufacturing techniques and process control and the resulting joints are evaluated for structural integrity.

Coincident with the development program for the machine and for the process, Solar has been evaluating suitable NDE techniques for inspection of the resulting joint. One technique being considered is AE and AE data for joints similar to the Solar joint has been reported in Reference 5. The data indicates that AE has potential for the application.

The purpose of this program was to evaluate the feasibility of using AE for NDE of joints made on the Solar machine using the titanium alloy Ti-6Al-4V. In the context of this report, evaluate means to identify problem areas affecting practicality and reliability of such an NDE system, estimate the magnitude of the problems and determine AE signatures for representative test specimens and methods.

2/ BACKGROUND

Acoustic Emission (AE) technology is being used at Rohr Industries for NDE of brazed and diffusion bonded structural honeycomb sandwich. The technique is referred to as the Acoustic Inspection Method (AIM) and is described in references 1, 2 and 3. Related AE technology is reported in References 4 and 5.

The AIM technique makes use of a scheduled test load applied to honeycomb sandwich which causes AE. The AE signature is used to estimate joint strength quality (JSQ) parameters such as ultimate strength and room temperature creep. Estimates of JSQ for sandwich are based on a comparison of an AE signature of the test article with predetermined standards.

3/ PROGRAM

A block diagram of the evaluation program is shown in Figure 1. The diagram outlines the sequence of operations used to evaluate the feasibility of several test methods and also to identify factors which impact on test methods such as the specimen design and the standard or criteria used for JSQ.

To be feasible, in the sense used here, the method must be capable of:

1. Detecting AE related to properties or characteristics of the bond which affect ultimate tensile strength (UTS).
2. Producing an AE signature which can be used to predict UTS.
3. Being adapted to testing of production type hardware having longitudinal joints in circular or irregular tubular cross sections.

Two NDE test methods were considered for use in a production environment.

1. Internal pressurization which would cause tension in the bond joint for a circular section and tension and compression for non-circular sections such as an ellipse.

2. A locally applied scanning load which would be applied by either a mechanical or thermal device. The mechanical device could be either a ram load applied at intervals along the joint or a continuously moving load applied by a roller. The thermal load could be applied by radiant heat from a flame, quartz lamp or similar device and could be applied at intervals or continuously along the joint.

The initial JSQ parameter considered was ultimate tensile strength. Other potential JSQ parameters are creep strength, fatigue life, metallurgical properties, void size and number or size of void per unit of joint length.

4/ TEST MODES

Three laboratory type test modes were used to evaluate the principals implicit in the tests being considered for production hardware.

1. A thin column fixed at each end and loaded by end compression induced by thermal expansion.
2. A thin cantilevered beam having a concentrated load at or near the outboard end.
3. A tensile coupon loaded by axial tension.

The thermally loaded column and the cantilevered beam modes were selected for evaluation because the conclusions could be applied, within limits, to the production hardware tests.

The tensile coupon test mode was selected because:

1. It could be used to evaluate correlation between AE testing techniques and JSQ of the bonded specimens.
2. It is representative of the stress in a circular pressurized tube.
3. The test could be used as a control for the thermal or cantilever tests.

5/ TEST SPECIMENS

The specimen selected for testing is shown in Figure 2. It was selected as the initial configuration because it could be adapted to the three laboratory test modes being evaluated and could be made from available test panels. In this regard, the configuration of the available test panels, and therefore the specimens, were fixed by a capability limitation of the Solar Bonding machine; the limitation being that the panels were four inches wide and had a joint down the middle.

Eighteen specimens were made in accordance with the design shown in Figure 2; six by Rohr Industries and twelve by Solar International.

The six Rohr specimens, none of which had a diffusion bonded joint, were used during development and evaluation of the initial test fixtures and procedures.

The twelve Solar specimens included six parent metal specimens used for control and six bonded specimens used for evaluation of the process. The bonded specimens had an undetermined range of JSQ.

6/ INSPECTION

The bonded specimens were radiographic inspected for voids by Solar prior to the tests.

All specimens were inspected for pertinent physical dimensions by Rohr before and after testing.

Evaluation of the specimens after testing was to be conducted by Solar. The major purpose of the post-evaluation was to detect defects or other characteristics which could be related to AE.

7/ TEST PROCEDURE

A standard test procedure was selected for each of the three test modes and the specimens were, as nearly as was practical, all tested in the same manner. Acoustic emission amplification was 90 dB.

The test sequence was:

1. Thermal
2. Cantilever - Short moment arm.
3. Cantilever - Long moment arm.
4. Tensile proof.
5. Tensile ultimate.

By sequential testing at successively higher stress levels, the same specimens could be used in each of the test modes.

7.1 THERMAL LOAD TEST

The thermal loading method was evaluated to gain experience with fixtures, equipment and AE characteristics which could be used to simulate a production test. The test fixture and method are shown in Figure 3. The heat source used was an oxygen-acetylene flame. Thermal stress was caused by heating the specimen in the area of the bonded joint while the ends of the specimen were held clamped to prevent longitudinal movements. The flame temperature was stabilized while the flame was off-set from the specimen.

After stabilization of the flame temperature, the flame was moved across the specimen in a direction parallel to the joint. The velocity of movement was about 0.40 inches per second. The resulting specimen temperature measured by the thermocouple method was about 300°F.

Thermal scan signatures for the Solar diffusion bonded specimens are summarized in Figure 4. The high emission for the bonded specimens was probably due to the effects of the foil bonded to the surface of the coupon during the joining process.

Conclusions reached for this thermal loading method were:

1. Thermal loading is a convenient method to apply a stress to the coupon and may be convenient for a longitudinal joint in a tube.
2. Background emission from the fixture-specimen interface occurs but could probably be adequately controlled.
3. Background emission during tube testing in production would be insignificant because fixture constraint would be minimal.
4. A detailed and exact thermal stress distribution could be determined but would not be necessary provided the thermal input is held constant.

7.2 CANTILEVER BEAM LOAD TEST

The cantilever beam test was evaluated to gain experience with the fixtures, equipment, and AE signatures which could be used to simulate a production test involving tube wall bending.

The specimens were loaded in two modes: a short moment arm (SMA) mode which produced predominately shear and contact stress and a long moment arm (LMA) mode which produced predominately tension and compression stresses due to bending.

The SMA test was used to evaluate the effects of ram contact force on the AE signatures and the LMA test to evaluate bending stress

requirements necessary to produce meaningful AE. It is expected that the results of the LMA tests could be related, to some extent, to the results of tensile coupon tests.

Load signatures for each specimen are shown with their respective AE signatures.

7.2.1 SHORT MOMENT ARM TEST -- The SMA test is shown in Figure 5. Stress in the plane of the joint is predominately shear.

AE signatures were recorded for a test stress of 34500 PSI tension due to bending and are summarized in Figure 6. Significant background emission resulted from the contact stress between the ram and specimen and between the specimen and clamping fixture. The contact stress and therefore the AE was variable and depended on the surface condition of the specimen, contour of the ram face and clamping force of the fixture.

Contact emission between the ram and specimen could be reduced by pre-stressing the contact areas of the ram and specimen. The prestressing technique would be difficult to adapt to a production test.

Contact emission between the specimen and fixture can be reduced by increasing the clamping force and using a thin nylon shim between metal surfaces. For the production test, fixture emission could be reduced by the use of nylon insulated clamping fixtures.

7.2.2 LONG MOMENT ARM TEST -- The LMA test is shown in Figure 7. Stress in the plane of the joint is predominately tension and compression due to beam bending. The test would be sensitive to the location of the defect with respect to the surface.

AE signatures were recorded for a test stress of 50000 PSI tension due to bending and an example is shown in Figure 8.

Background emissions from ram contact and fixture clamping for the LMA tests were significantly reduced compared to the SMA test.

Conclusions reached from the cantilever beam test evaluation were:

1. Contact emission was high and nylon pads would be needed.
2. For a production test, optimum conditions occur where a small applied force can be used to cause significant bending stress (i.e., a LMA is preferred).
3. A nylon wheel could probably be used to apply a continuously moving load.

7.3 TENSILE COUPON TESTS

The tensile coupon test was evaluated to gain experience with the fixtures, equipment, AE characteristics and its potential for correlating AE and JSQ for bonded specimens.

7.3.1 ROHR CALIBRATION SPECIMENS

The six Rohr Calibration Specimens (RCS) were tested during this phase to determine requirements for:

1. Transducer placement
2. Presetting pin holes
3. Loading rate and holding time
4. AE amplification
5. AE and load signature display.

Several methods for attaching the transducer were evaluated and rejected for the following reasons:

1. Directly on the specimen; the specimen was too small and the surface too uneven for good transducer contact.
2. Mounted on the side plate; the background emission from the fixture was too great.
3. Mounted on a wave guide clamped between the specimen and side plate and insulated from the side plate; was not repeatable.

The method found to be most suitable was to mount the transducer on a contoured wave guide clamped to the specimen. The method was awkward to assemble but was repeatable.

The pin holes were preset by applying a compression load to each end of the coupon while supported on the pins. The preload was twice the test load used.

The test fixture selected from these tests is shown in Figure 9; the test stress used in Figure 10; and examples of the selected loading rates, holding times, AE amplification and AE load signatures in Figure 11.

The AE signatures were recorded using two formats; total acoustic emission (TAE) and total acoustic emission with a periodic reset (TAE-R). The two methods were used to improve signature visibility.

The tests were run in an ascending order of test stress to:

1. Check for fixture background noise (AE from the test article will not repeat because of the Kaiser effect).
2. Help select the optimum holding stress. The optimum stress in this case would be below the proportional limit but high enough to produce a significant AE signal.

Conclusions for the tensile coupon tests were:

1. Background emission from the fixtures was suitably low.
2. AE from the specimen at the higher holding stress appeared to be adequate for the intended purpose.
3. The rising and holding load sequence has potential for NDE of titanium coupons and possibly for bonded specimens.

7.3.2 SOLAR BONDED SPECIMEN TESTS -- The Solar tensile coupon tests were used to evaluate correlation between AE and JSQ for the bonded specimens.

Prior to testing, the specimens were arranged into groups of two; one control and one bonded. The purpose of the grouping was to permit evaluation of up to six potential loading methods. The groups and the specimens tested are shown in Figure 12. The single unit sample size was justified on the basis that AE signatures would be affected more by the test method than by variations between each of the six control and bonded specimens.

Three loading methods were actually evaluated:

1. Multiple rising and holding loads at successively higher stress levels until near failure.
2. A single rising load to failure.
3. A single rise and hold to near the proportional limit.

The test stress for each, and observations made for each coupon after test are shown in Figure 13. Examples of AE signatures are shown in Figure 14.

The primary conclusion was that a rise and holding load just below the proportional limit for the material offered the most potential for an NDE test.

Because of the limited number of specimens, no effort was made to evaluate correlation between bond imperfections and AE. For this task, a modified tensile coupon configuration and multiple tests would be required.

8/ CONCLUSIONS

The primary conclusions reached were:

1. The thermal loading method was convenient to use and background emission associated with testing production hardware would probably be low.
2. The cantilever beam method could be used to simulate bending stress encountered in testing production hardware but background emission control would require special consideration.
3. The tensile coupon test would probably be a useful control test because the background emission can be made low and the correspondence between AE and stress is reasonable.
4. A test load cycle comprising a single rise and hold sequence may be a suitable NDE test. The hold stress would be slightly below the proportional limit.

Summarizing; the test results indicated that AE technology has potential for NDE of diffusion bonded titanium in a production environment but a demonstration of feasibility would require additional testing.

The additional testing could be approached in three phases:

1. Select a standard tensile coupon specimen and test method and test sufficient number of bonded coupons to establish the necessary correlation between the AE signature and a significant JSQ parameter.
2. Develop a prototype production test (i.e., thermal or beam bending) and demonstrate correlation with JSQ.
3. Adapt the prototype test to production hardware.

9/ EQUIPMENT

Equipment used in the test program included:

1. A hydraulic operated loading frame. The frame, described in Reference 1, was adapted for applying loads to the cantilever beam and tensile coupon.

2. A clamping fixture for the thermal load tests.

3. A Dunegan two-channel system for acoustic emission detection.

4. A Minneapolis Honeywell X-Y-Y recorder for recording the AE and load signatures.

10/ REFERENCES

1. D. B. Weir, "Acoustic Emission NDT Technique for Structural Sandwich," Rhr-73-138, Rohr Industries, Inc.

2. D. B. Weir, "Loading Methods for Acoustic Emission Testing of Structural Sandwich," Rohr-74-508, Rohr Industries, Inc.

3. D. B. Weir, "Acoustic Emission and Thermal Scanning for Structural Sandwich," Rhr-75-016, Rohr Industries, Inc.

4. T. F. Drouillard, "Acoustic Emission, A Bibliography for 1970-1971-1972. Dow Chemical.

5. Nondestructive Testing of Diffusion Bonded Titanium Alloys for Engine and Airframe Components, AFML-TR-74-215, July 1974.

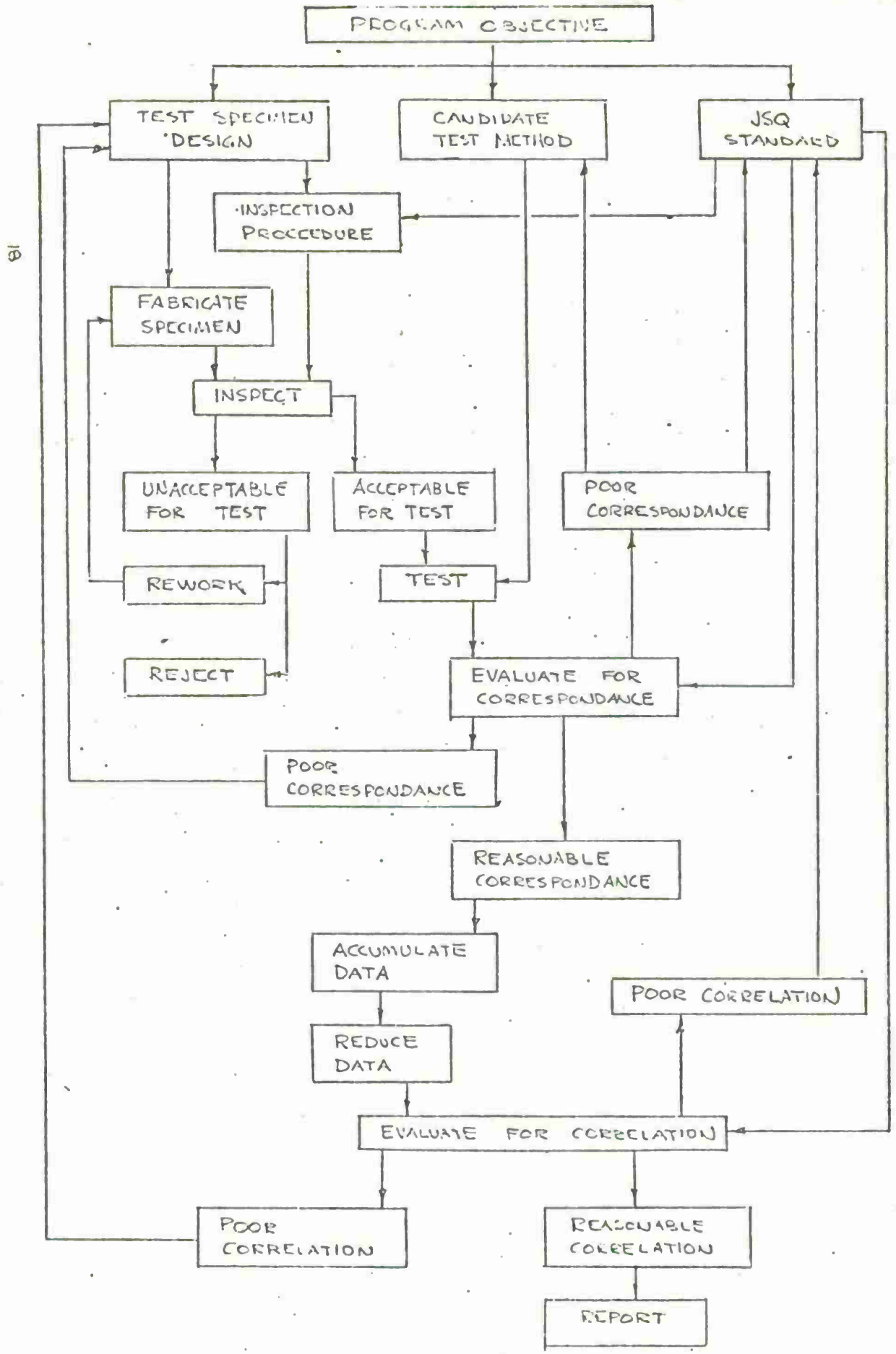

FIGURE A-1 EVALUATION PLAN

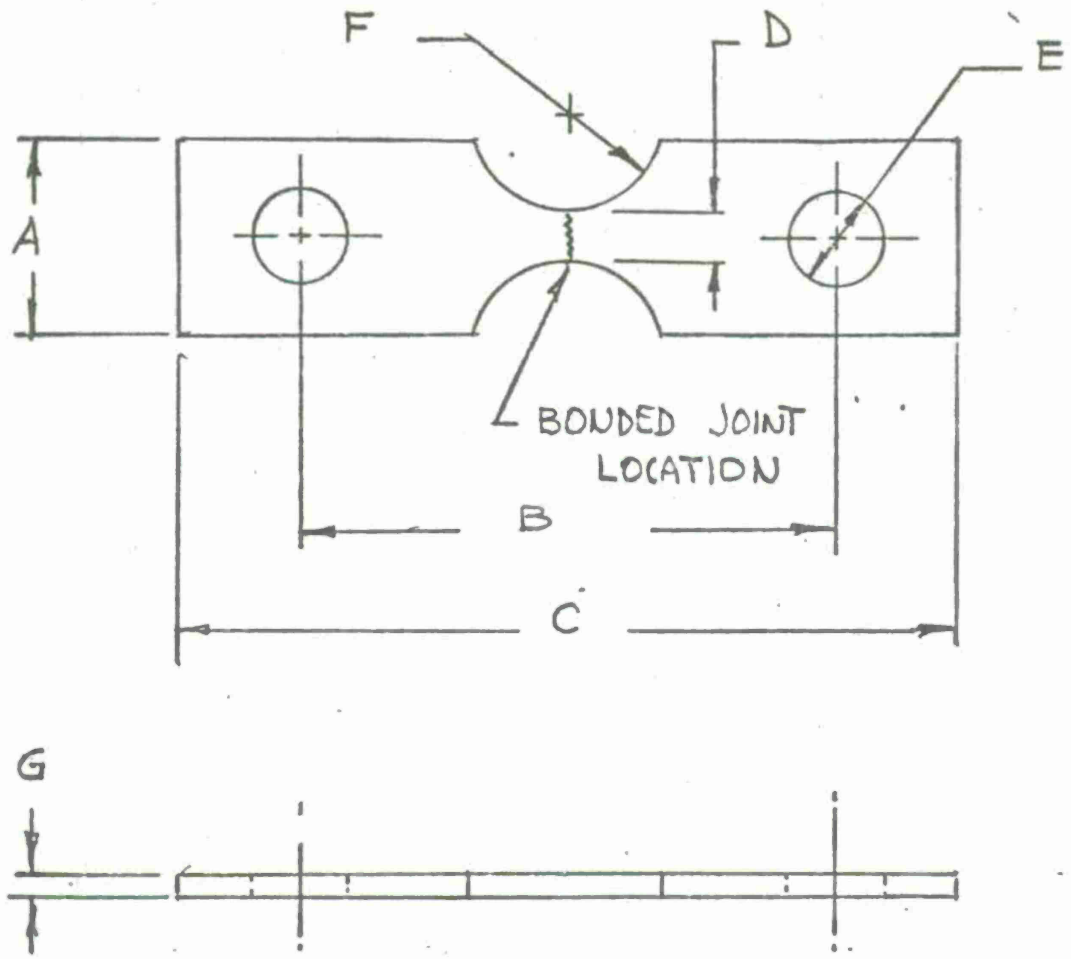

SPECIMEN								
NO.	DIMENSION (INCHES)							TYPE
	A	B	C	D	E	F	G	
1	1.0	2.75	4.0	0.25	0.38	0.75	0.12	RECOMMENDED
2	1.0	2.75	4.0	0.25	0.50	0.75	0.12	AVAILABLE

FIGURE A-2. TEST SPECIMEN

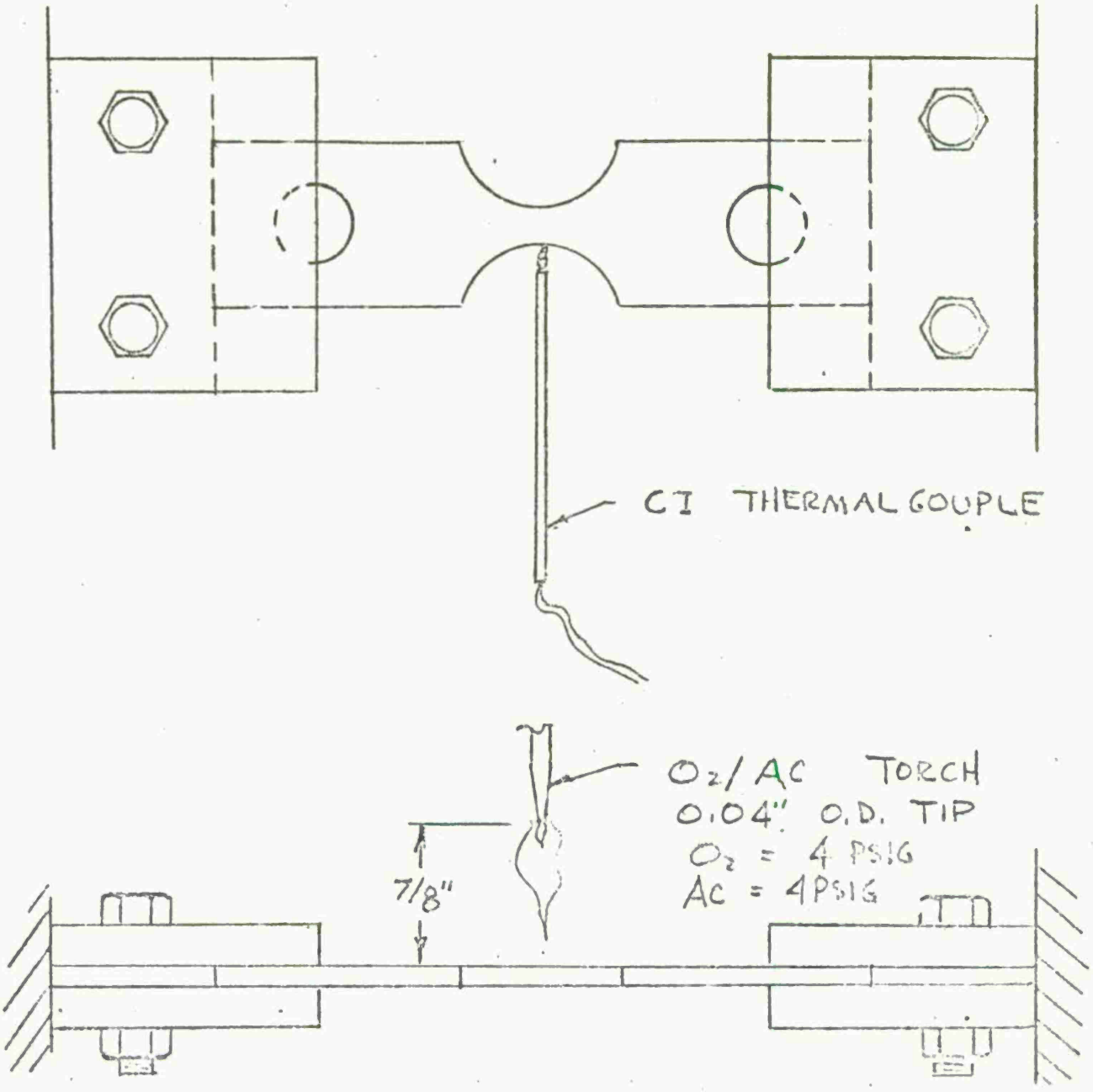

FIGURE A-3. THERMAL LOAD TEST

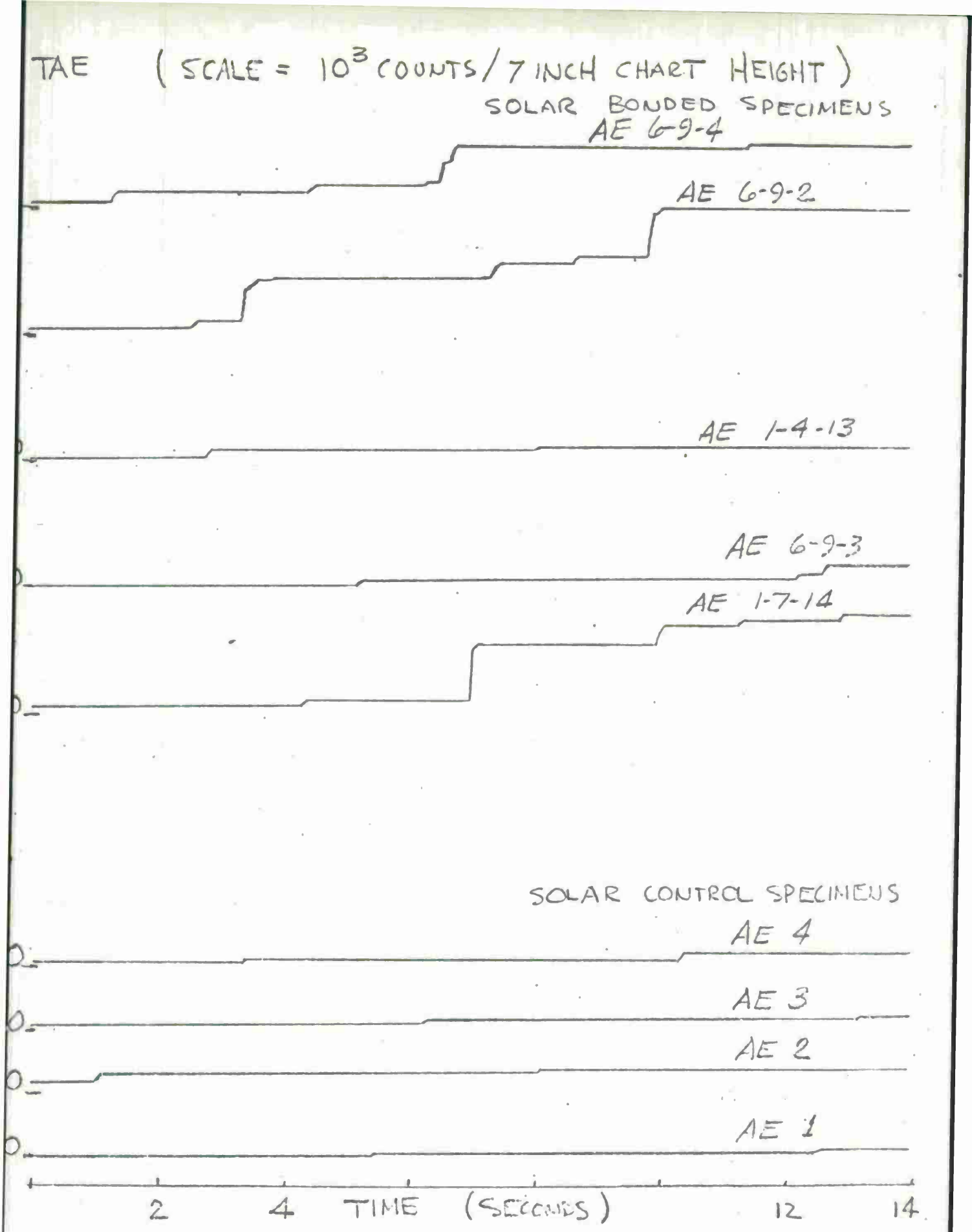

FIGURE A-1. THERMAL LOAD AE SIGNATURES

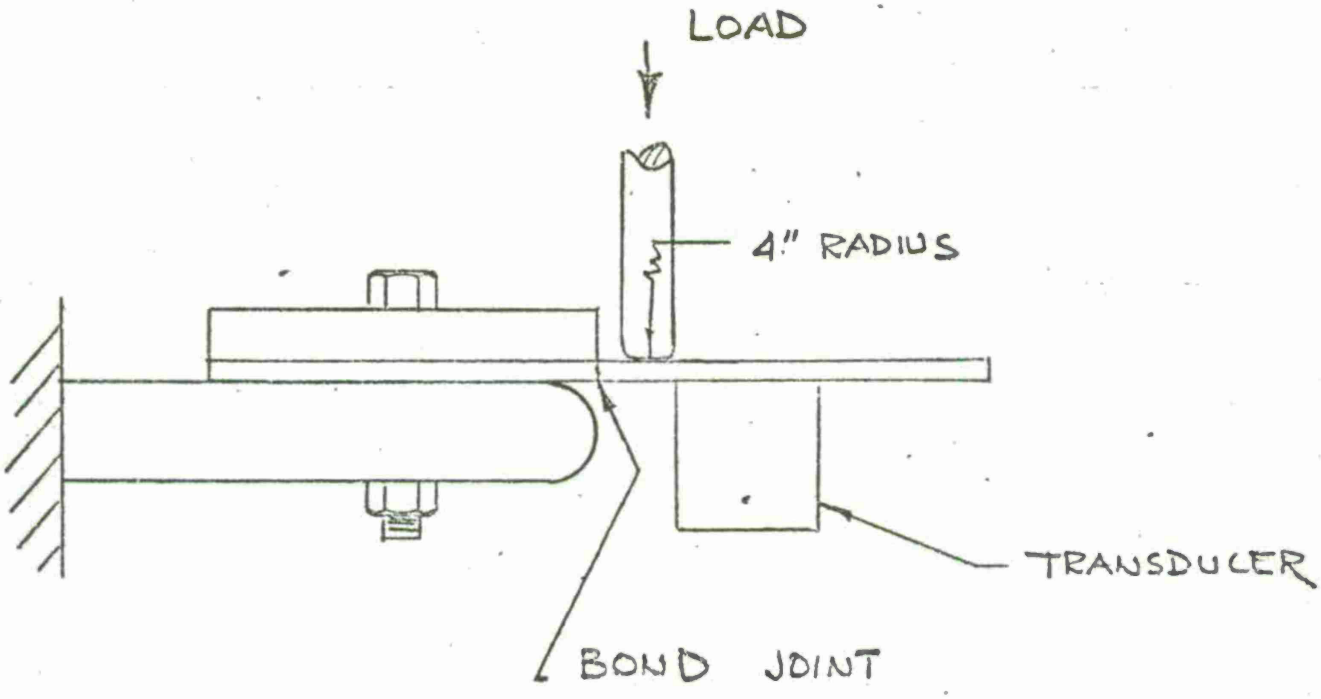

FIGURE A-5. CANTILEVER BEAM - SHORT MOMENT ARM TEST

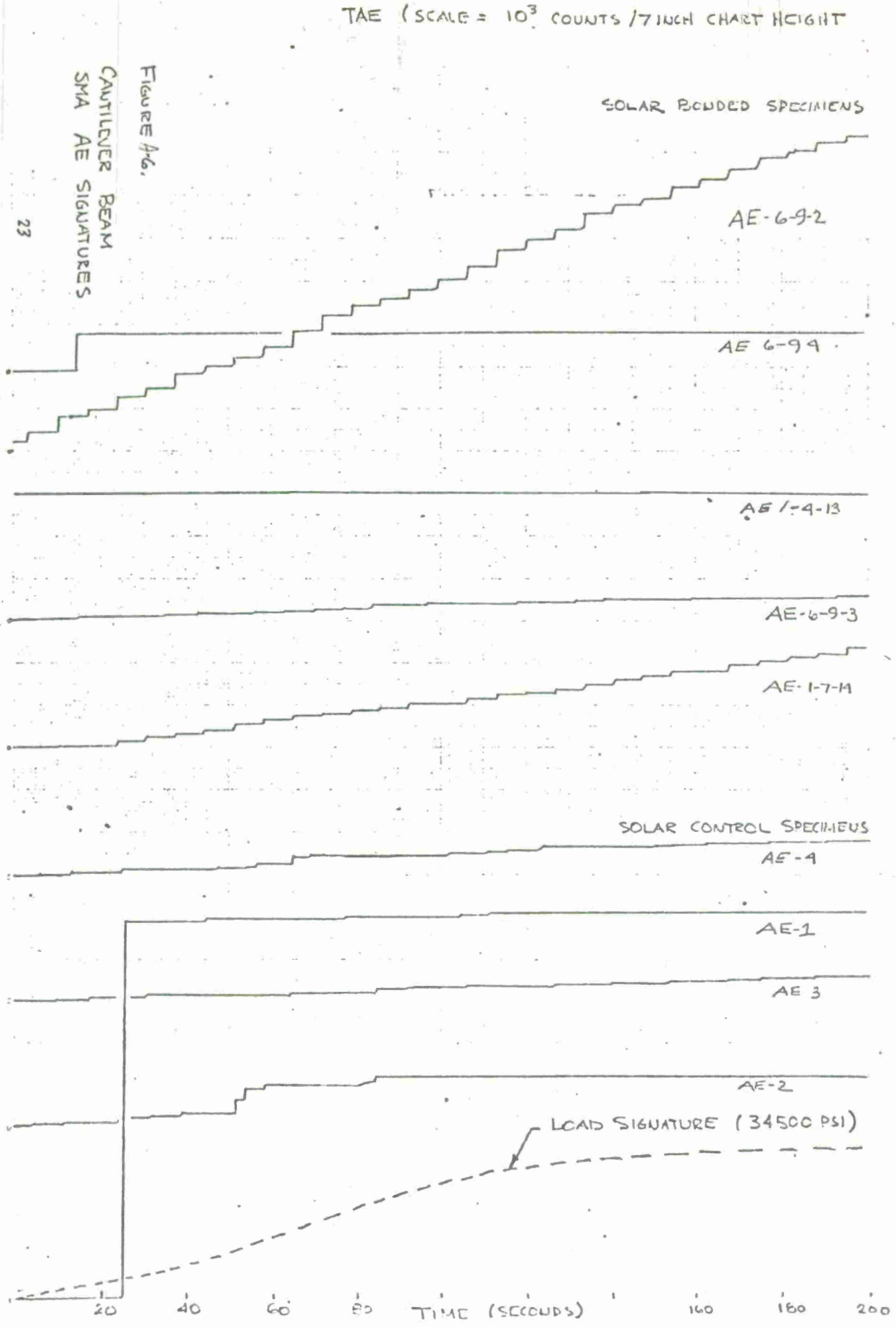

FIGURE A-6.

CANTILEVER BEAM SMA AE SIGNATURES

23

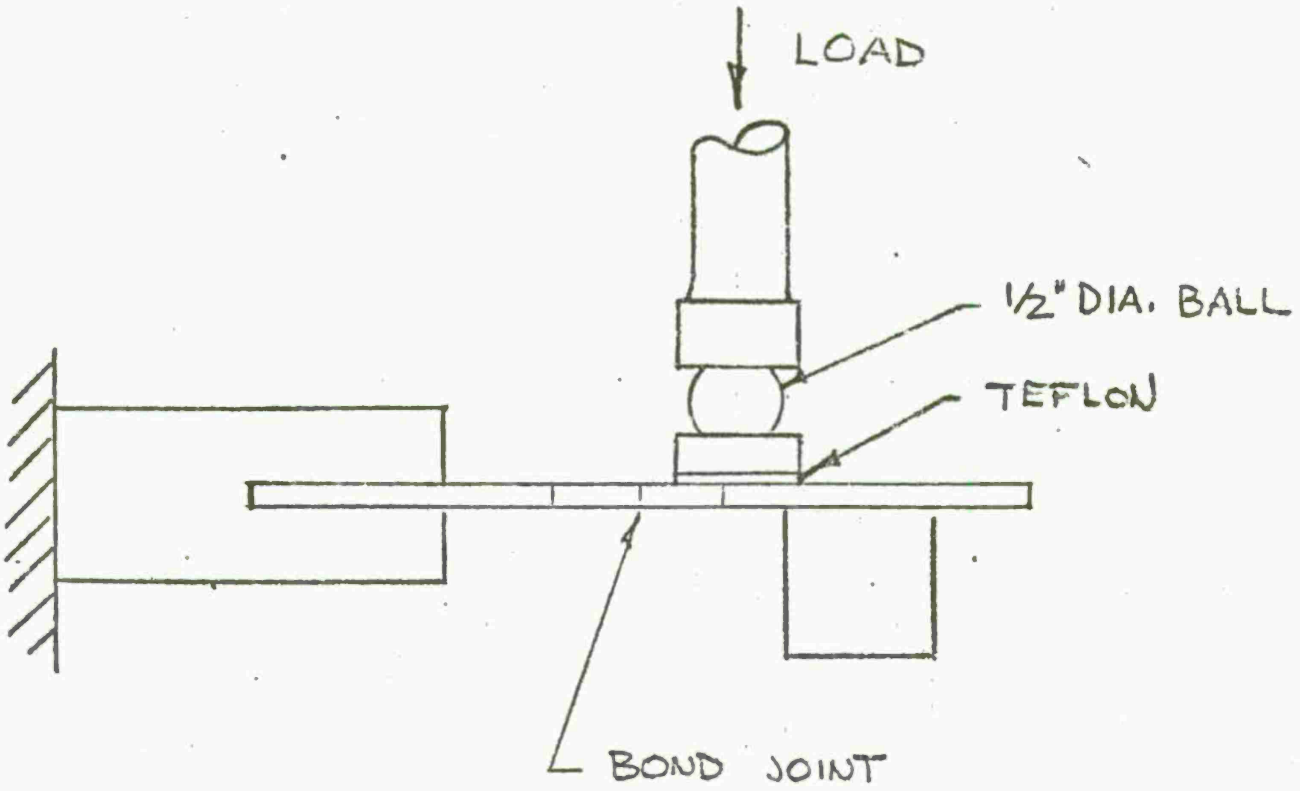

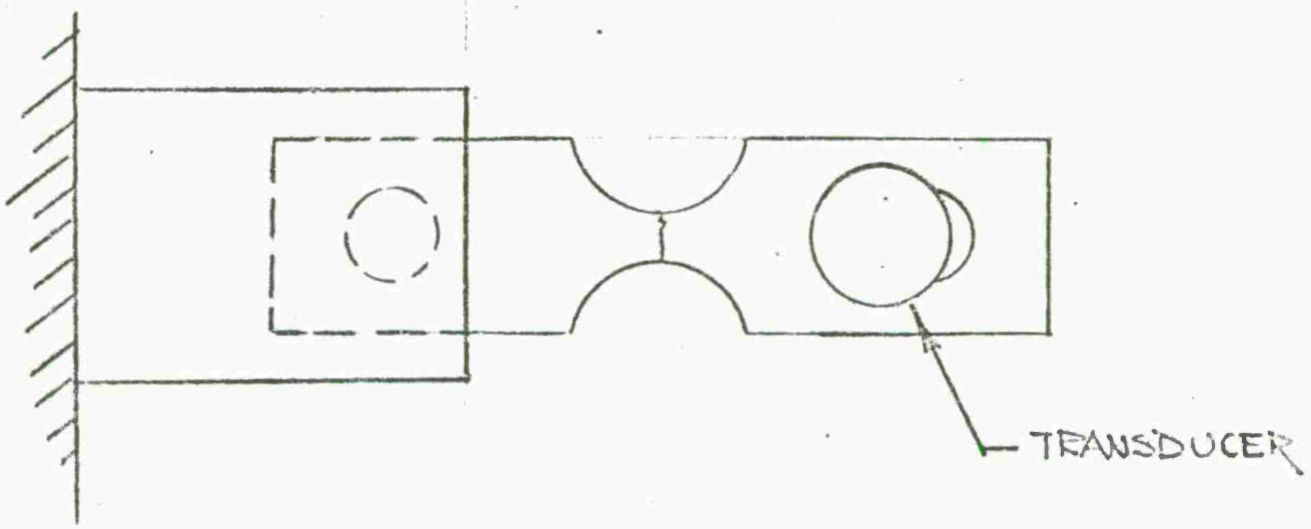

FIGURE A-7. CANTILEVER BEAM - LONG MOMENT ARM TEST

TAE x 10^5

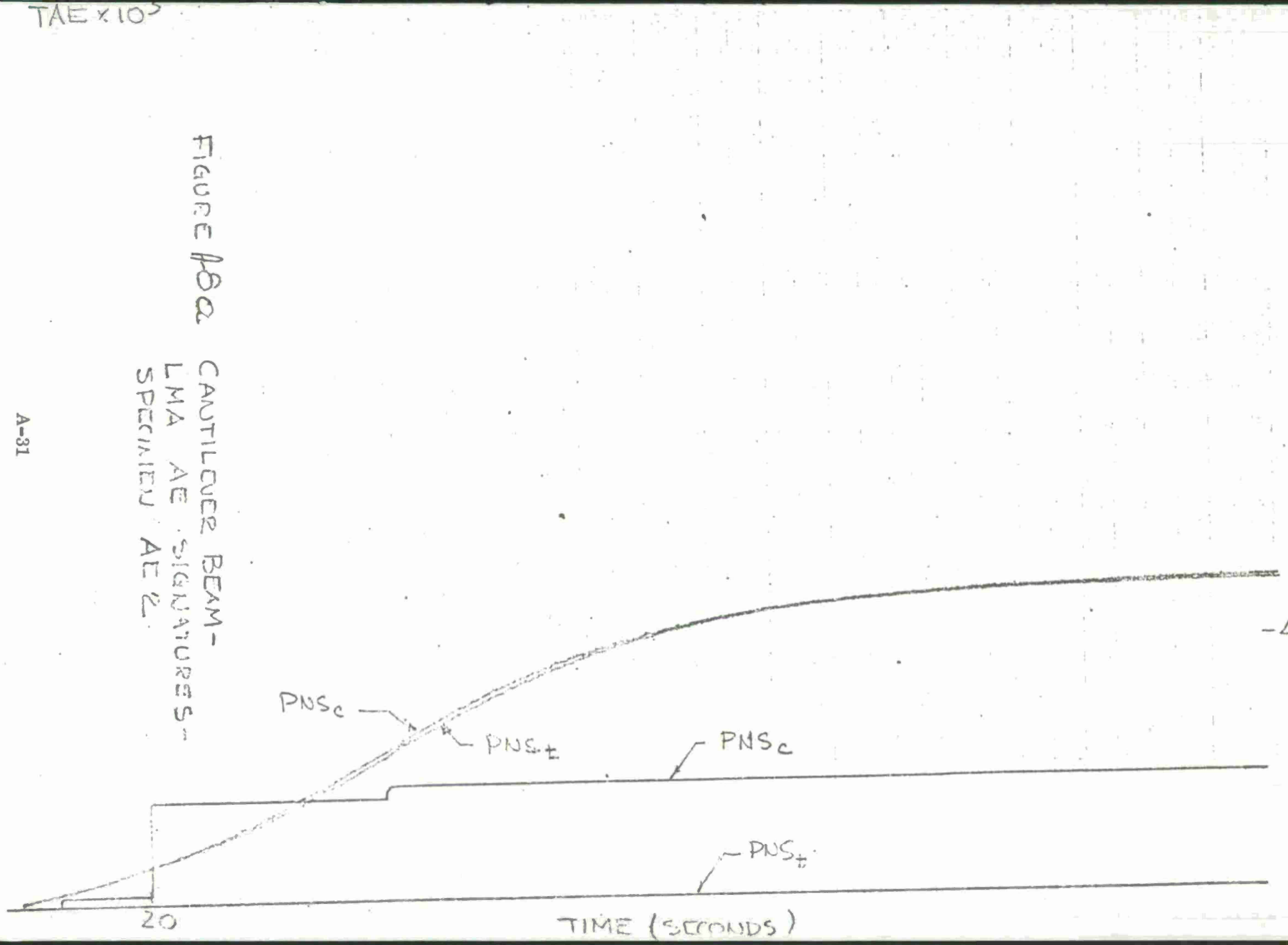

FIGURE A8a CANTILEVER BEAM-LMA AE SIGNATURES-SPECIMEN AE 2.

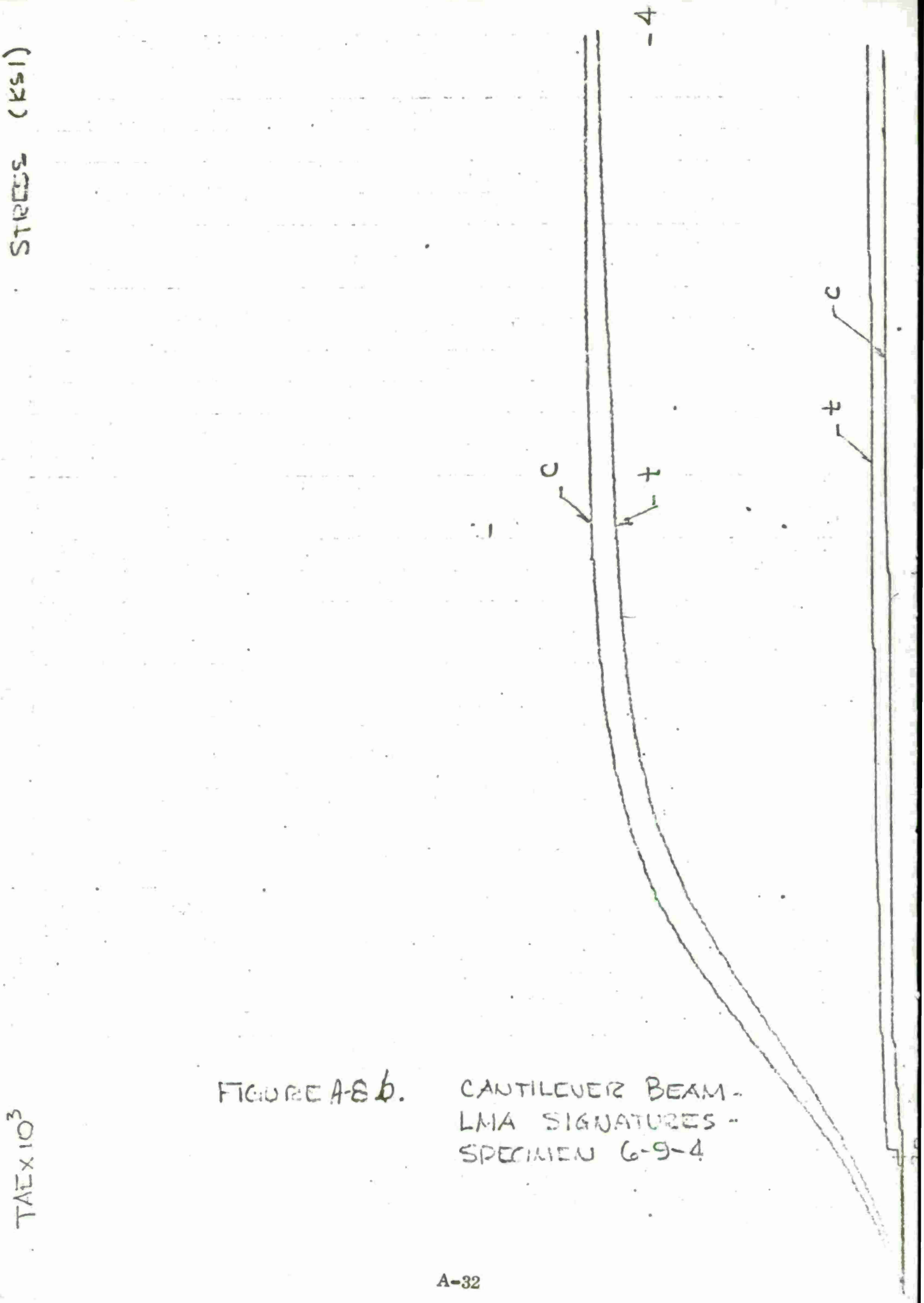

FIGURE A-8b. CANTILEVER BEAM - LMA SIGNATURES - SPECIMEN 6-9-4

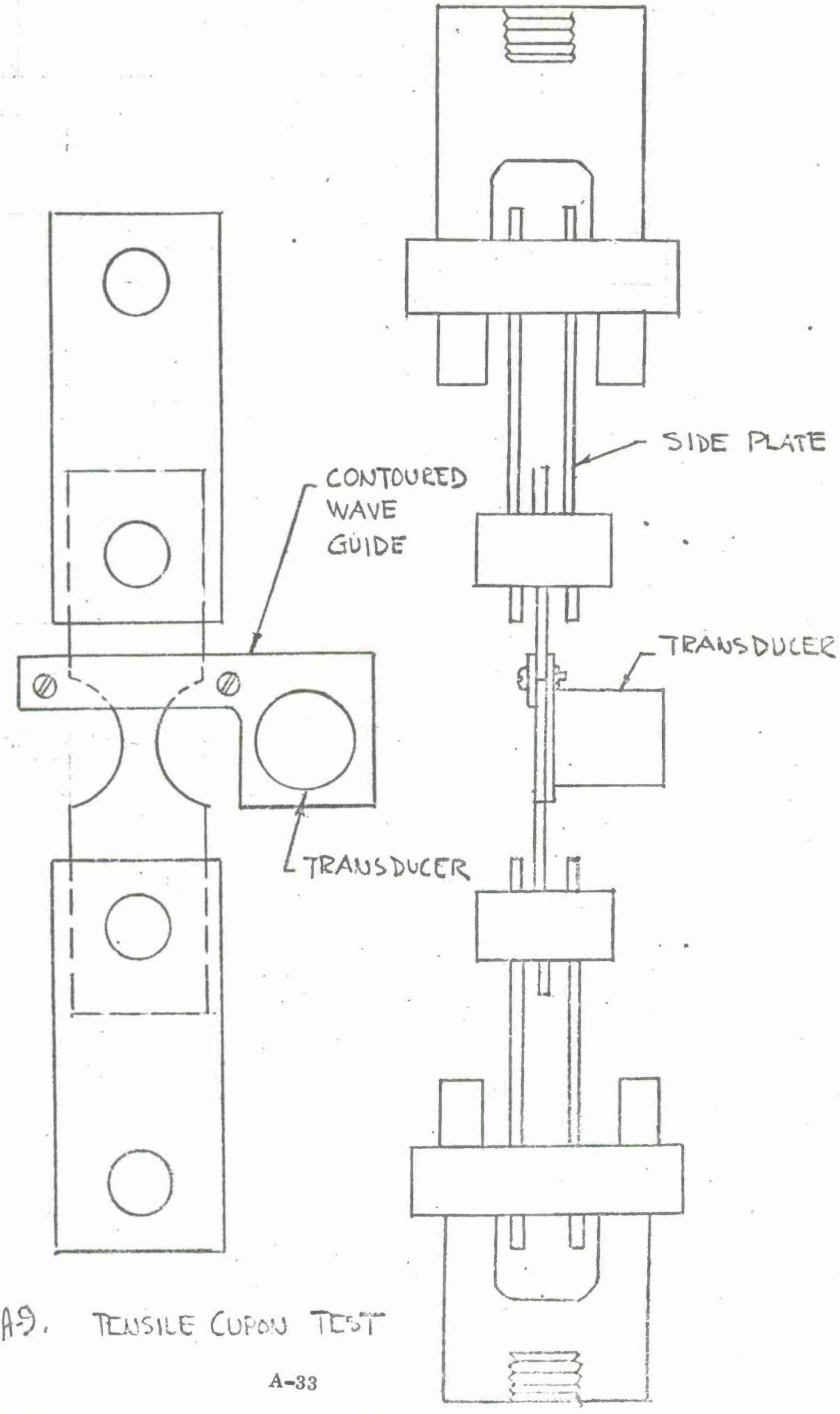

FIGURE A-9. TENSILE CUPON TEST

RUN	MAXIMUM STRESS (PSI)
1	110 400
2	121 000
3	135 000
4	141 000
5	145 000
6	148 500
7	151 400
8	157 000
9	155 000 UTS

FIGURE A-10. TEST STRESS, ROHR CALIBRATION SPECIMEN No. 3

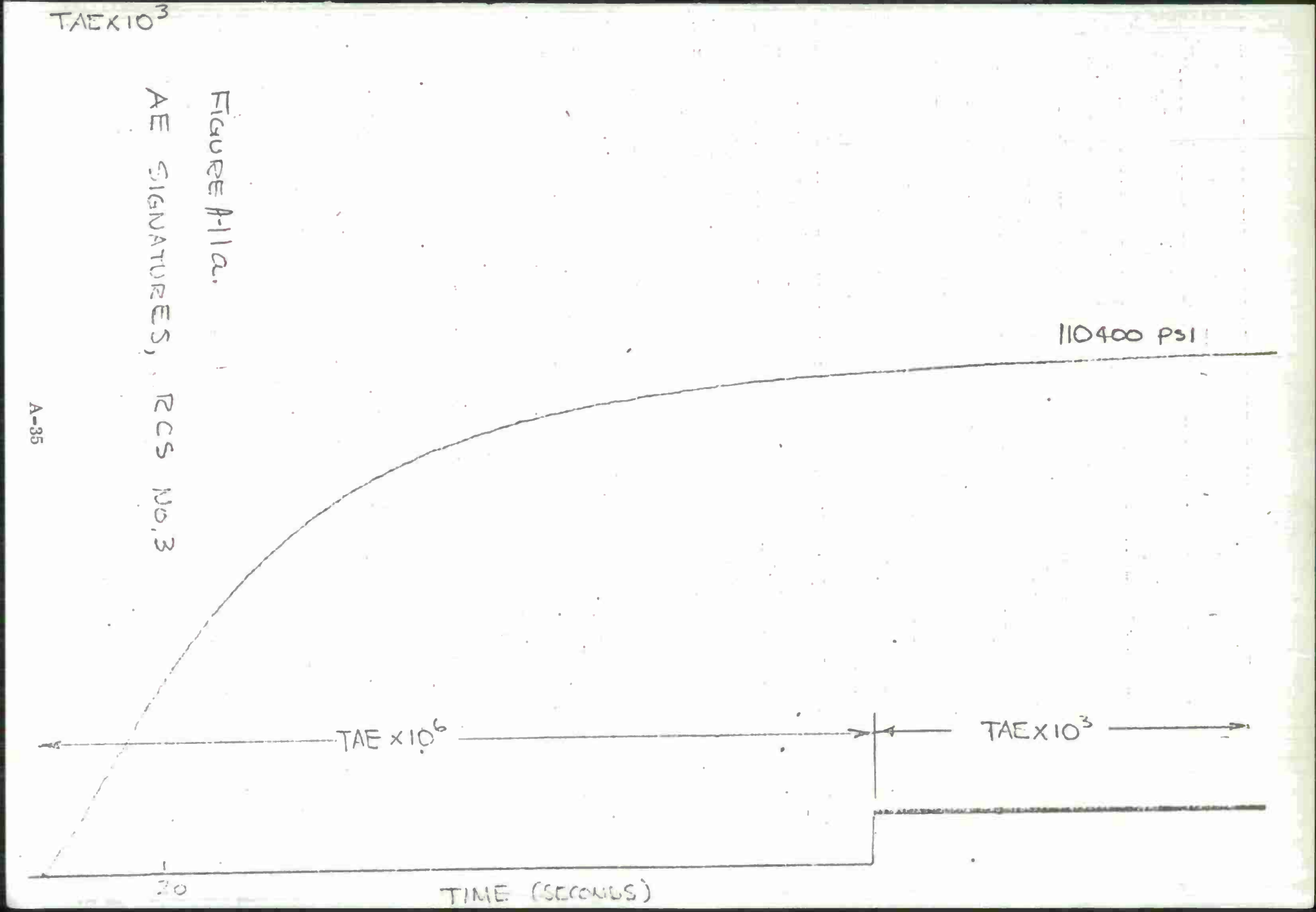

FIGURE A-11a.

AE SIGNATURES, RCS NO. 3

TAE x 10^2, REEFT 0.2 SECONDS
(110 400 PSI)

FIGURE A-11b.

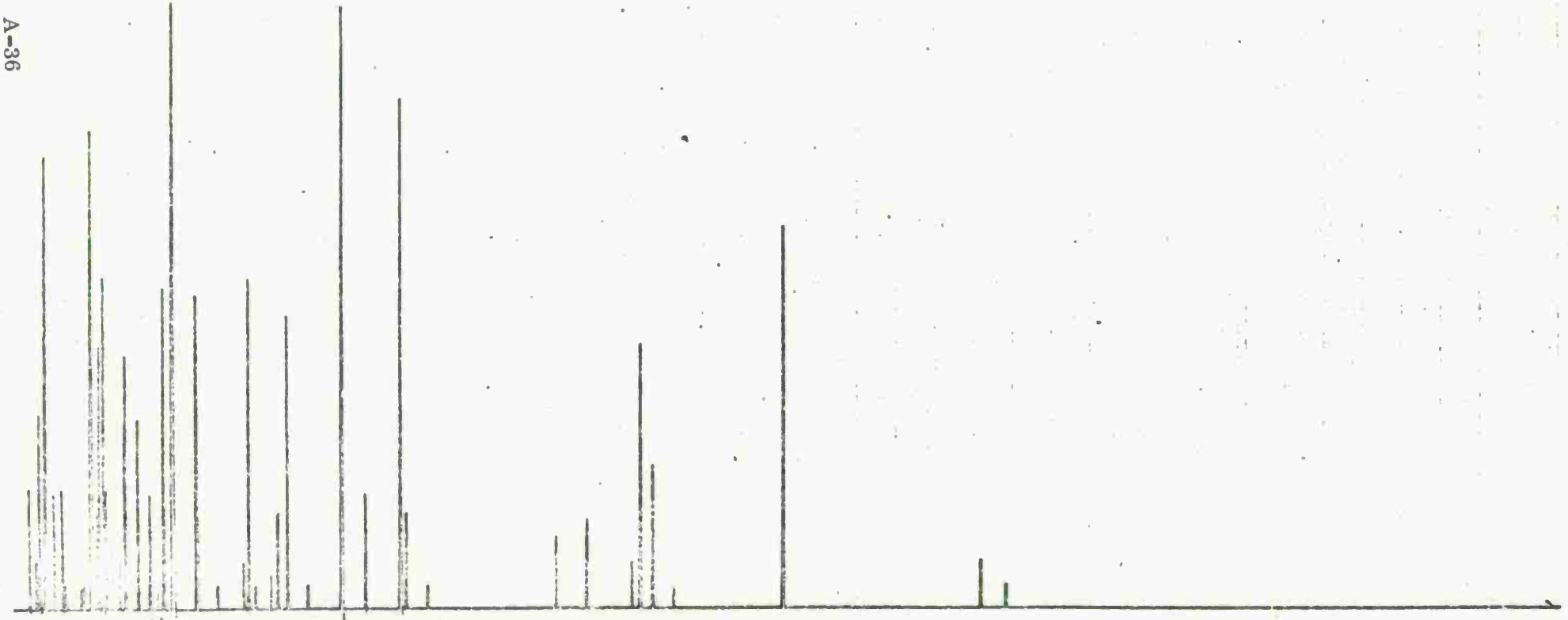

SPECIMEN TYPE		TENSILE COUPON TEST FOR AE
CONTROL	BONDED	
AE 1	1-7-14	YES
2	6-9-3	YES
3	1-4-13	YES
4	6-9-2	NO
5	1-7-13	NO
6	6-9-4	NO

FIGURE A-12. TEST GROUPS, SOLAR SPECIMENS

TEST	TEST STRESS (KSI)					
	RISING/HOLDING SEQUENCE		RISE TO FAILURE		ONE RISE AND HOLD SEQUENCE	
	AE 1	1-7-14	AE 2	6-9-3	AE 3	1-4-13
1	47.3	48.5	148.6	147.0	120.0	120.0
2	58.9	59.0			154.0	152.8
3	114.5	121.0				
4	124.0	142.0				
5	137.0	149.0				
6	149.0	153.0				
FAILURE	NO	NO	NO	YES	YES	YES
LOAD CURVE DROP	NO	YES	YES	NO	YES	YES
SPECIMEN NECKING	YES	YES	YES	—	—	—

FIGURE A-13. TEST STRESS, SOLAR SPECIMENS

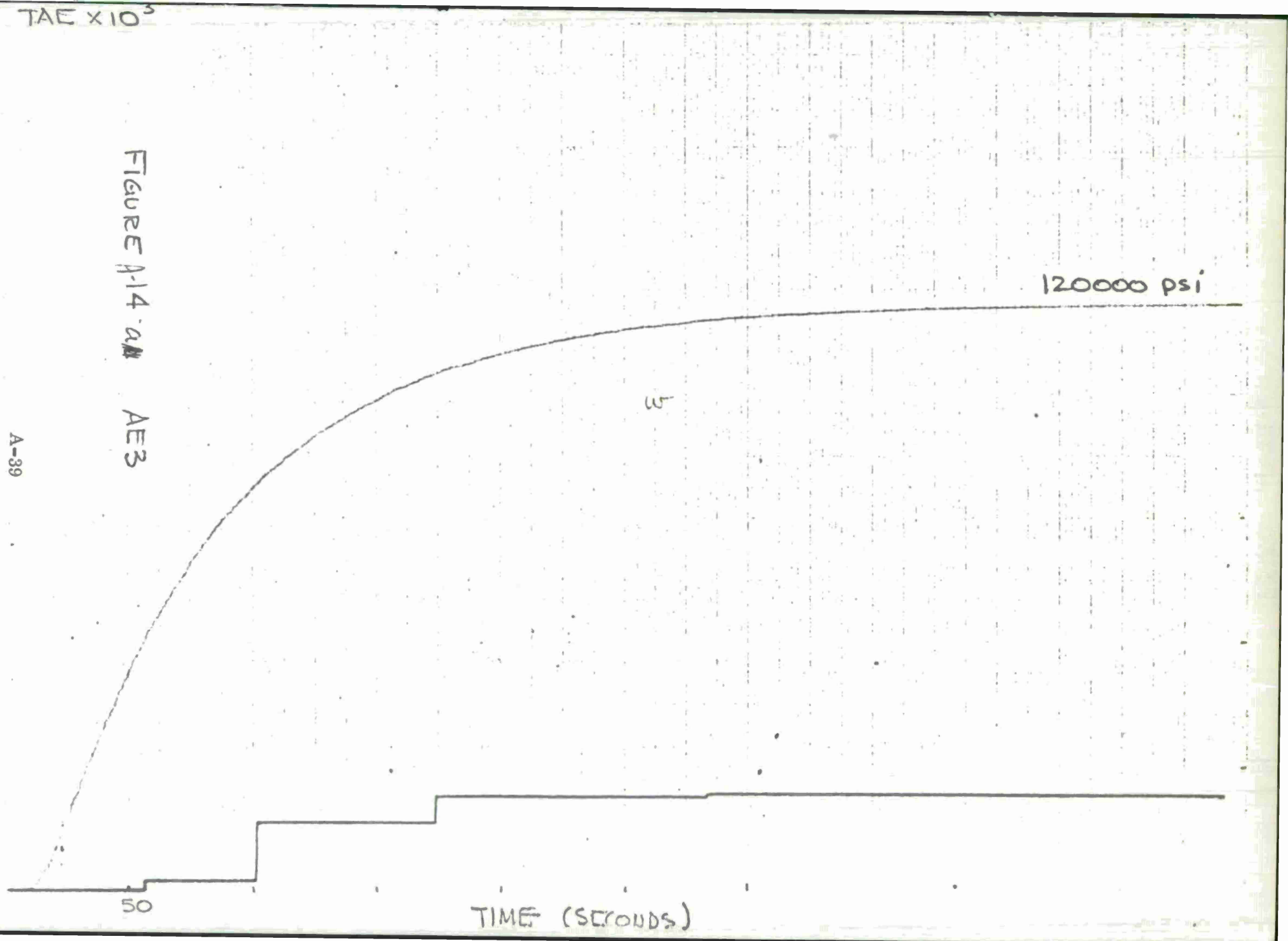

FIGURE A-14 AE3

TAE $\times 10^2$, RESET 0.2 SECONDS
(120 000 PSI)

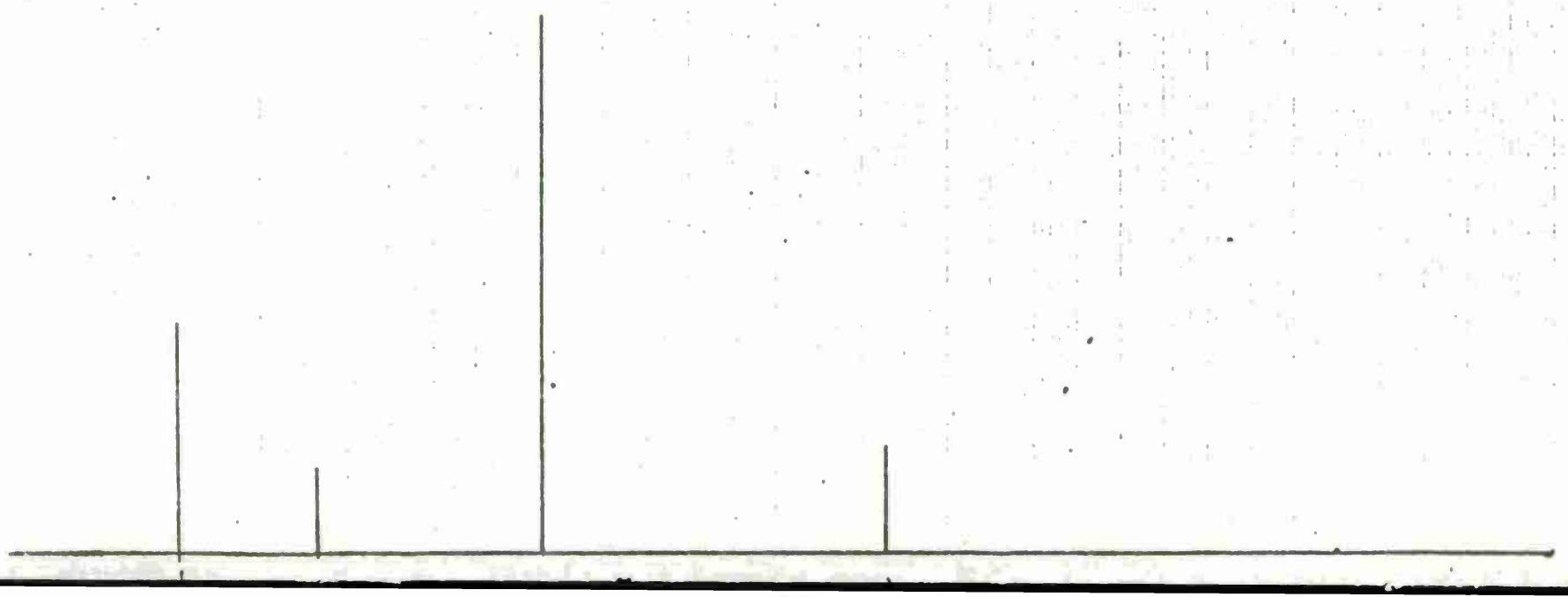

FIGURE A-14 b AE 3

FIGURE A14 ~~AEC~~ 1-4-13

TAEX 16?

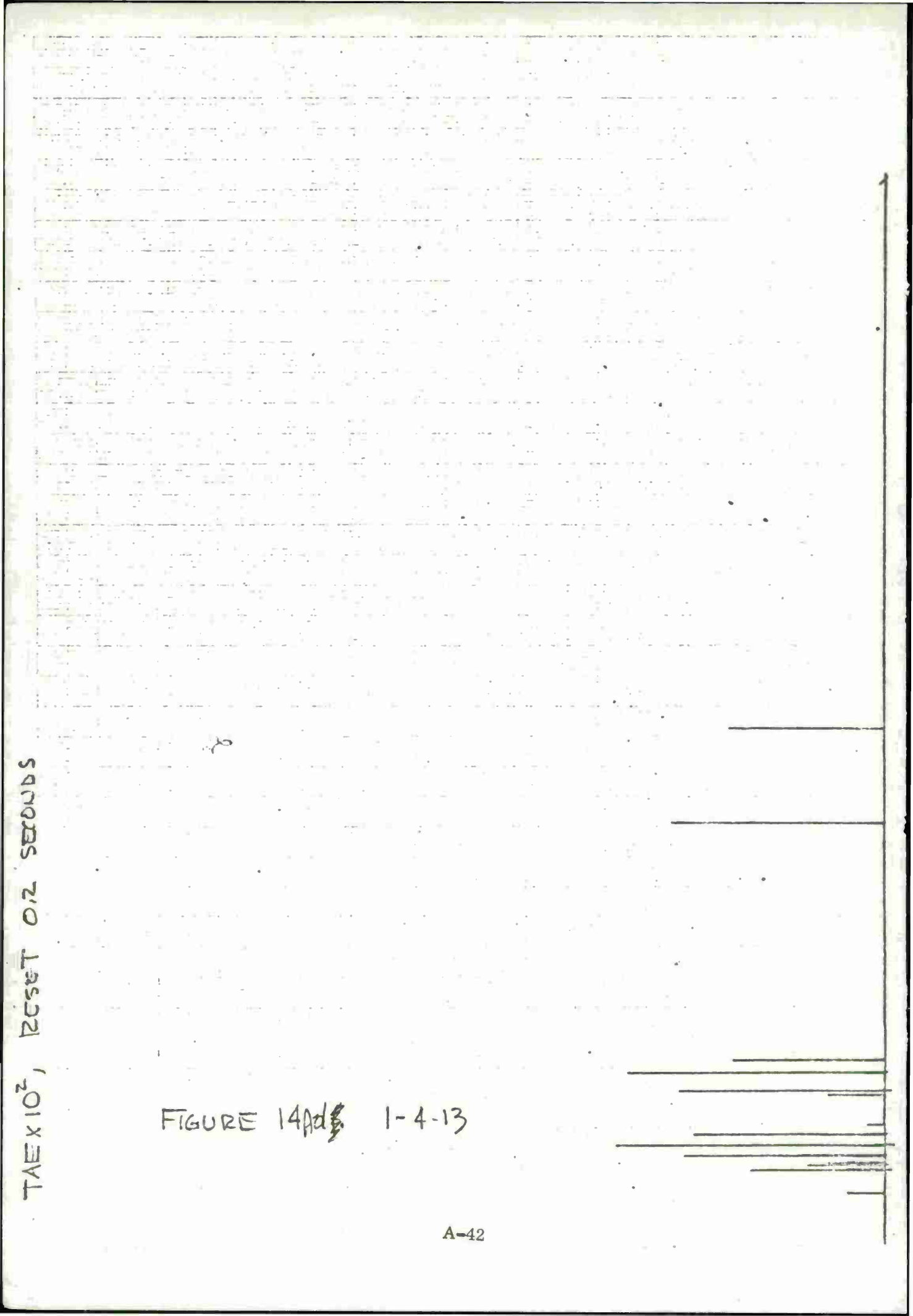

FIGURE 14 Add'g 1-4-13

TECHNICAL REPORT DISTRIBUTION

No. of Copies	To
1	Office of the Director, Defense Research and Engineering, The Pentagon, Washington, D. C. 20301
12	Commander, Defense Documentation Center, Cameron Station, Alexandria, Virginia 22314
1	Advanced Research Projects Agency, The Pentagon, Washington, D. C. 20315
	Metals and Ceramics Information Center, Battelle Memorial Institute, 505 King Avenue, Columbus, Ohio 43201
2	ATTN: Mr. Daniel Maykuth
	Chief of Research and Development, Department of the Army, Washington, D. C. 20310
2	ATTN: Physical and Engineering Sciences Division
1	Dr. Bernard R. Stein
	Commander, U. S. Army Materiel Command, 5001 Eisenhower Avenue, Alexandria, Virginia 22333
1	ATTN: AMCRD-DE, Development Division
1	AMCRD-RS, Research Division
1	AMCRD-RS, Scientific Deputy
1	AMCRD-TC
	Commander, U. S. Army Aviation Systems Command, P. O. Box 209, Main Office, St. Louis, Missouri 63166
1	ATTN: AMSAV-LEP, Mr. J. M. Thorp
1	AMSAV-ER, Dr. I. Peterson
	Commander, U. S. Army Missile Command, Redstone Arsenal, Alabama 35809
1	ATTN: AMSMI-IE, Mr. J. E. Kirshtein
1	AMSMI-R, Mr. John L. McDaniel
1	AMSMI-RBLD, Redstone Scientific Information Center
1	Chief Scientist, Dr. W. W. Carter
1	Directorate of R&D
1	Dr. B. Steverding
	Commander, U. S. Army Mobility Equipment Command, 4300 Goodfellow Boulevard, St. Louis, Missouri 63120
1	ATTN: AMSME-PLC, Mr. J. Murphy
1	Commander, U. S. Army Tank-Automotive Command, Warren, Michigan 48090
1	ATTN: AMSMO-PPS, Mr. David Siegel
1	Mr. J. P. Jones

No. of Copies	To
	Commander, U. S. Army Armament Command, Rock Island, Illinois 61201
2	ATTN: Technical Library
1	AMSAR-SC, Dr. C. M. Hudson
1	AMSAR-PPW-PB, Mr. Francis X. Walter
	Commander, Aberdeen Proving Ground, Maryland 21005
3	ATTN: Technical Library, Building 313
	Commander, U. S. Army Foreign Science and Technology Center, 220 7th Street, N. E., Charlottesville, Virginia 22901
1	ATTN: AMXST-SD3
	Frankford Arsenal, Philadelphia, Pennsylvania 19137
1	ATTN: Pitman-Dunn Institute of Research
	Commander, Picatinny Arsenal, Dover, New Jersey 07801
1	ATTN: Feltman Research Laboratories
	Commander, Rock Island Arsenal, Rock Island, Illinois 61201
1	ATTN: SWERI-RDL
	Director, Eustis Directorate, U. S. Army Air Mobility Research and Development Laboratory, Fort Eustis, Virginia 23604
1	ATTN: Mr. J. Robinson, SAVDL-EU-SS
	Commander, U. S. Army Ballistic Research Laboratories, Aberdeen Proving Ground, Maryland 21005
1	ATTN: Dr. D. Eichelberger
	Director, U. S. Army Materiel Systems Analysis Activity, Aberdeen Proving Ground, Maryland 21005
1	ATTN: AMXSY-D
	Commander, U. S. Army Electronics Command, 225 South 18th Street, Philadelphia, Pennsylvania 19103
1	ATTN: AMSEL-PP/P/IED-2, Mr. Wesley Karg
	Commander, U. S. Army Mobility Equipment Research and Development Center, Fort Belvoir, Virginia 22060
2	ATTN: Technical Documents Center, Building 315
	Commander, U. S. Army Production Equipment Agency, Manufacturing Technology Branch, Rock Island Arsenal, Illinois 61202
1	ATTN: AMXPE, Mr. Ralph Siegel
	Commander, U. S. Army Research and Engineering Directorate, Warren, Michigan 48090
1	ATTN: SMOTA-RCM.1, Mr. Edward Moritz
1	SMOTA-RCM.1, Mr. Donald Phelps

No. of Copies	To
	Commander, Watervliet Arsenal, Watervliet, New York 12189
1	ATTN: SWEWV-R
1	Dr. Robert Weigle
1	Chief, Bureau of Naval Weapons, Department of the Navy, Room 2225, Munitions Building, Washington, D. C.
	Chief, Bureau of Ships, Department of the Navy, Washington, D. C. 20315
1	ATTN: Code 341
	Chief of Naval Research, Arlington, Virginia 22217
1	ATTN: Code 472
	Hq., USAF/RDPI, The Pentagon, Washington, D. C. 20330
1	ATTN: Major Donald Sponberg
	Headquarters, Aeronautical Systems Division, 4950 TEST W/TZHM (DH 2-5 Mgr), Wright-Patterson Air Force Base, Ohio 45433
1	ATTN: AFML-MATB, Mr. George Glenn
2	AFML-LAE, E. Morrissey
1	AFML-LMD, D. M. Forney
1	AFML-LC
1	AFML-MBC, Mr. Stanley Schulman
	National Aeronautics and Space Administration, Washington, D. C. 25046
1	ATTN: AFSS-AD, Office of Scientific and Technical Information
1	Mr. B. G. Achhammer
1	Mr. G. C. Deutsch, Chief, Materials Research Program, Code RR-1
	National Aeronautics and Space Administration, Lewis Research Center, 21000 Brookpark Road, Cleveland, Ohio 44135
1	ATTN: Mr. G. Mervin Ault, Assistant Chief, M&S Division
	National Aeronautics and Space Administration, Marshall Space Flight Center, Huntsville, Alabama 35812
1	ATTN: S&E-ME-MM, Mr. W. A. Wilson, Building 4720
1	R-P&VE-M, R. J. Schwinghamer
	Albany Metallurgy Research Center, Albany, Oregon 97321
1	ATTN: Mr. R. R. Wells, Research Director
	Defense Materials Service, General Services Administration, Washington, D. C. 20405
1	ATTN: Mr. Clarence A. Fredell, Director, Technical R&D Staff

No. of Copies	To
	Director, Army Materials and Mechanics Research Center, Watertown, Massachusetts 02172
2	ATTN: AMXMR-PL
1	AMXMR-PR
1	AMXMR-CT
1	AMXMR-XC
1	AMXMR-AP
1	AMXMR-M
1	AMXMR-PT, Mr. R. Farrow
1	Author